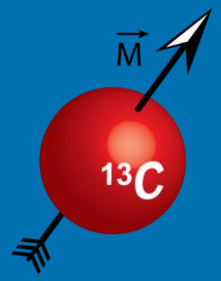

CIBM
Center for Biomedical Imaging

INTERPRETATION OF DYNAMIC X-NUCLEI EXPERIMENTS WITH METABOLIC MODELLING

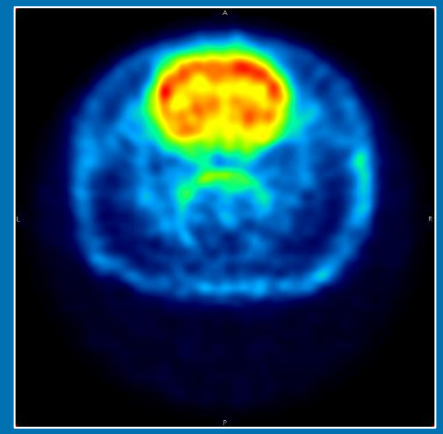

Bernard Lanz, PhD

CIBM MRI EPFL

01.05.2023

PHYS-760

CIBM translational MR neuroimaging & spectroscopy

EPFL

IN VIVO STUDIES OF BRAIN ACTIVITY

- Electromagnetic activity (action potential):
  - Electroencephalography (EEG)
  - Magnetoencephalography (MEG)
- Oxygen demand and hemodynamic response (oxy/deoxyhemoglobin)
  - Functional magnetic resonance imaging (fMRI)

- Energy metabolism (use of plasma energy substrates)
  - Dynamic magnetic resonance spectroscopy:
    - ^{1}H MRS (fMRS) without tracer injection
    - ^{13}C MRS with tracer injection
    - ^{15}N MRS with tracer injection
    - ^{31}P MRS without tracer injection
  - Radionuclides emission tomography (PET, SPECT)

WHAT CAN WE MEASURE WITH MRS ?

In vivo magnetic resonance spectroscopy (MRS)
gives extended chemical information on the compounds involved
in brain metabolism and biochemical processes

^{1}H MRS spectrum:

Measures total concentrations of
more than 20 compounds at high field
(static acquisition in one voxel)

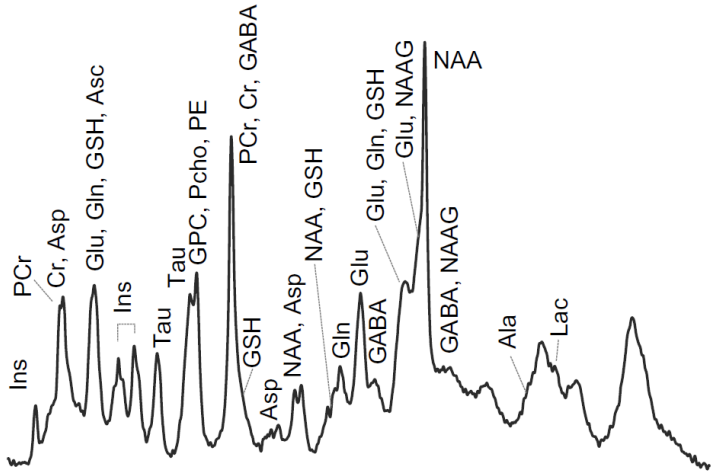

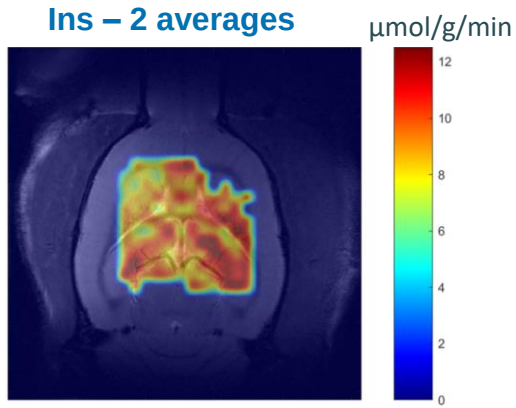

Courtesy of D Simicic, C Cudalbu

Extend spatial information:

Magnetic resonance spectroscopic imaging (MRSI)

It is an equilibrium information on the compounds
Does not carry information on their interaction

Extend temporal information:

Dynamic magnetic resonance spectroscopy (typically X-nuclei),
to measure metabolic fluxes / reactions

UNDERLYING BIOCHEMICAL MECHANISMS ?

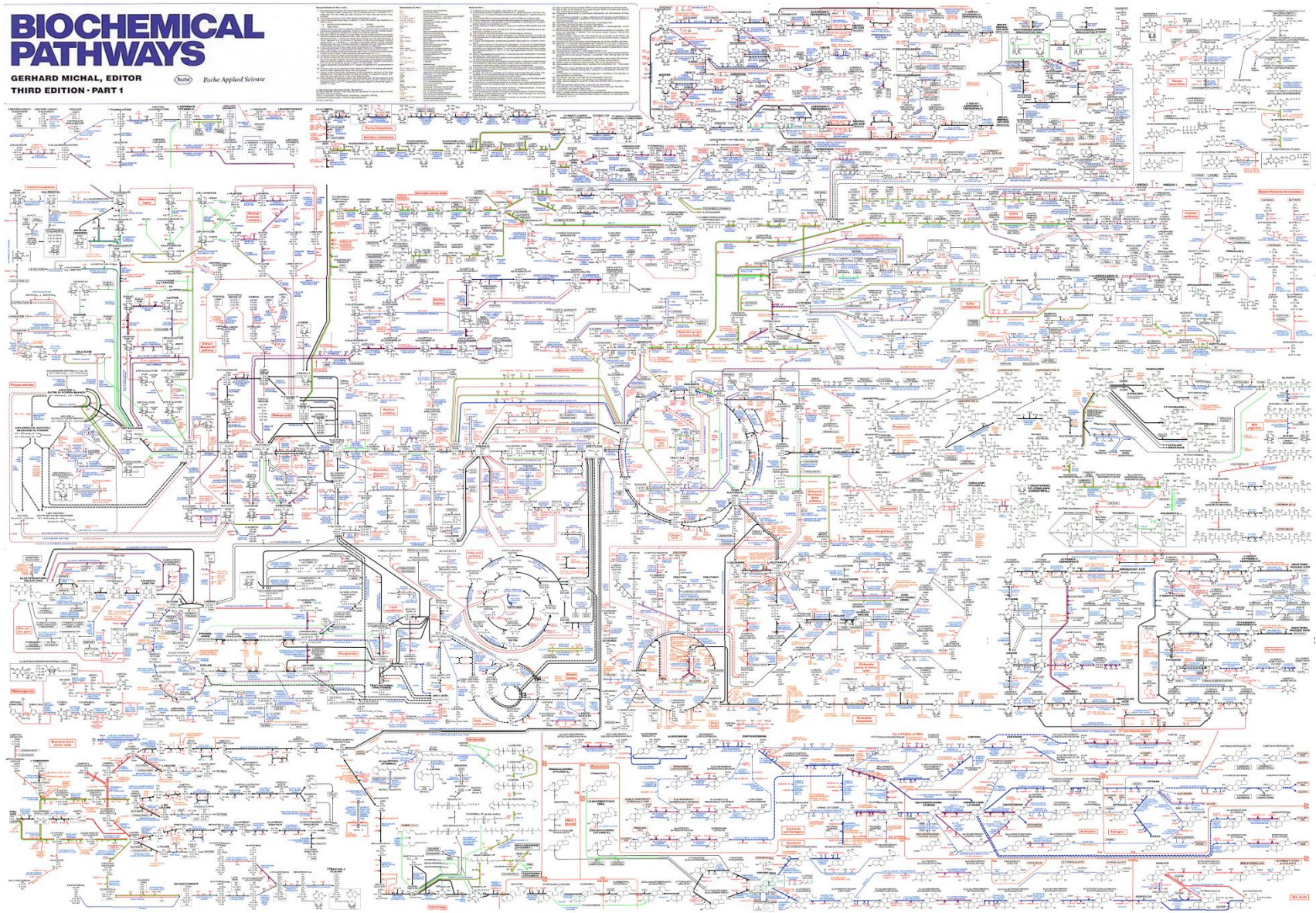

UNDERLYING BIOCHEMICAL MECHANISMS ?

TCA cycle:

(or Krebs cycle)

Main oxidative reaction chain producing ATP for the various cellular needs in energy.

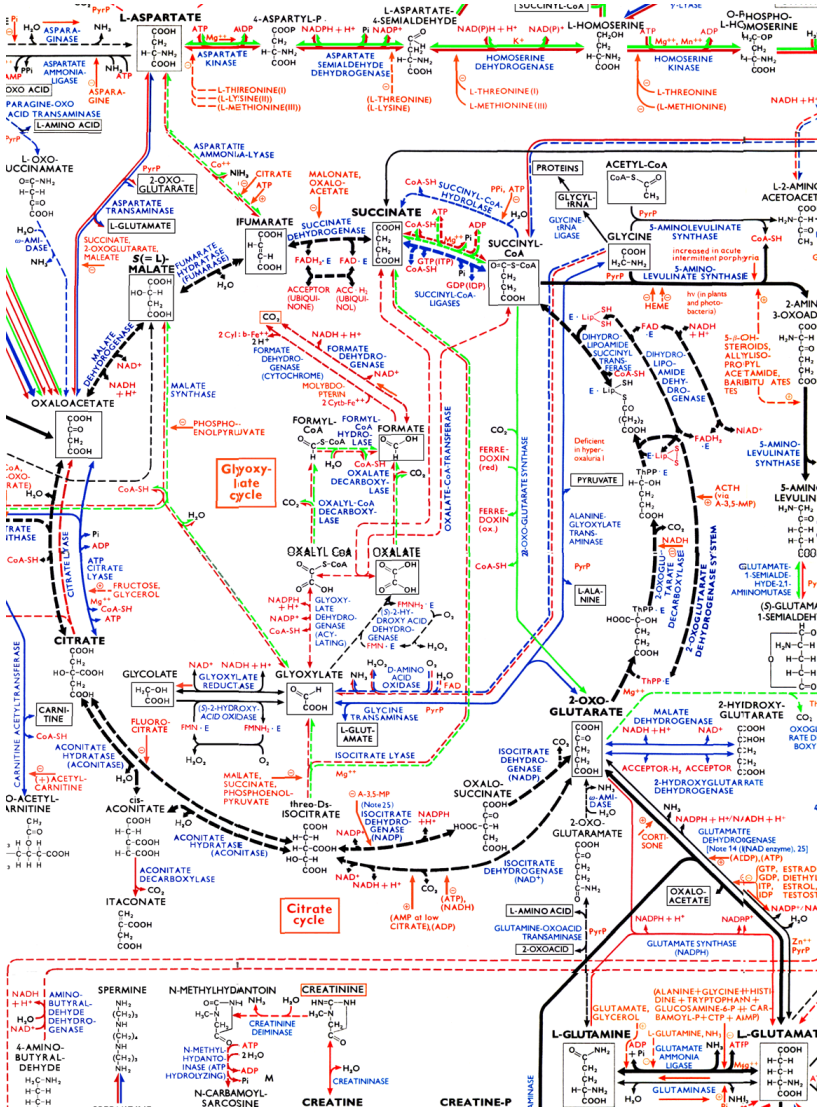

BRAIN ENERGY METABOLISM:
UNDERLYING BIOCHEMICAL MECHANISMS ?

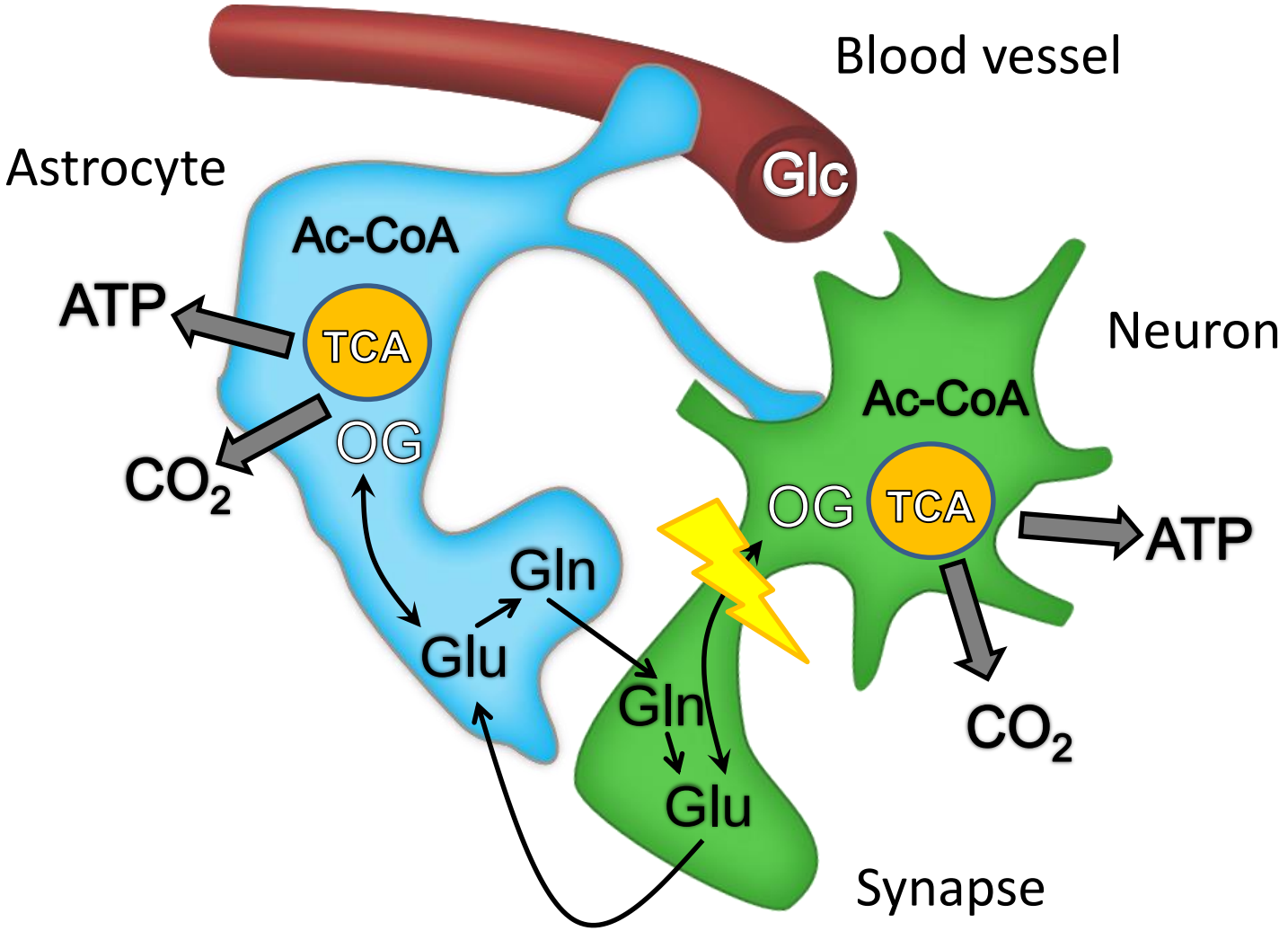

BIOCHEMICAL MOTIVATIONS

Network:

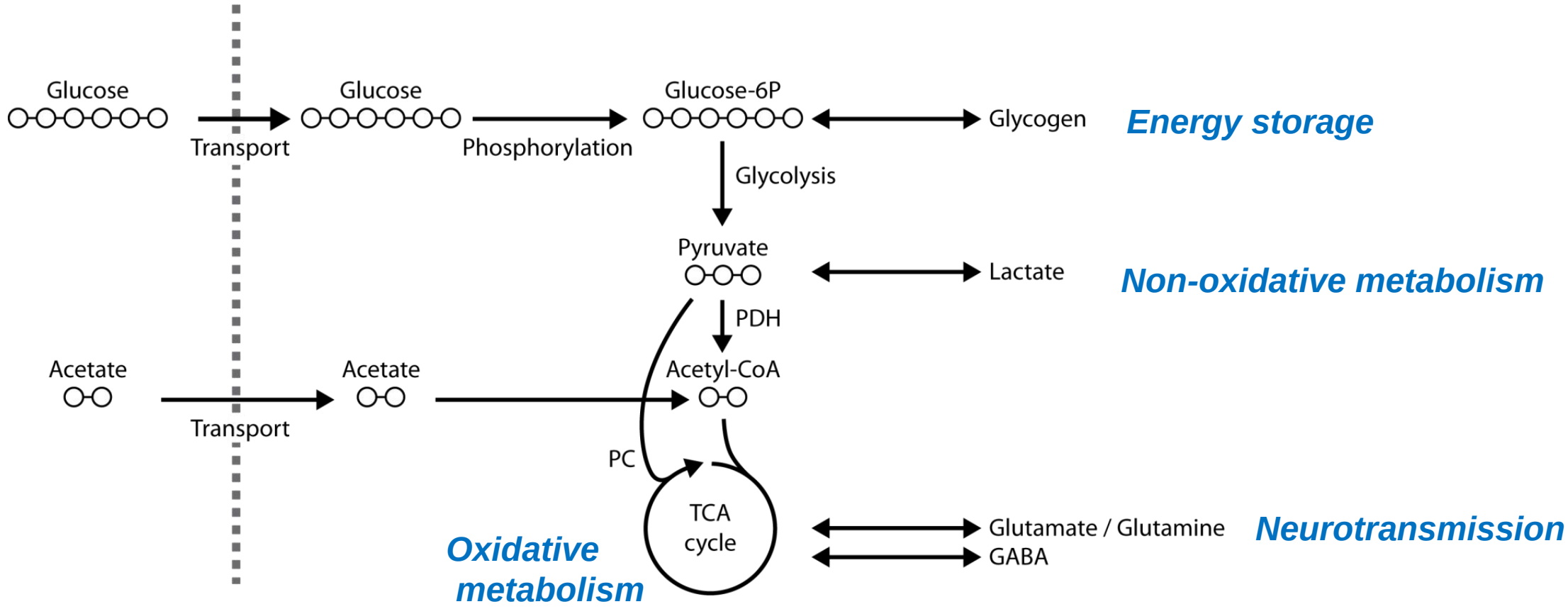

MAIN BIOCHEMICAL PATHWAYS

IN BRAIN ENERGY METABOLISM

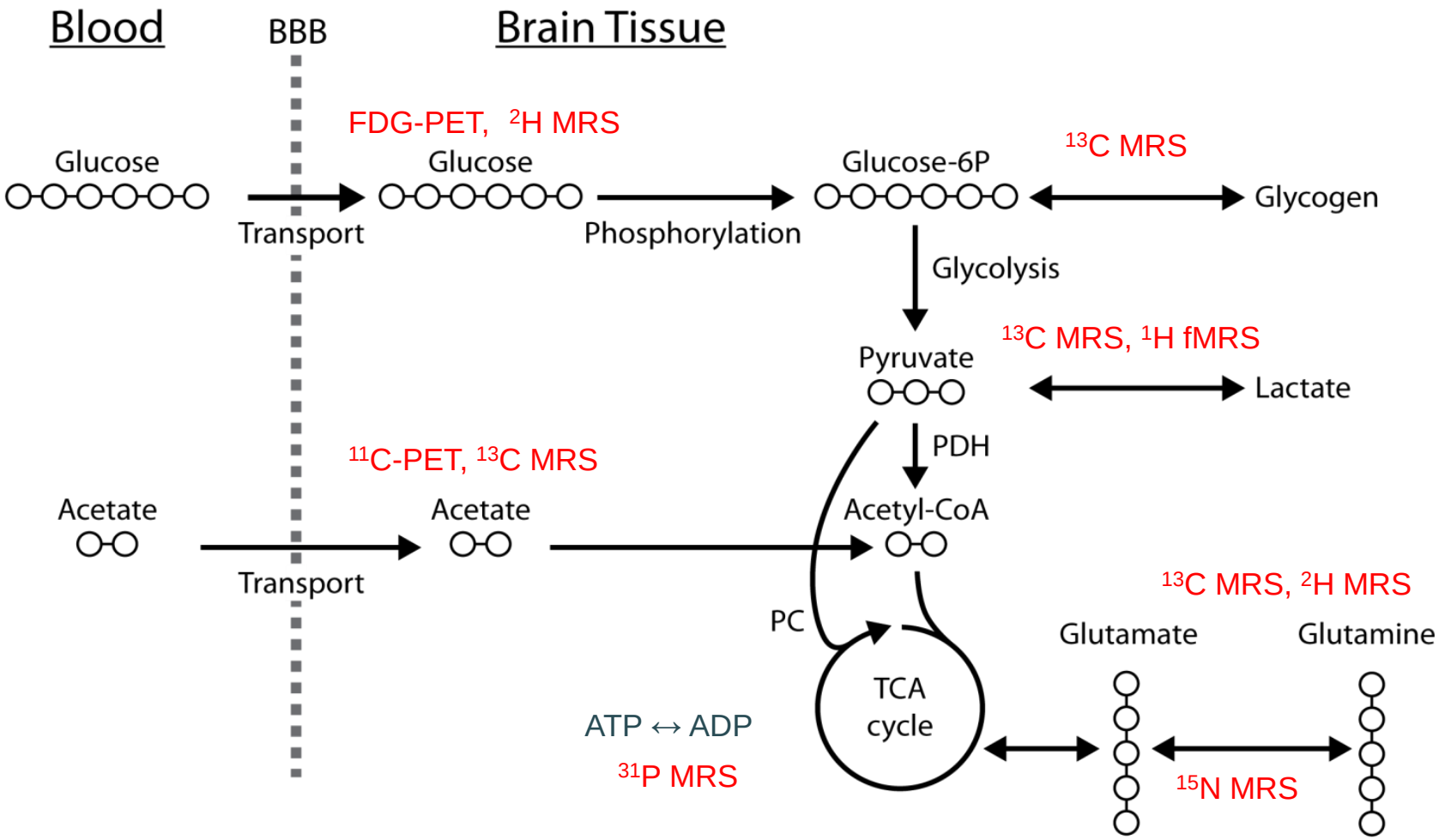

OVERVIEW ^{13}C MRS *IN VIVO*

The Carbon nucleus

- Spin I=1/2

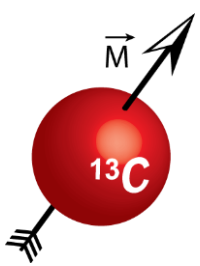

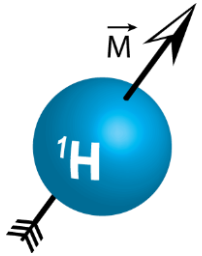

- Natural abundance

98.9 %

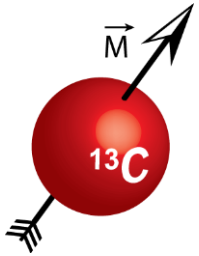

1.1 %

- Low sensitivity

$\gamma(^{13}C) = 10.7$ MHz/T ($\gamma(^{1}H) = 42.6$ MHz/T)

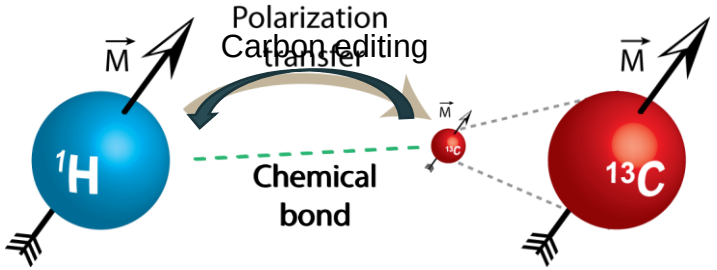

^{13}C MRS

Separate detection of carbon positions

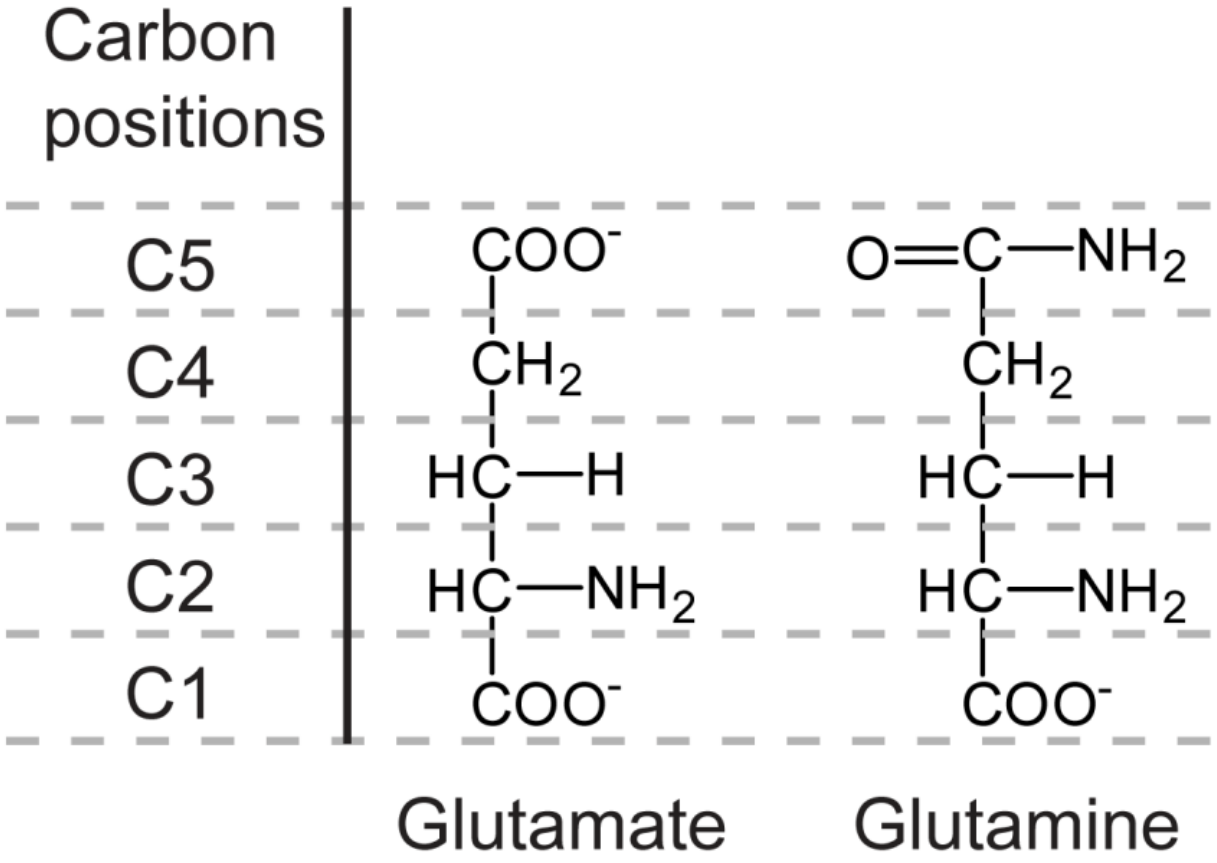

^{13}C MRS

Separate detection of carbon positions

Large chemical shift:

\+ Good spectral resolution

\+ Flat baseline

\- Large chemical shift artefacts

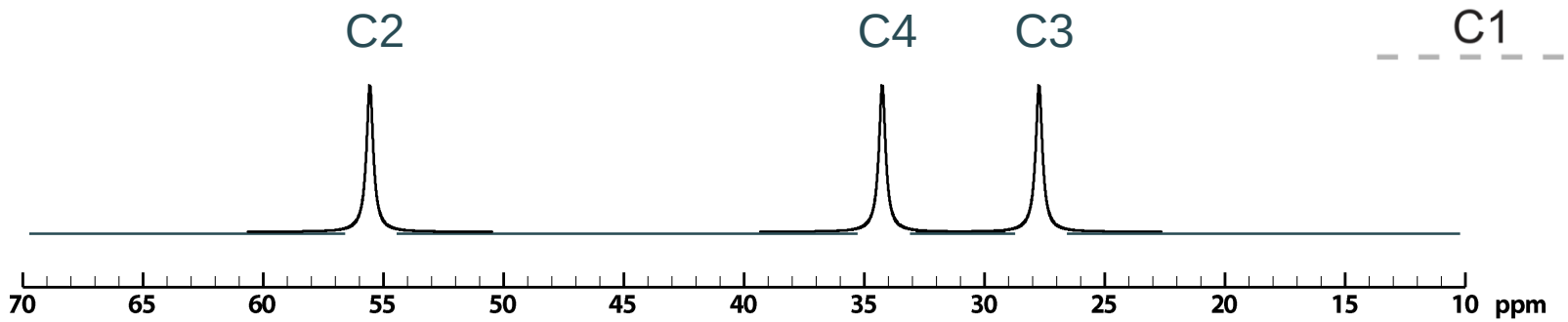

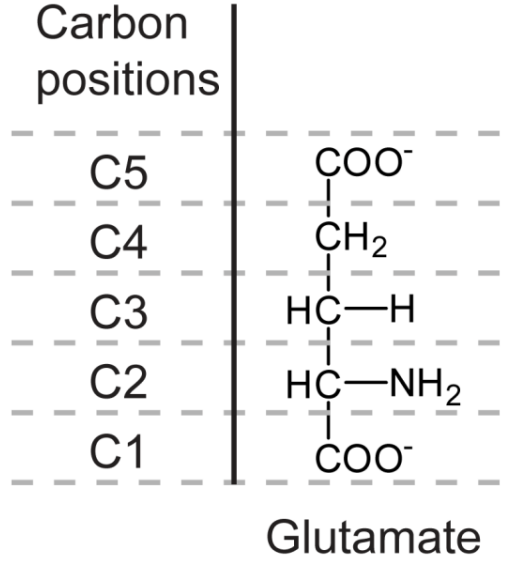

Methine groups Methylene groups

Carboxyl / amide groups (C5 and C1) (170-185 ppm)

^{13}C MRS

Detection of multiple ^{13}C labelling

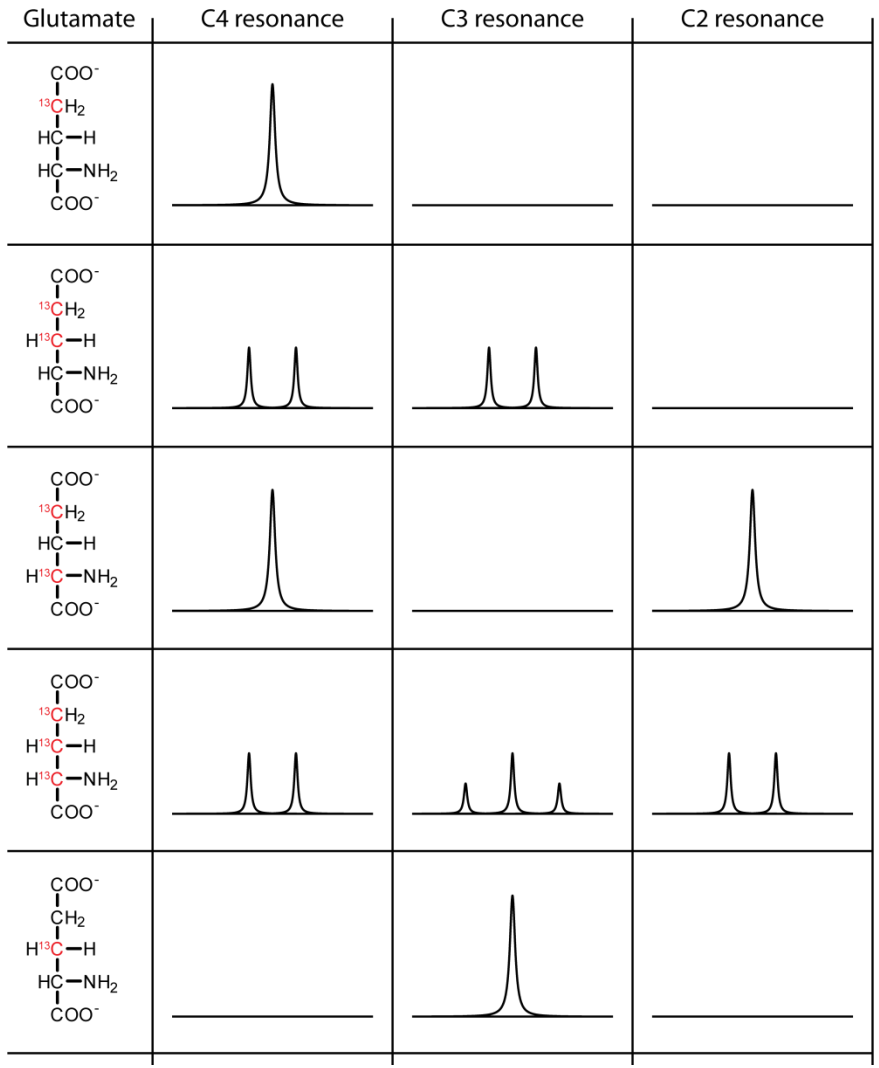

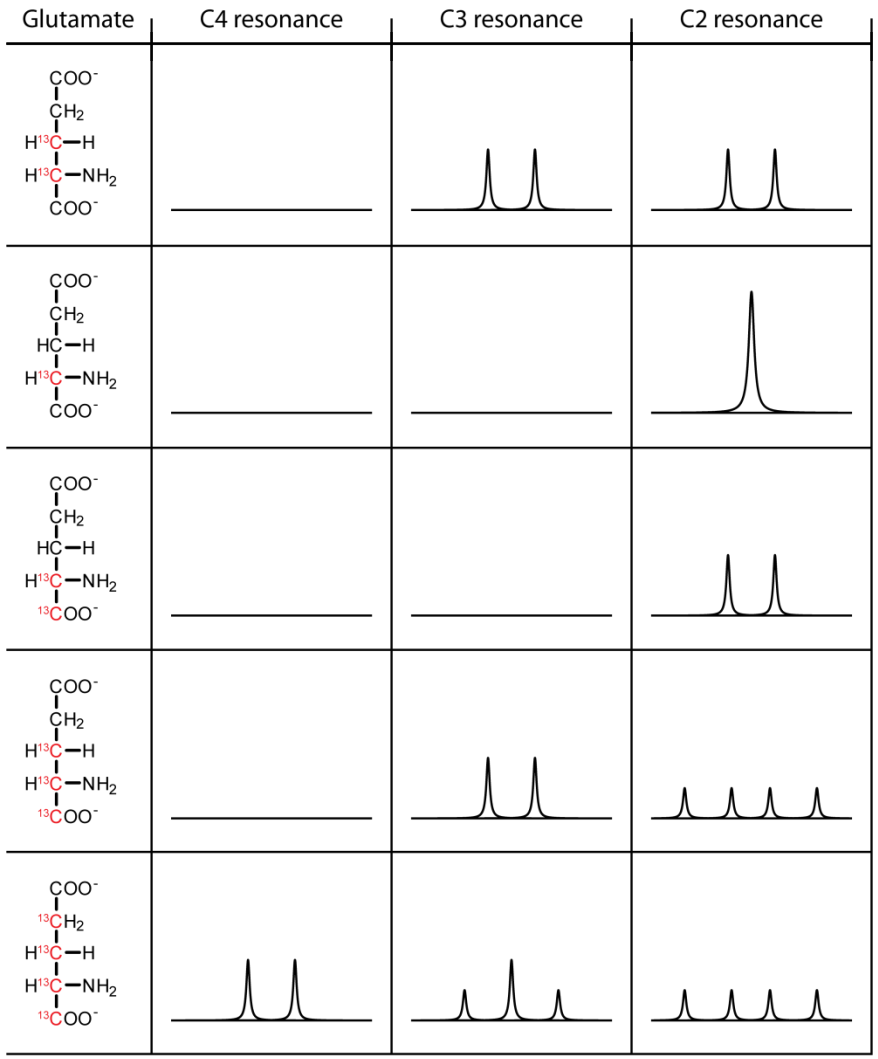

^{13}C MRS NMR SIGNAL STRENGTH

- Zeeman energy: $\gamma_C \cong \frac{1}{4}\gamma_H$

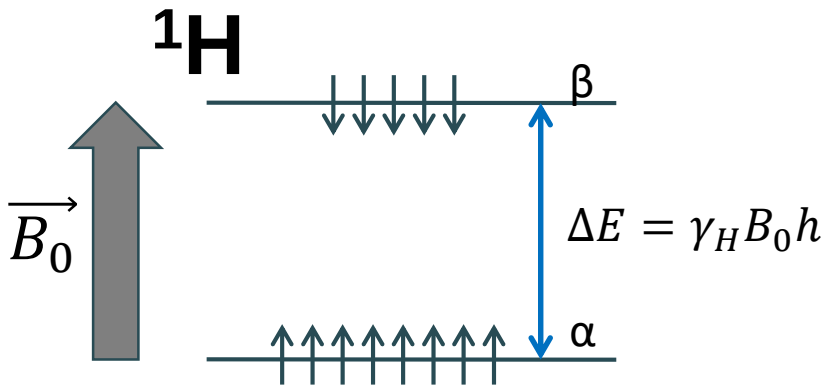

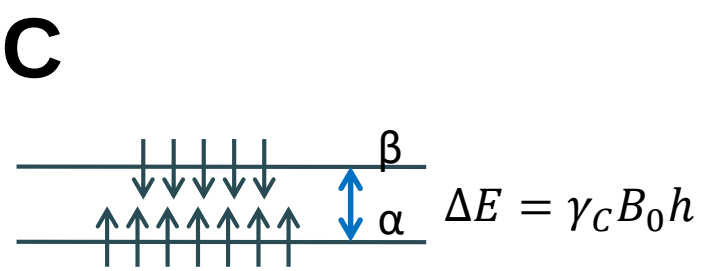

Boltzmann distribution: $(n_\alpha - n_\beta) \approx \left(\frac{nh\gamma B_0}{2kT}\right)$

- Amplitude of the magnetization: $M_0 = (n_\alpha - n_\beta)\mu_z = (n_\alpha - n_\beta)\,\gamma\,\frac{h}{2}$
- Total magnetization: $M_0 = n\,\frac{1}{2}(\gamma h)^2\left(\frac{B_0}{2kT}\right) \propto \gamma^2$

$$M_0(^{13}\mathrm{C}) \cong \frac{1}{16} M_0(^{1}\mathrm{H})$$

THEORETICAL GAIN IN SNR

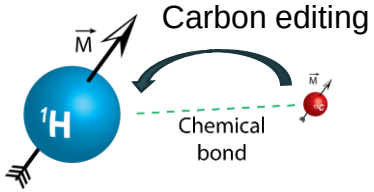

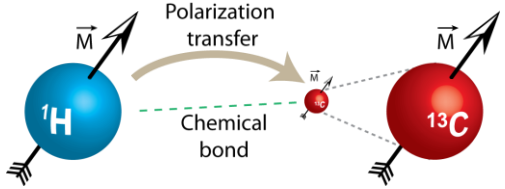

	^{1}H-[^{13}C]MRS	Polarization transfer ^{13}C MRS
Polarization $\Delta E \propto \gamma$	^{1}H	^{1}H
Magnetic moment $\mu_z \propto \gamma$	^{1}H	^{13}C
Detection sensitivity $emf \propto freq. \propto \gamma$ Noise $\propto \gamma^{1/2}$	^{1}H	^{13}C
Overall SNR	$\propto \gamma_H^{5/2}$ (32x)	$\propto \gamma_H \gamma_C^{3/2}$ (4x)

(neglecting T1 saturation effects)

^{13}C MRS ACQUISITION STRATEGIES

Indirect ^{13}C detection

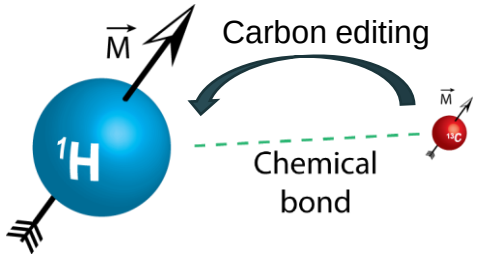

- Indirect ^{1}H-[^{13}C] localized MRS detection
  - High sensitivity of ^{1}H detection
    (of advantage for higher temporal resolution / lower enrichment studies)
    -> lower chemical shift range

Indirect ^{13}C MRS spectroscopy:
([2-^{13}C] Ace infusion)

BISEP-SPECIAL ^{1}H-[^{13}C]MRS (at 14T)

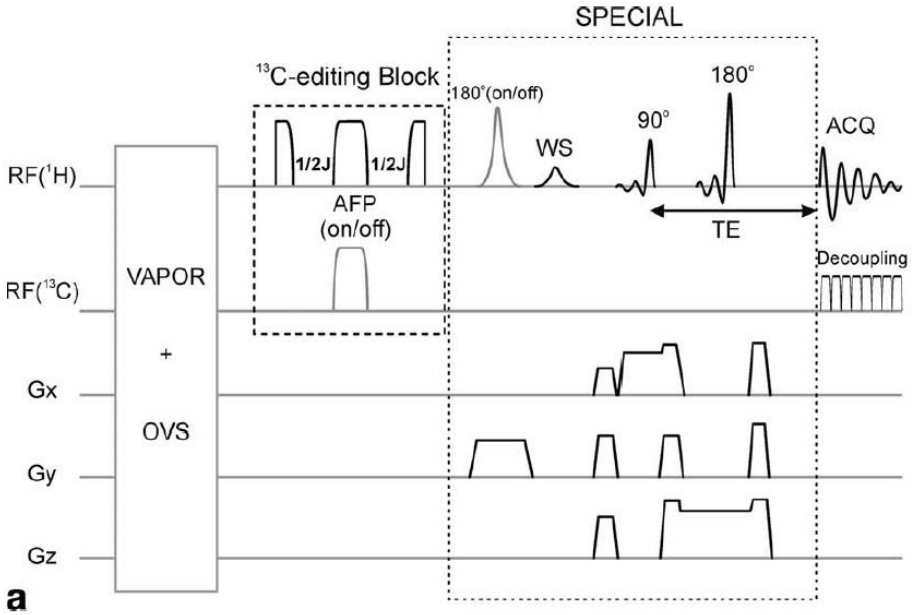

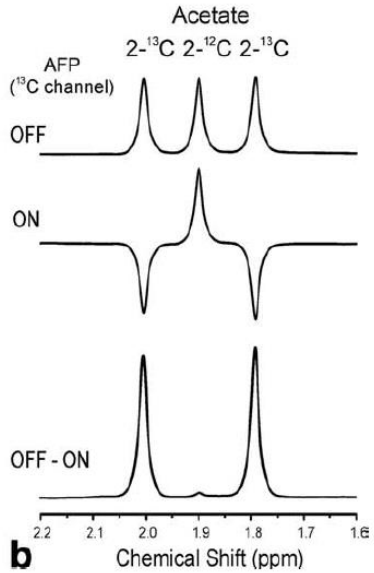

Xin et al., MRM, 2010

^{13}C MRS ACQUISITION STRATEGIES

Direct ^{13}C detection

- Direct ^{13}C localized MRS detection with polarization transfer
  - Higher chemical shift range of ^{13}C spectra (many carbon resonances measurable)
    -> labelling positions clearly dissociable

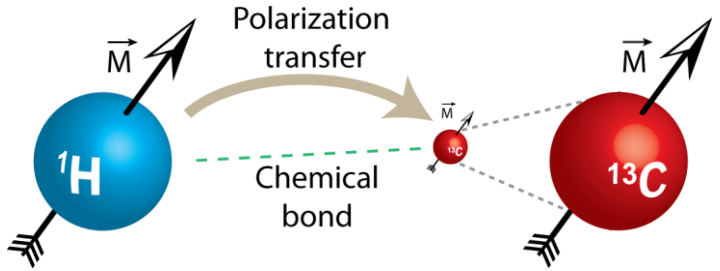

Localized DEPT:

Henry et al., MRM, 2003

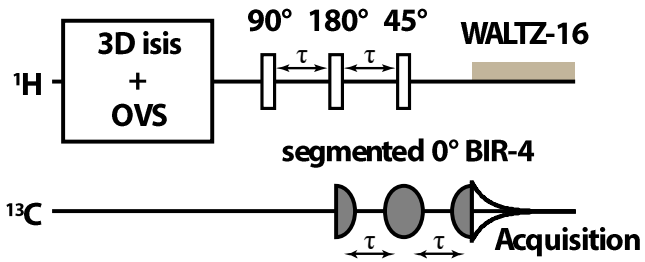

with $\tau = 1/2J_{CH}$

^{13}C MRS spectrum:

([1,6-^{13}C] Glc infusion rat, 9.4T, 320 µl, last 50 min)

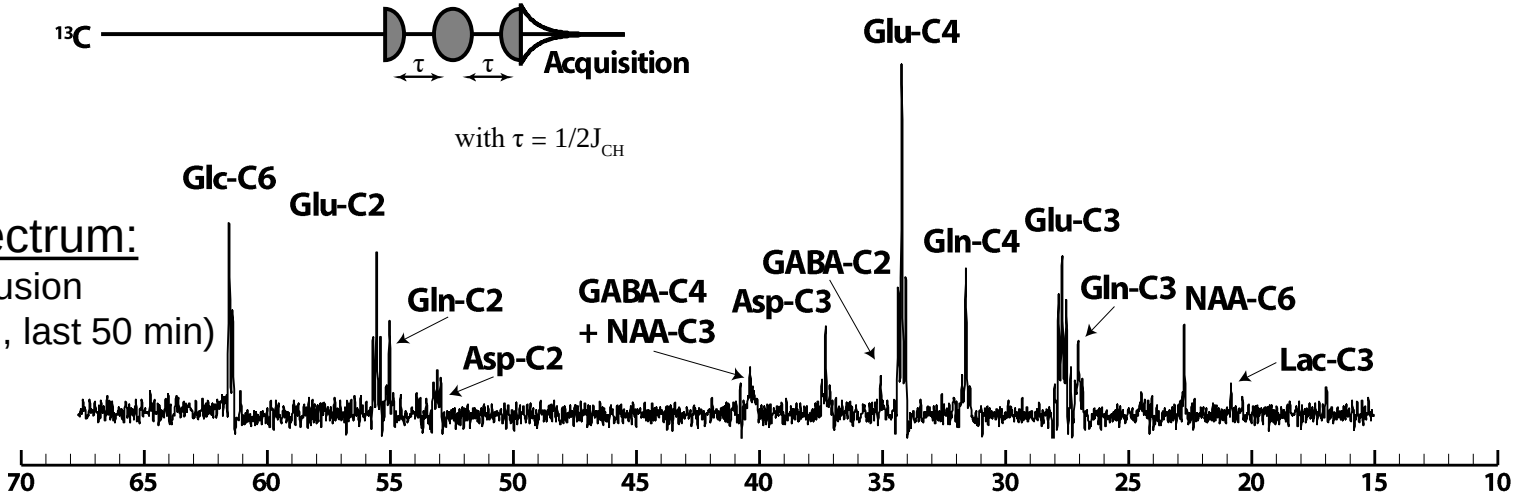

MISSING INTERNAL REFERENCE

^{1}H MRS : water signal

- Frequency reference

- Power calibration

- Concentration reference

- …

MISSING INTERNAL REFERENCE

^{13}C MRS : no carbon in water

- No frequency reference

- No reference for power calibration

- No concentration reference

- …

^{13}C-FORMIC ACID CALIBRATION

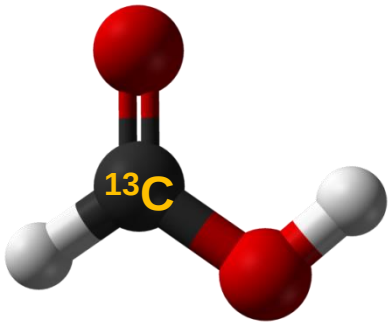

Formic acid-^{13}C

95 wt. % in H_2O, 99 atom % ^{13}C

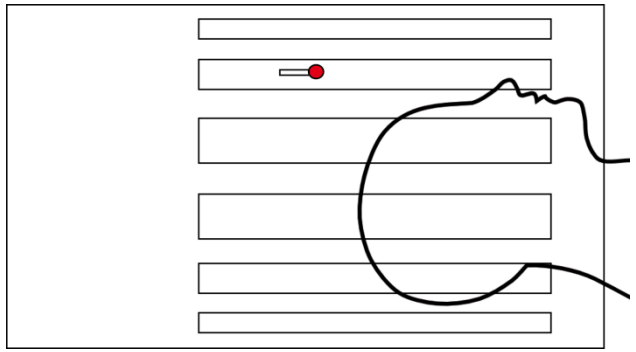

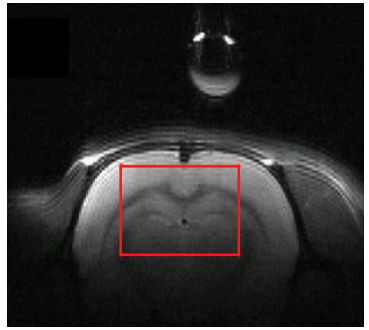

T_1 relaxation:

Reduced from ~6 to 0.5 second with Gd contrast agent (Dotarem)

$$\frac{1}{T_{1,Obs}} = \frac{1}{T_1} + r_1[CA]$$

with $[CA]$ the concentration of contrast agent.

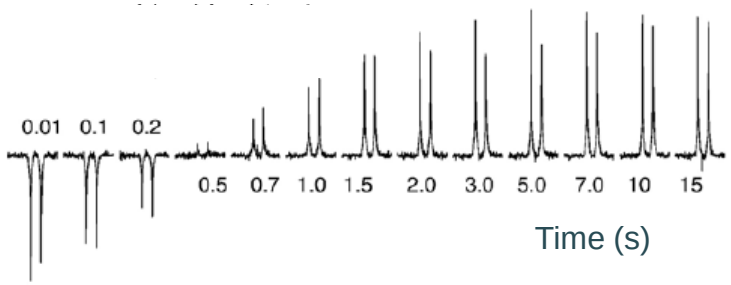

^{13}C spectrum

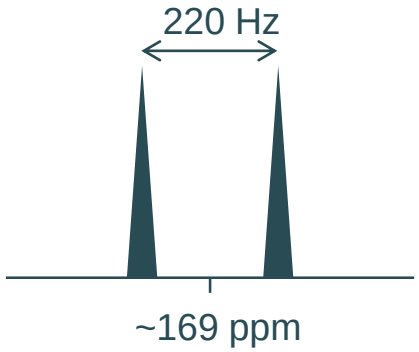

R. van Heeswijk et al., MRM 2007

BRAIN METABOLIC MODELLING

Metabolic modelling is a two-step process.

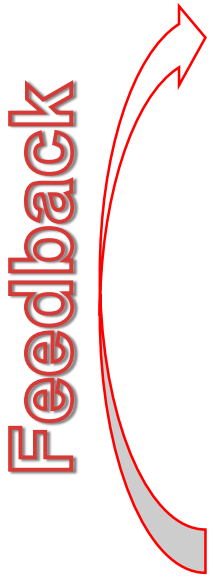

1. The metabolic system is formalized as a schematic,
   taking into account the current physiological and biochemical knowledge on the biological system.
   It is adapted to the available information, since part of the system is not measurable or not relevant for the measured processes.

   → set of mathematical equations

2. The model is used to estimate the metabolic parameters involved in the studied metabolic process by fitting it to the experimental data.
   - appropriateness of the model
   - parameter values describing the current data
   - precision of these estimations.

TRACER / TRACEE

- The study of brain metabolism with dynamic labelling studies is intrinsically linked with the use of **a particular tracer**.

Definitions: **A tracer** is defined as an isotope-labelled and detectable molecule, used to follow the fate of unlabelled chemical species that it is transformed into through metabolism.

The tracee is the corresponding unlabelled species, whose dynamics is of interest in the analysed metabolic process.

- The chemical structure of the tracer is commonly close to the chemical structure of the tracee (identical in the case of ^{13}C MRS)

FDG / glucose [1,6-^{13}C]glucose / glucose [2-^{13}C]acetate / acetate

TRACER / TRACEE

Characteristics of the ideal tracer :

1. It should be detectable by the applied bioimaging measurement technique and should be measurable quantitatively as a concentration (mol of tracer/ g) or as a fractional enrichment ([amount of tracer] / [amount of tracer and tracee])
2. Its introduction should minimally affect the biochemical system that is studied
3. Its metabolism should be identical to the metabolism of the tracee
4. When entering a metabolic pool, it should mix uniformly and instantly throughout
5. The natural abundance of the tracer should be very low, to avoid additional measurement errors due to background contamination
6. It should provide chemical specificity, in the sense that the detection system should be able to determine in which molecule and in which position in this molecule the labelled isotope is located
7. It should be safe for the experimentalist and for the subject and should be detectable in the tissue in a non-destructive way
8. It should enable a site-specific detection, meaning that the researcher should be able to measure the uptake and metabolism of the tracer locally in any physical space of a chosen organ

COMPARTMENTAL MODELLING

- The different biochemical species (or group of species) are modelled as idealized stores of substance called metabolic pools (also called labelling pools)
  - Describes molecules that share the same behaviour
  - Each pool is supposed homogeneous (instantaneous mixing of the tracer with the tracee, uniform volume distribution)

→ The probability of leaving the labelling pool through any of the available effluxes is the same for all the molecules present in the pool

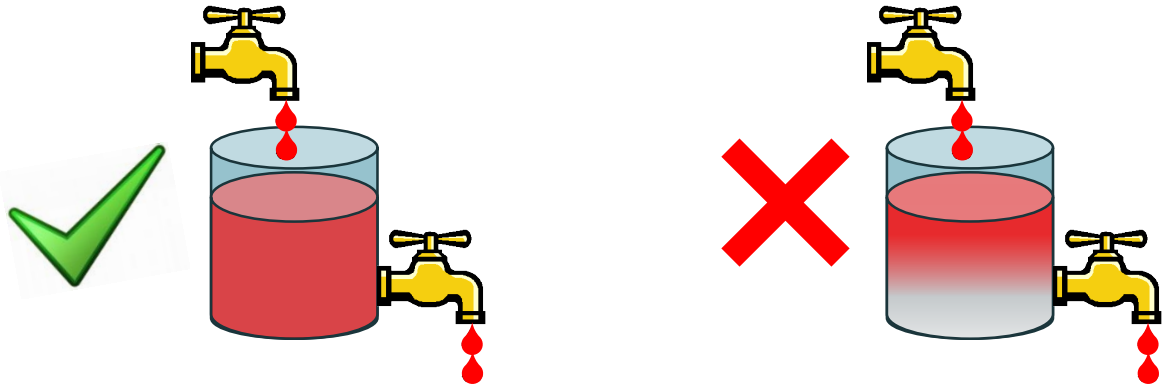

OBJECTIVES OF THE MODEL

The objectives of a metabolic model can be the following:

- identification the structure of the system

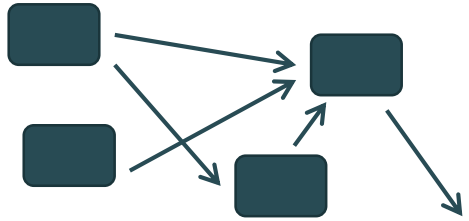

- estimation of the value of the internal metabolic parameters and their precision

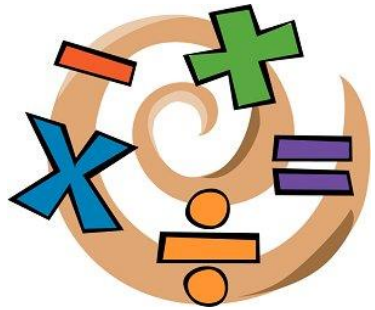

- prediction of the response of the system to external factors

MATHEMATICAL DESCRIPTION OF COMPARTMENTAL MODELS

The elementary unit, the labelling pool :

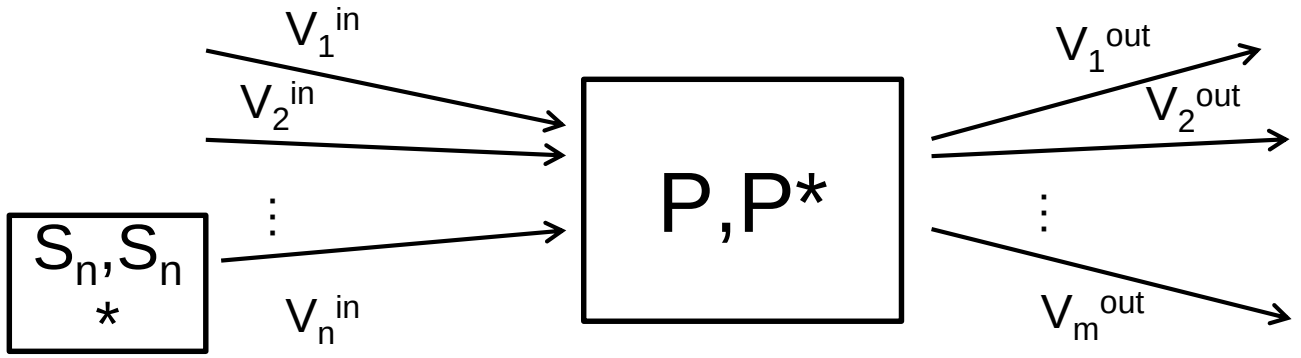

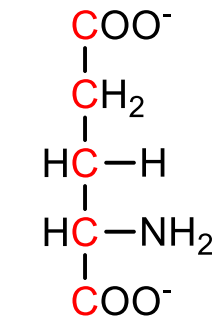

Glutamate

- Represents a labelling position in a given molecule, or simply a labelled molecule
- Is characterized by :
  - Its total concentration (P) in [µmol/g]
  - Its labelled concentration (P*) in [µmol/g] (typically ^{13}C), or equivalently by its fractional enrichment : [-], varying between 0 and 1

$$FE = \frac{P^*}{P}$$

MATHEMATICAL PRINCIPLES OF COMPARTMENTAL MODELLING

The labelling equations:

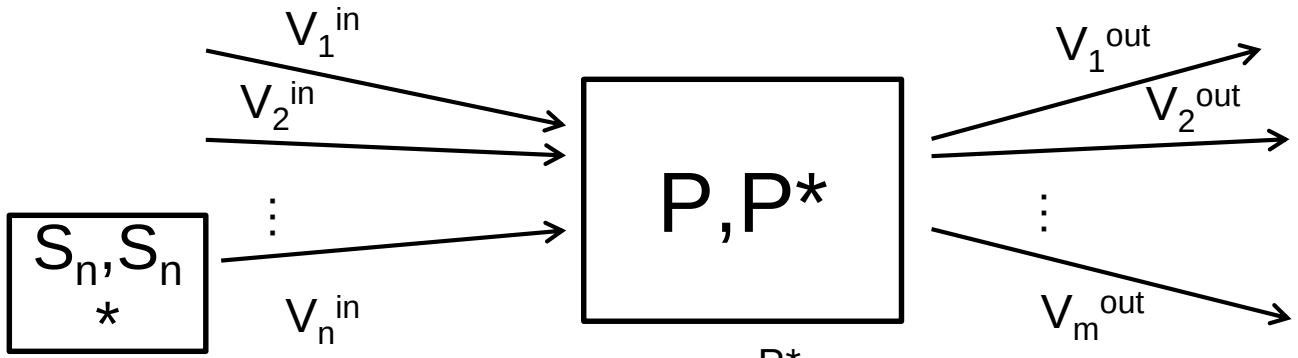

Mass balance equation: $\frac{dP(t)}{dt} = \sum_i V_i^{in} - \sum_j V_j^{out}$ at metabolic steady-state

Labelling equation : $\frac{dP^*(t)}{dt} = \sum_i V_i^{in} \cdot \underbrace{\frac{S_i^*(t)}{S}}_{\textbf{FE}} - \sum_j V_j^{out} \cdot \underbrace{\frac{P^*(t)}{P}}_{\textbf{FE}}$

In compartment modelling of PET data :

$$\frac{dP^*(t)}{dt} = \sum_i K_i^{in} \cdot S_i^*(t) - \sum_j K_j^{out} \cdot P^*(t) \qquad \text{with } K_i^{in} = \frac{V_i^{in}}{S} \text{ and } K_j^{out} = \frac{V_j^{out}}{P}$$

MATHEMATICAL PRINCIPLES OF COMPARTMENTAL MODELLING

The measurement of the substrate concentration:

The arterial input function (AIF)

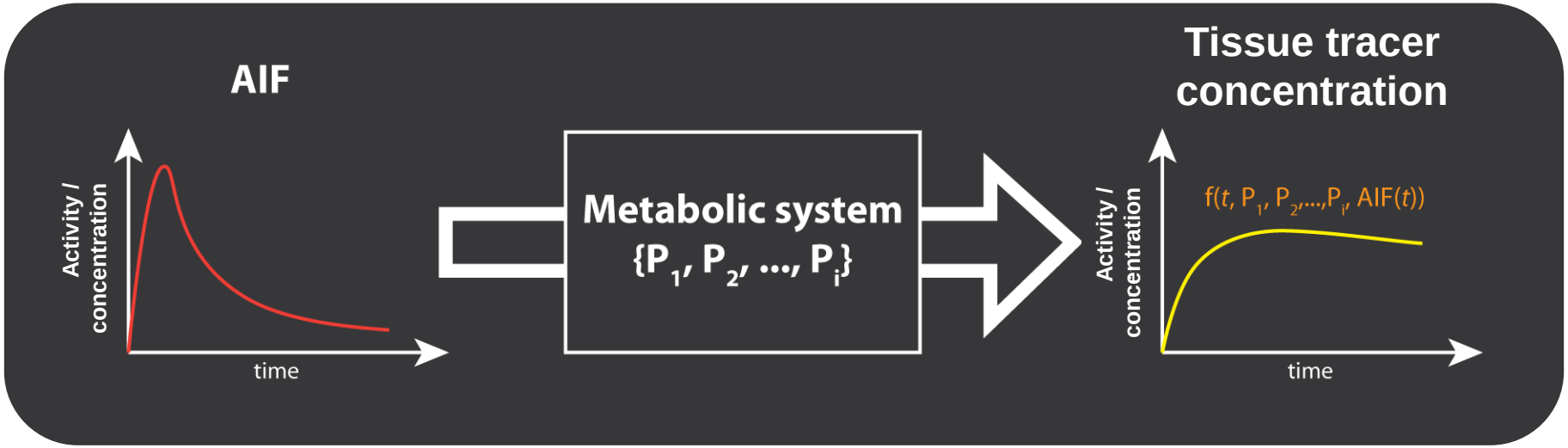

The AIF needs to be measured continuously over the entire infusion period or

The infusion protocol is designed to reach a desired input function.

SIMPLE ONE-PRODUCT POOL EXAMPLE

The labelling equations:

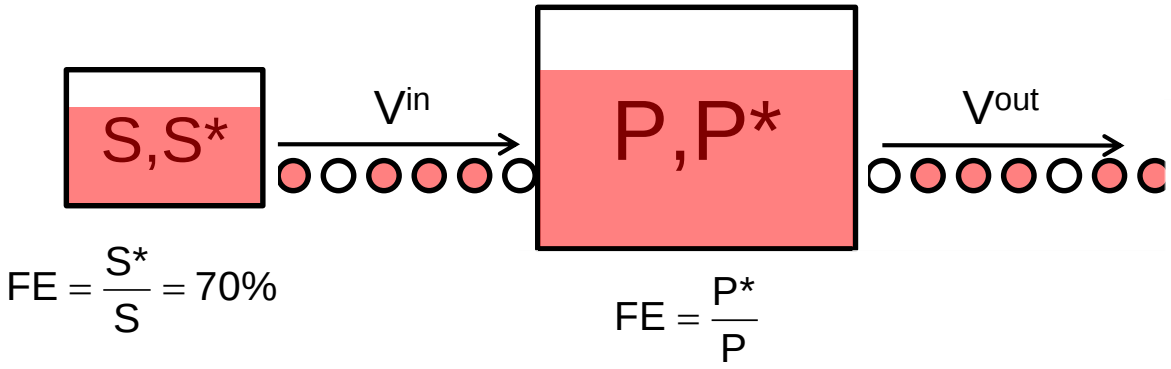

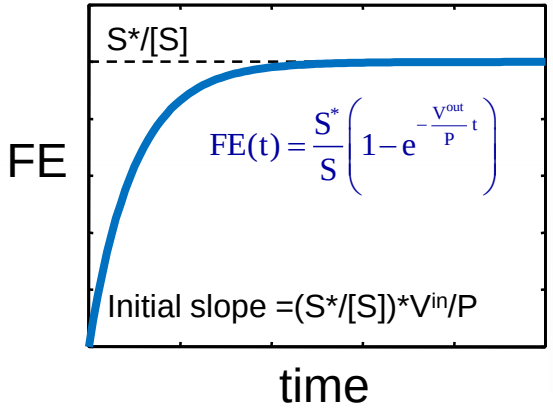

Mass balance equation : $\frac{dP(t)}{dt} = V^{in} - V^{out} = 0$ (metabolic steady-state)

Labelling equation : $\frac{dP^*(t)}{dt} = V^{in} \cdot \frac{S^*(t)}{S} - V^{out} \cdot \frac{P^*(t)}{P}$

(we assume $P^*(0) = 0$)

SIMPLE ONE-PRODUCT POOL EXAMPLE

The labelling equations:

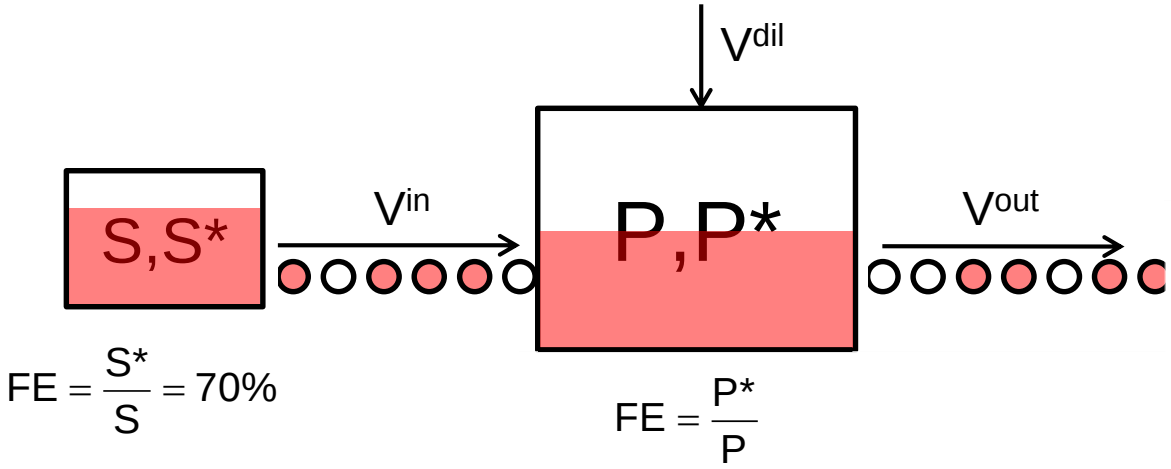

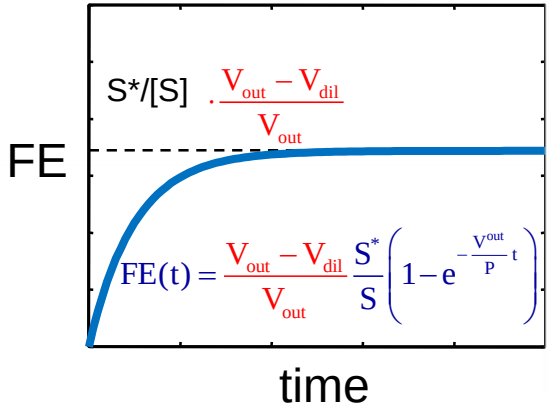

$$\begin{cases} \text{Mass balance equation :} & \dfrac{dP(t)}{dt} = V^{in} + V^{dil} - V^{out} = 0 \qquad \text{(metabolic steady-state)} \\ \text{Labelling equation :} & \dfrac{dP^*(t)}{dt} = V^{in} \cdot \dfrac{S^*(t)}{S} - V^{out} \cdot \dfrac{P^*(t)}{P} \end{cases}$$

(we assume $P^*(0) = 0$)

MATHEMATICAL PRINCIPLES OF COMPARTMENTAL MODELLING

General equations for a compartmental model:

Mass balance equation :

$$\frac{d}{dt}\begin{pmatrix} P_1(t) \\ P_2(t) \\ \dots \\ P_n(t) \end{pmatrix} = \begin{pmatrix} V_{S1} & V_{21} & \dots & V_{n1} \\ V_{S2} & V_{22} & \dots & V_{n2} \\ \dots & \dots & \dots & \dots \\ V_{Sn} & V_{2n} & \dots & V_{nn} \end{pmatrix} \begin{pmatrix} 1 \\ 1 \\ \dots \\ 1 \end{pmatrix} \overset{\text{(metabolic steady-state)}}{=} \begin{pmatrix} 0 \\ 0 \\ \dots \\ 0 \end{pmatrix}$$

Labelling equation :

$$\frac{d}{dt}\begin{pmatrix} P_1^*(t) \\ P_2^*(t) \\ \dots \\ P_n^*(t) \end{pmatrix} = \begin{pmatrix} V_{S1} & V_{21} & \dots & V_{n1} \\ V_{S2} & V_{22} & \dots & V_{n2} \\ \dots & \dots & \dots & \dots \\ V_{Sn} & V_{2n} & \dots & V_{nn} \end{pmatrix} \begin{pmatrix} S^*(t)/[S] \\ P_2^*(t)/[P_2] \\ \dots \\ P_n^*(t)/[P_n] \end{pmatrix}$$

System of linear differential equations with constant coefficients

Numerical solutions

EXTRACTING METABOLIC PARAMETERS FROM THE EXPERIMENTAL DATA

- The mathematics needed in metabolic modelling can be schematically separated into two steps.

  - The first is to find a general solution to the set of equations that describes the biochemical model
  - The second is to find the particular set of model parameters that describe the observation.

→ REGRESSION

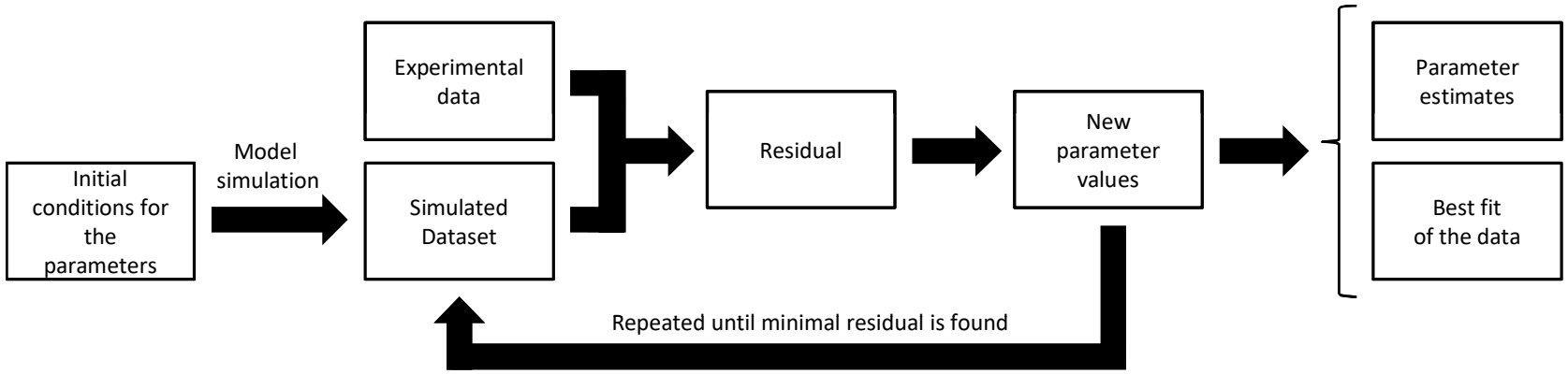

REGRESSION

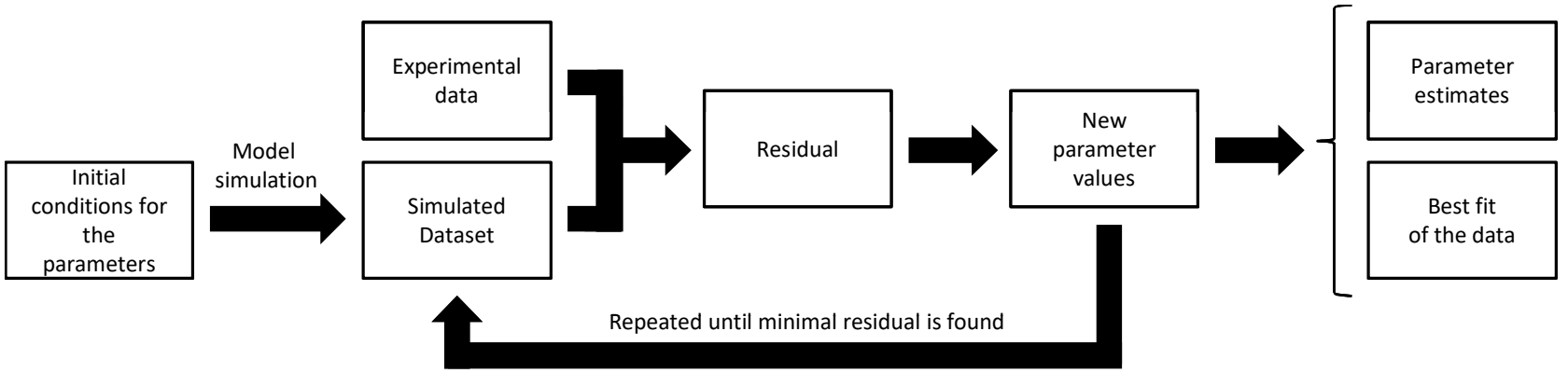

- A metabolic model is designed to explain the experimental observations and gives a number *j* of output functions *f* that describe the *j* dynamic datasets obtained from the measurement:

$$f_j(a_1, a_2, ..., a_m, t)$$

- The most common measurement of proximity of the data and simulation is the least-squares criterion:

$$WRSS = \sum_{j=1}^{J} \sum_{i=1}^{n} w_j \left[y_j(t_i) - f_j(a_1, a_2, ..., a_m, t_i) \right]^2$$

where $y_j(t_i)$ are the *i* sampling points of the *j*th uptake curve,

w_j the relative weight of the *j*th curve in the regression. (typically, $w_j = 1/Var_j$)

BASIC PRINCIPLES OF NON-LINEAR REGRESSION

PARAMETER PRECISION AND CORRELATION

- The precision of the parameter estimation can be estimated by error propagation from the regression in terms of the covariance matrix :

$$\boldsymbol{Cov}(\hat{\boldsymbol{a}}) = \begin{pmatrix} Var(\hat{a}_1) & Cov(\hat{a}_1,\hat{a}_2) & \dots & Cov(\hat{a}_1,\hat{a}_m) \\ Cov(\hat{a}_2,\hat{a}_1) & Var(\hat{a}_2) & \dots & Cov(\hat{a}_2,\hat{a}_m) \\ \dots & \dots & \dots & \dots \\ Cov(\hat{a}_m,\hat{a}_1) & Cov(\hat{a}_m,\hat{a}_2) & \dots & Var(\hat{a}_m) \end{pmatrix}$$

where $\hat{a}_1$, $\hat{a}_2$, …, are the optimized parameters of the system (metabolic fluxes)

Cobelli C., Foster D. and Toffolo G. (2000)
Tracer kinetics in biomedical research: from data to model, Vol. 1. Kluwer Academic/Plenum.

PARAMETER PRECISION AND CORRELATION

Similarly the correlation matrix of the parameters can be extracted

$$\boldsymbol{Corr}(\hat{\boldsymbol{a}}) = \begin{pmatrix} 1 & \frac{Cov(\hat{a}_1,\hat{a}_2)}{SD(\hat{a}_1)\,SD(\hat{a}_2)} & \dots & \frac{Cov(\hat{a}_1,\hat{a}_m)}{SD(\hat{a}_1)\,SD(\hat{a}_m)} \\ \frac{Cov(\hat{a}_2,\hat{a}_1)}{SD(\hat{a}_2)\,SD(\hat{a}_1)} & 1 & \dots & \frac{Cov(\hat{a}_2,\hat{a}_m)}{SD(\hat{a}_2)\,SD(\hat{a}_m)} \\ \dots & \dots & \dots & \dots \\ \frac{Cov(\hat{a}_m,\hat{a}_1)}{SD(\hat{a}_m)\,SD(\hat{a}_1)} & \frac{Cov(\hat{a}_m,\hat{a}_2)}{SD(\hat{a}_m)\,SD(\hat{a}_2)} & \dots & 1 \end{pmatrix}$$

BASIC PRINCIPLES OF NON-LINEAR REGRESSION

PARAMETER PRECISION AND CORRELATION

- Non-linearity of the system (model)
  -> Sometimes, small effects on the noise of the data can have huge impact on the estimated parameters

- An alternative method to evaluate the precision and correlation of the model parameters is Monte Carlo simulation

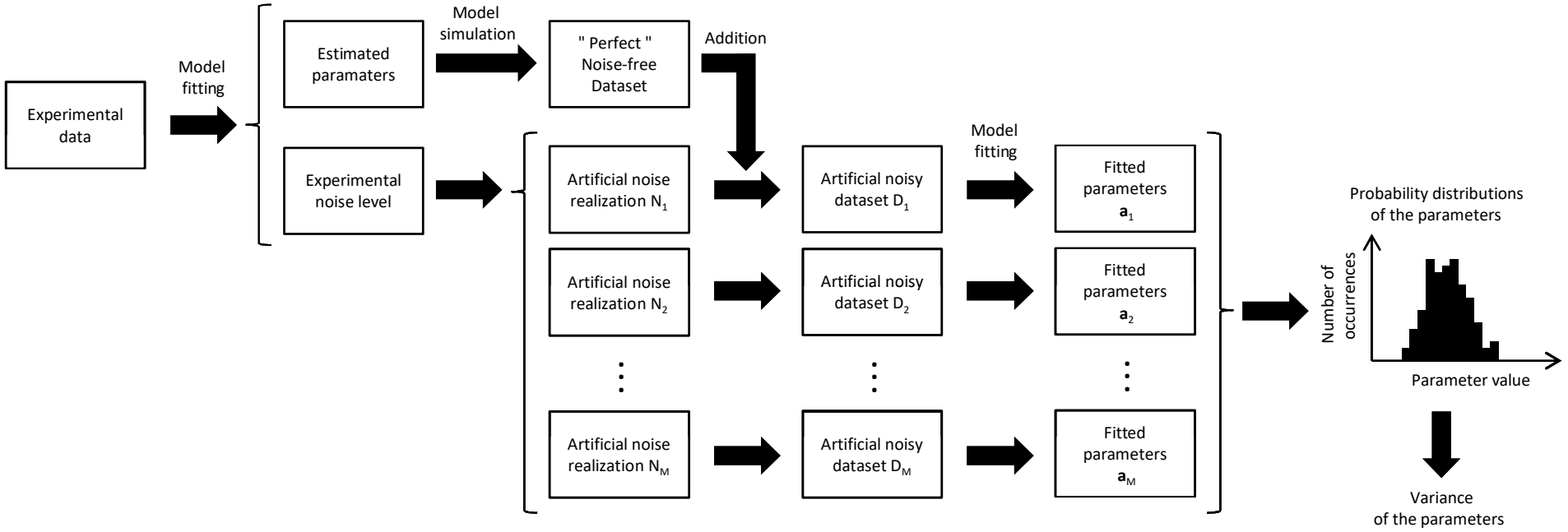

WARNINGS

- Although many optimized algorithm have been developed for non-linear regression, it is in practice never possible to be completely sure that the found optimum is a global minimum.

- The fact that the model functions fit the experimental data is necessary, but not sufficient.
  - Precision of the model parameters
    (sensitivity of the measurement to the given parameters)
  - Correlation between the parameters
    (close to ± 1 → parameters not individually identifiable)

- A compartmental model is therefore as good as the assumptions that are incorporated in it.

BIOCHEMICAL MOTIVATIONS

Brain energy metabolism

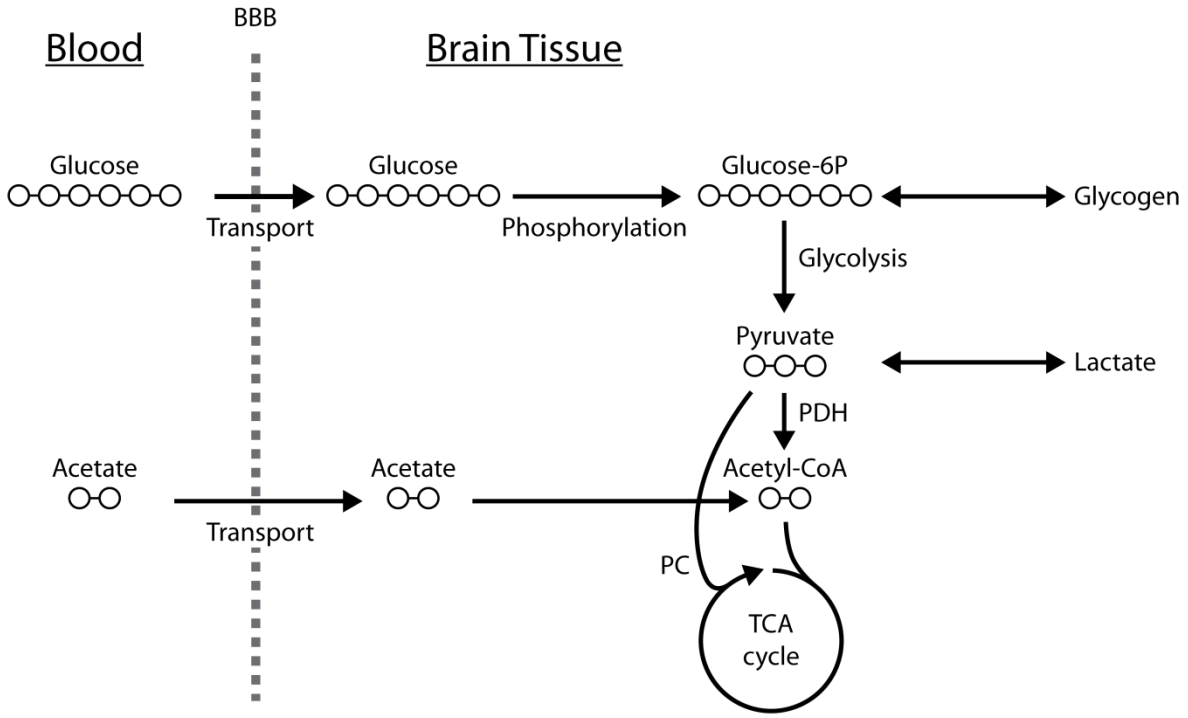

In vivo ^{13}C NMR spectroscopy:

- ^{13}C natural abundance is only 1.1%
- ^{13}C can be used as a tracer by infusing ^{13}C-enriched substrates

BRAIN ENERGY METABOLISM STUDIED WITH ^{13}C MRS

THE TRACER: [1,6-^{13}C] GLUCOSE OR [1-^{13}C] GLUCOSE

[1,6-^{13}C] glucose

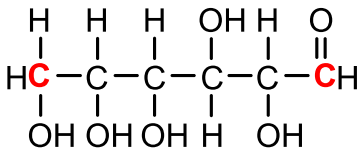

Glycolysis

2 x more enrichment

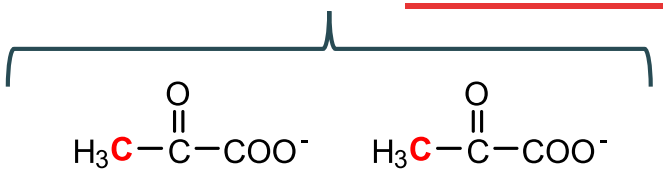

Pyruvate Pyruvate

TCA cycle,
Lactate metabolism

[1-^{13}C] glucose

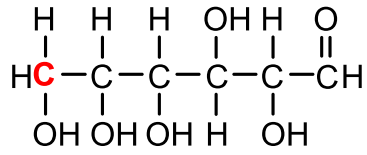

Glycolysis

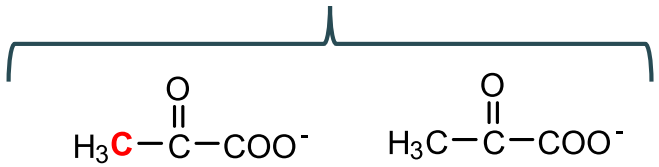

Pyruvate Pyruvate

TCA cycle,
Lactate metabolism

BRAIN ENERGY METABOLISM STUDIED WITH ^{13}C MRS

TCA CYCLE METABOLISM OF [1,6-^{13}C] GLUCOSE

Neuronal TCA cycle (1st turn)

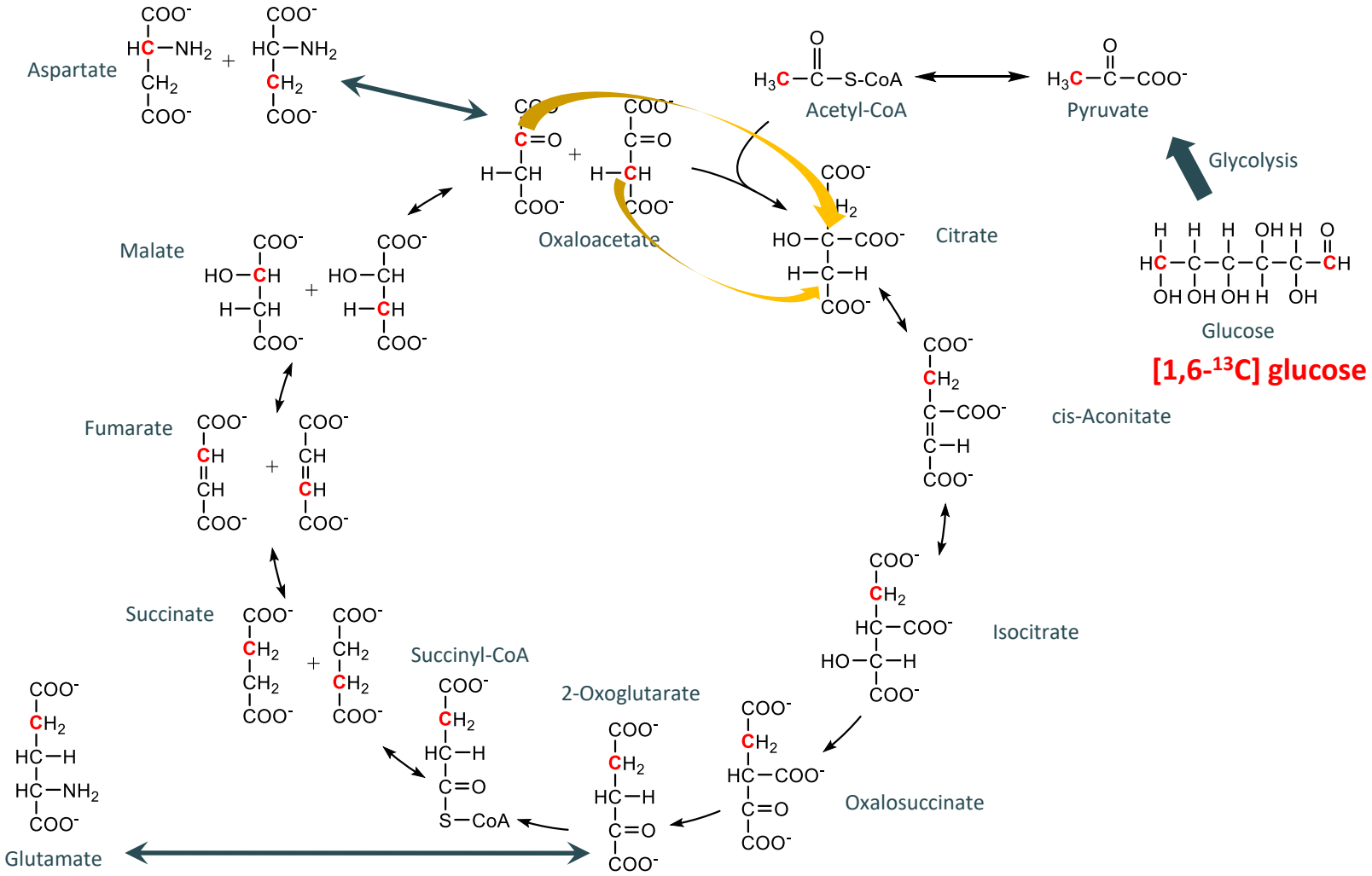

BRAIN ENERGY METABOLISM STUDIED WITH ^{13}C MRS

TCA CYCLE METABOLISM OF [1,6-^{13}C] GLUCOSE

Neuronal TCA cycle (2nd turn)

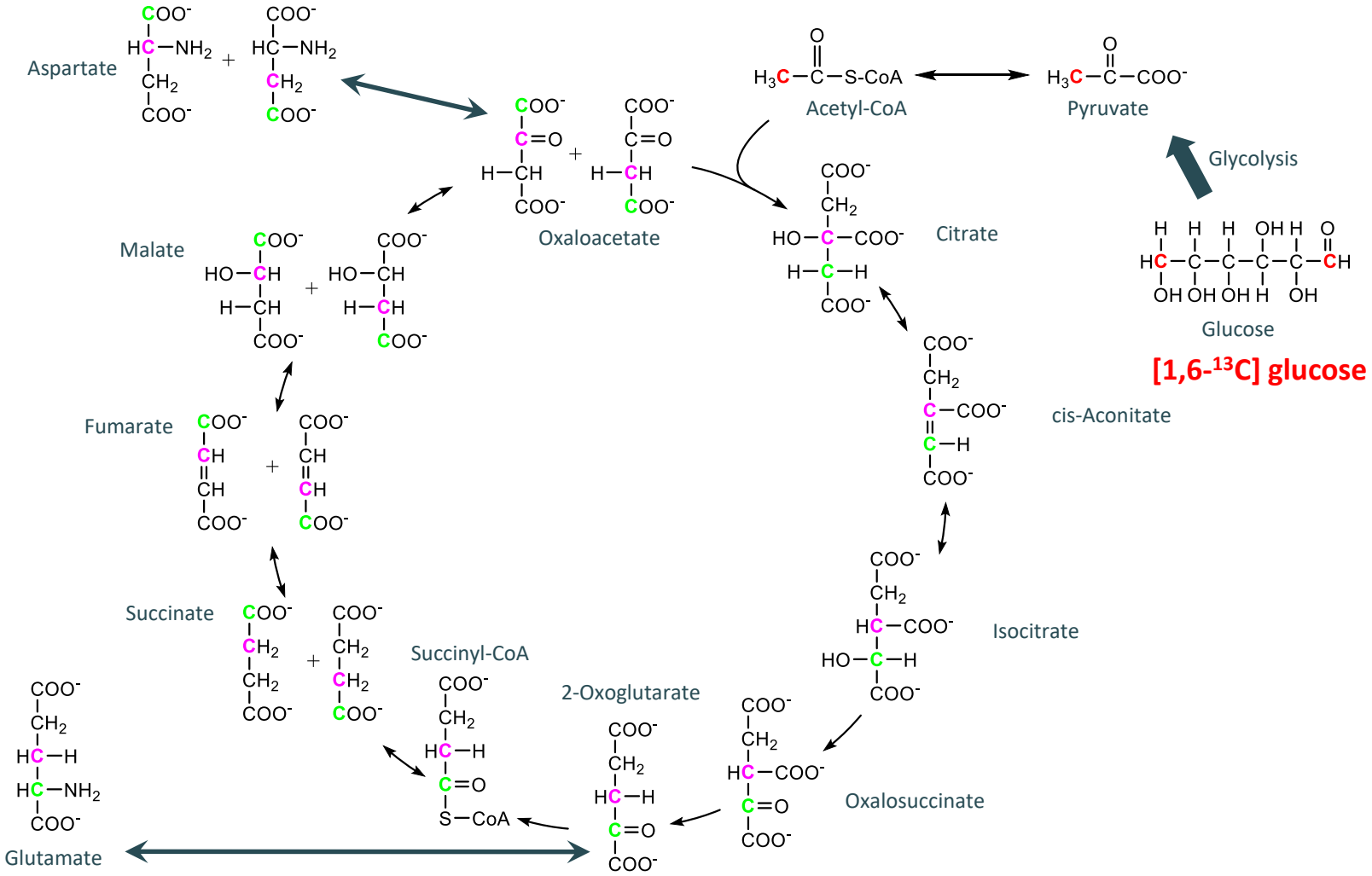

BRAIN ENERGY METABOLISM STUDIED WITH ^{13}C MRS

TCA CYCLE METABOLISM OF [1,6-^{13}C] GLUCOSE

Glial-specific reaction

- *pyruvate carboxylase*

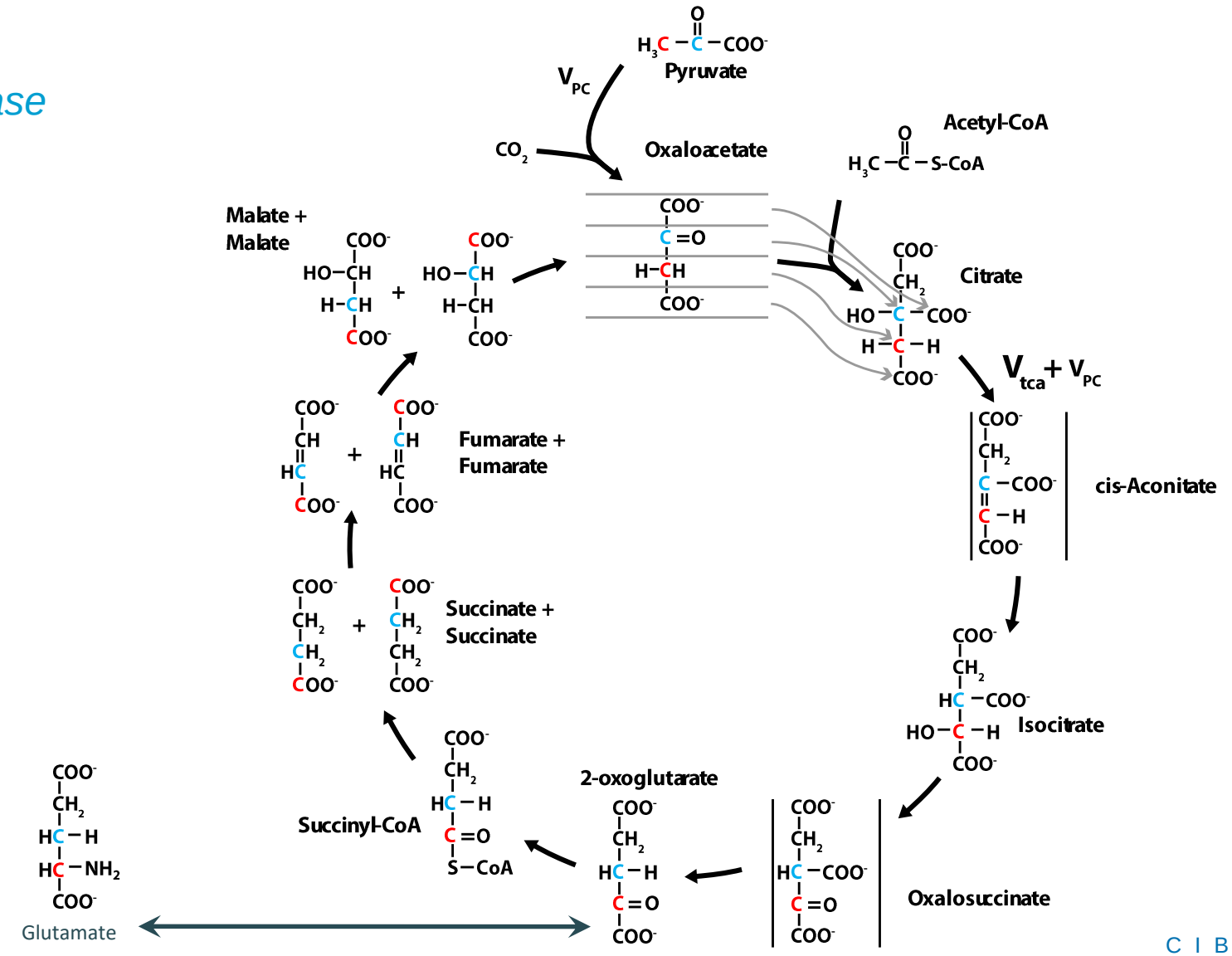

BRAIN ENERGY METABOLISM STUDIED WITH ^{13}C MRS

the two-compartment model

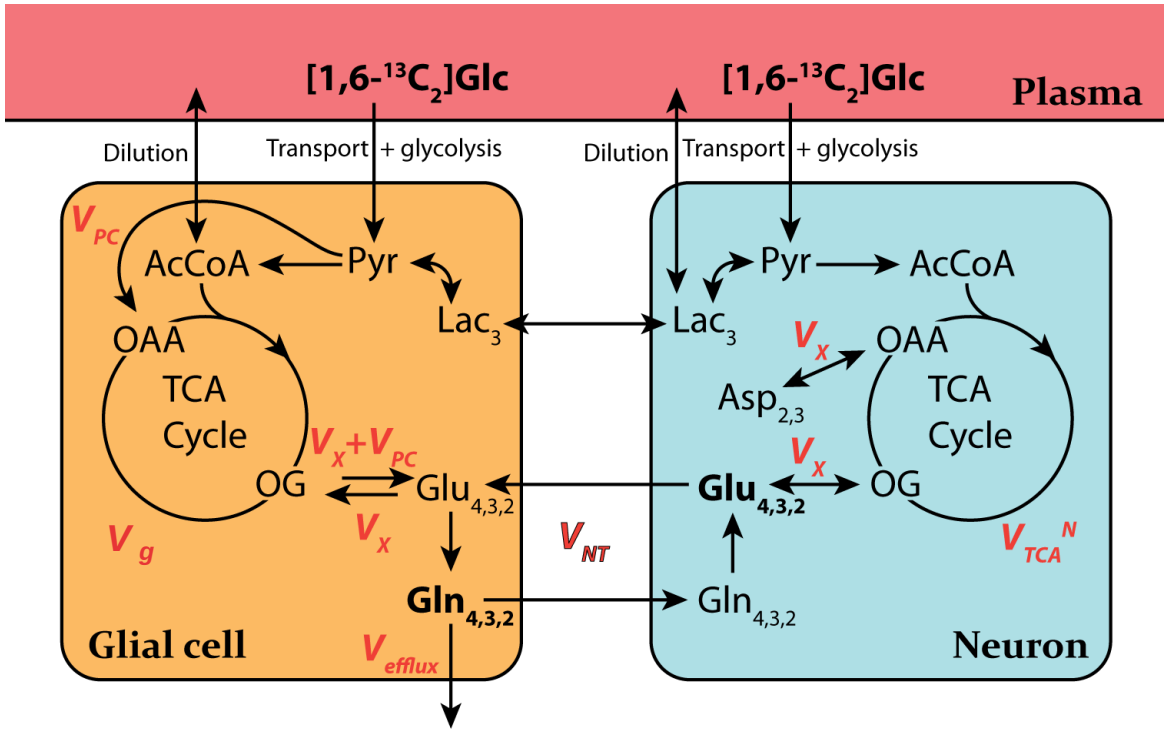

In ^{13}C MRS, the metabolites with sufficient concentration are measured (> 1mM)

→ **Glu, Gln, Asp and Lac**

[1] Gruetter et al., *Am. J. Physiol. Endocrinol. Metab.*, 2001

[2] Sibson et al., *J. Neurochem.* , 2001

TWO-COMPARTMENT MODELING

OF [1,6-13C] GLUCOSE BRAIN METABOLISM

1st TCA cycle turn labeling :

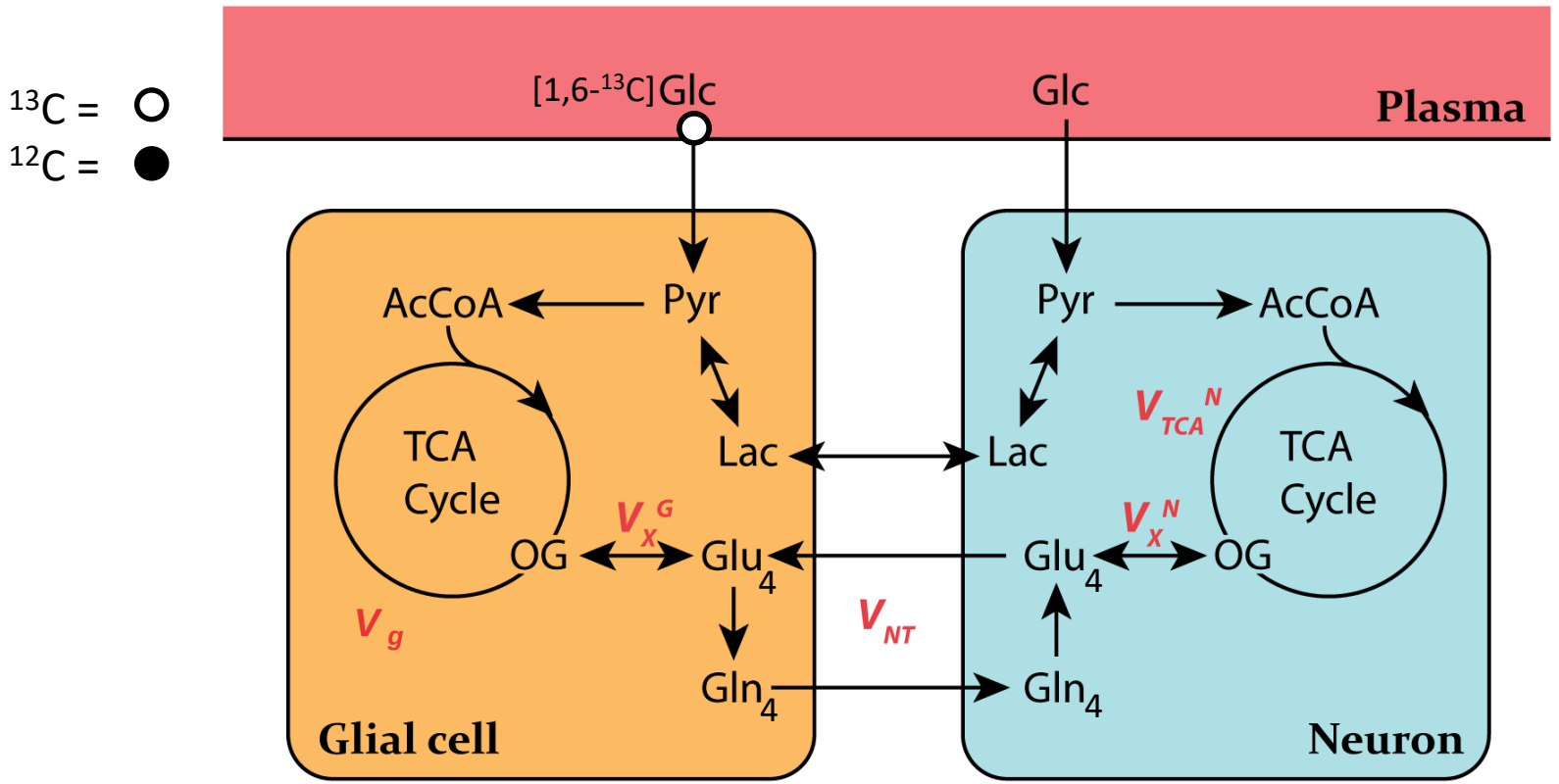

TWO-COMPARTMENT MODELING

OF [1,6-13C] GLUCOSE BRAIN METABOLISM

2nd TCA cycle turn labeling :

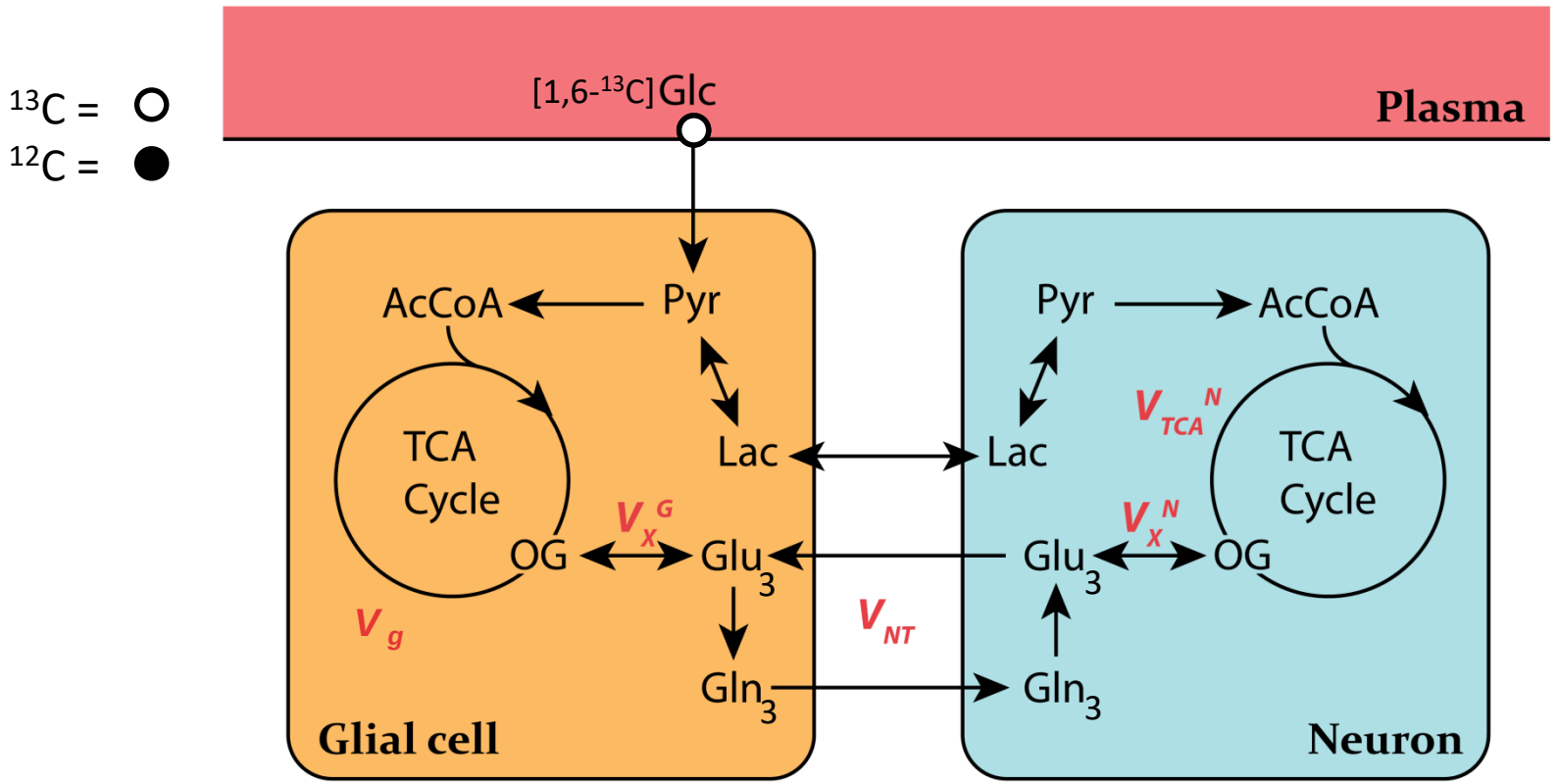

TWO-COMPARTMENT MODELING

OF [1,6-13C] GLUCOSE BRAIN METABOLISM

2nd TCA cycle turn labeling :

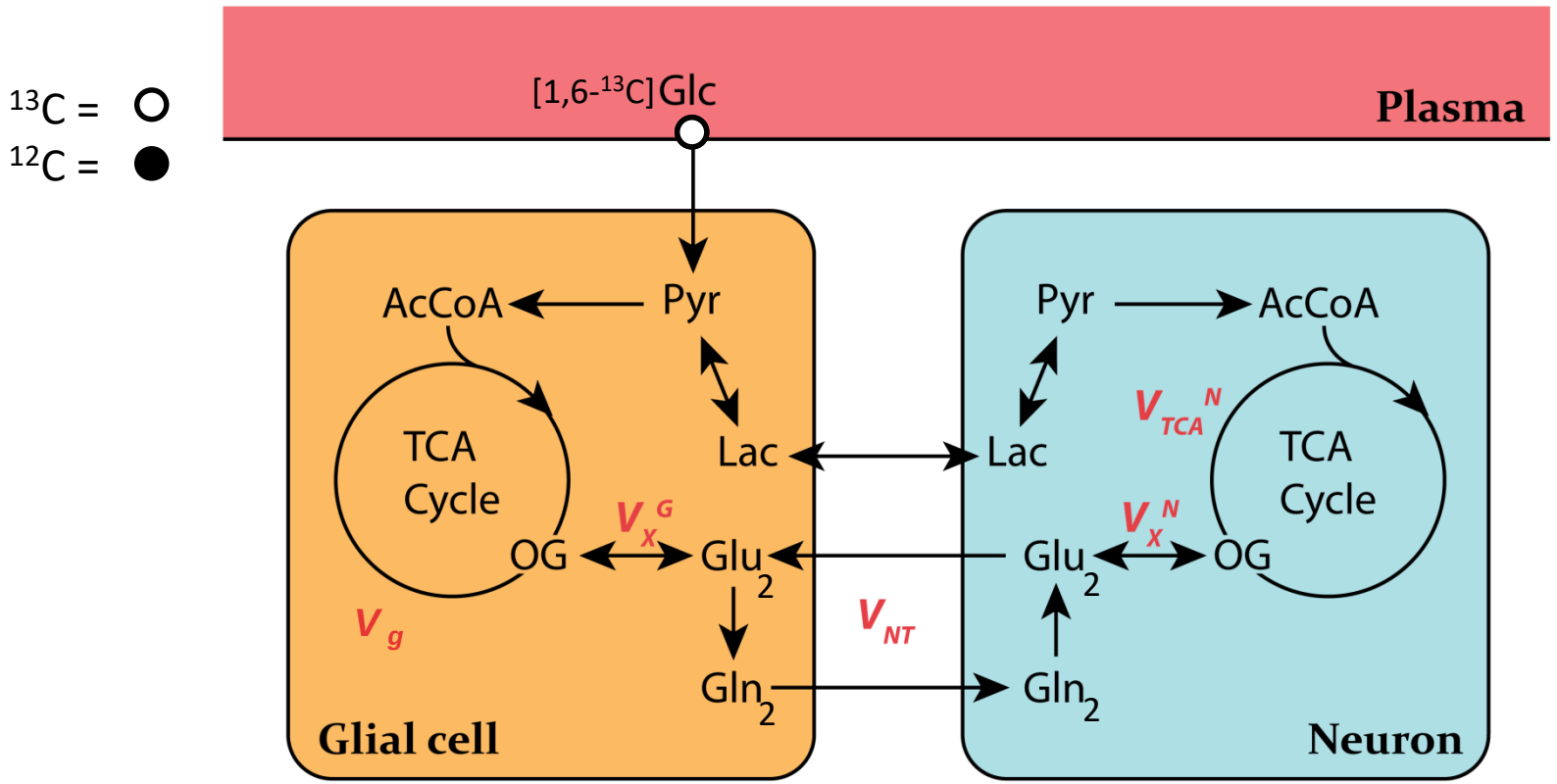

TWO-COMPARTMENT MODELING

OF [1,6-13C] GLUCOSE BRAIN METABOLISM

Dilution through PC:

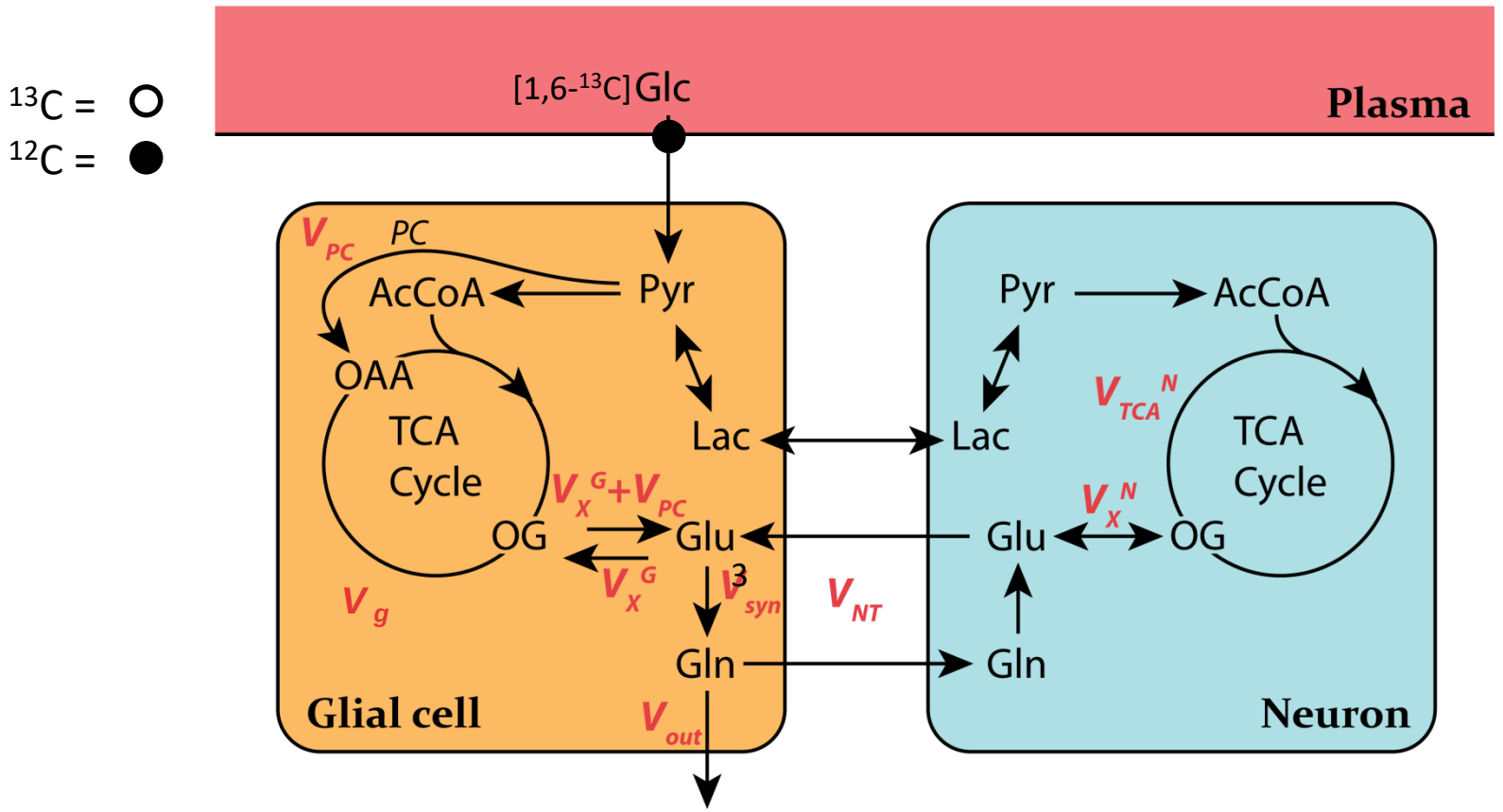

TWO-COMPARTMENT MODELING

OF [1,6-13C] GLUCOSE BRAIN METABOLISM

Labelling through PC:

Separate measurement of the C3 and C2 positions of Glu and Gln is required for a complete description of the 2-compartment model.

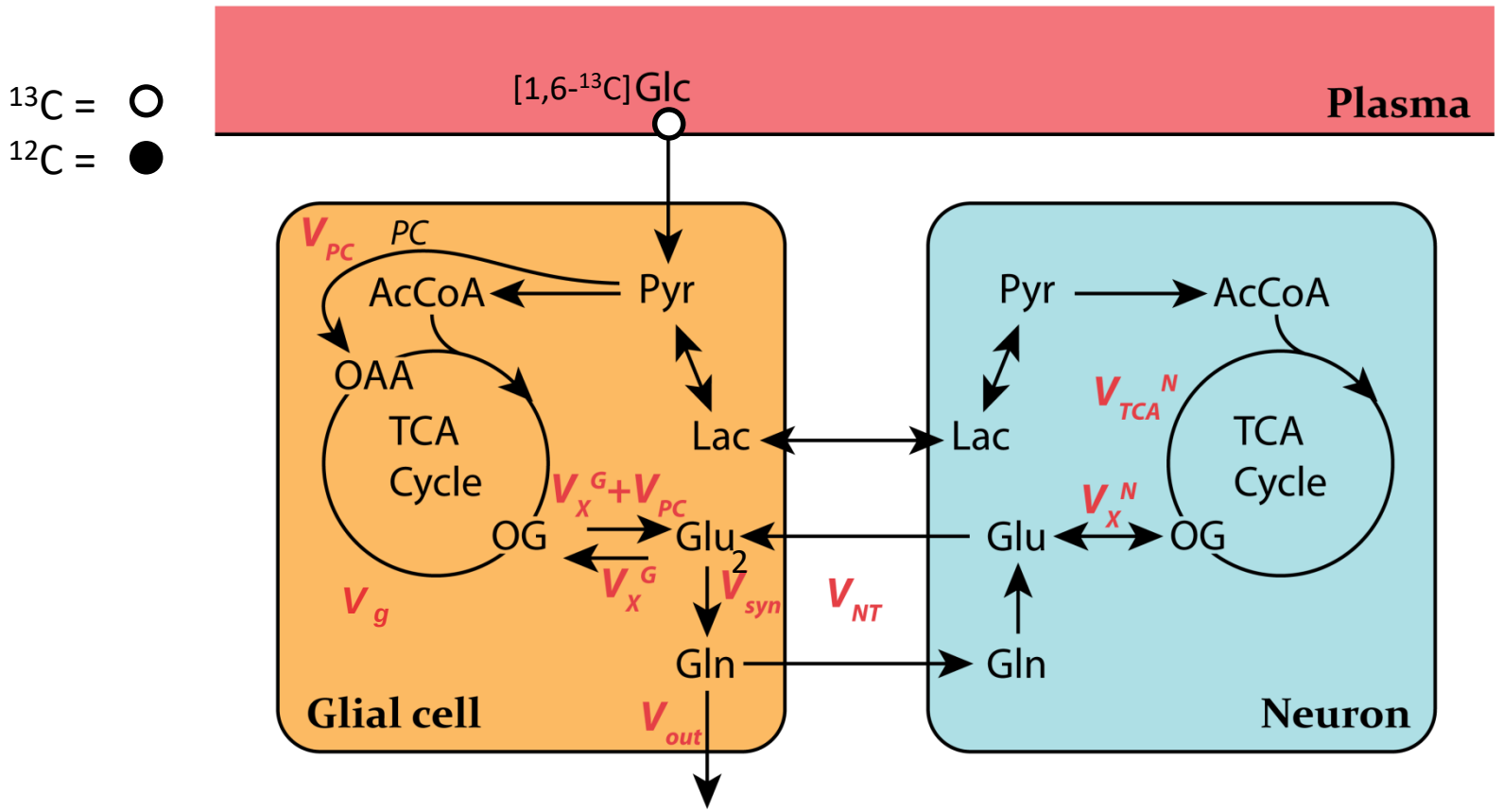

TWO-COMPARTMENT MODELLING OF BRAIN GLUCOSE METABOLISM

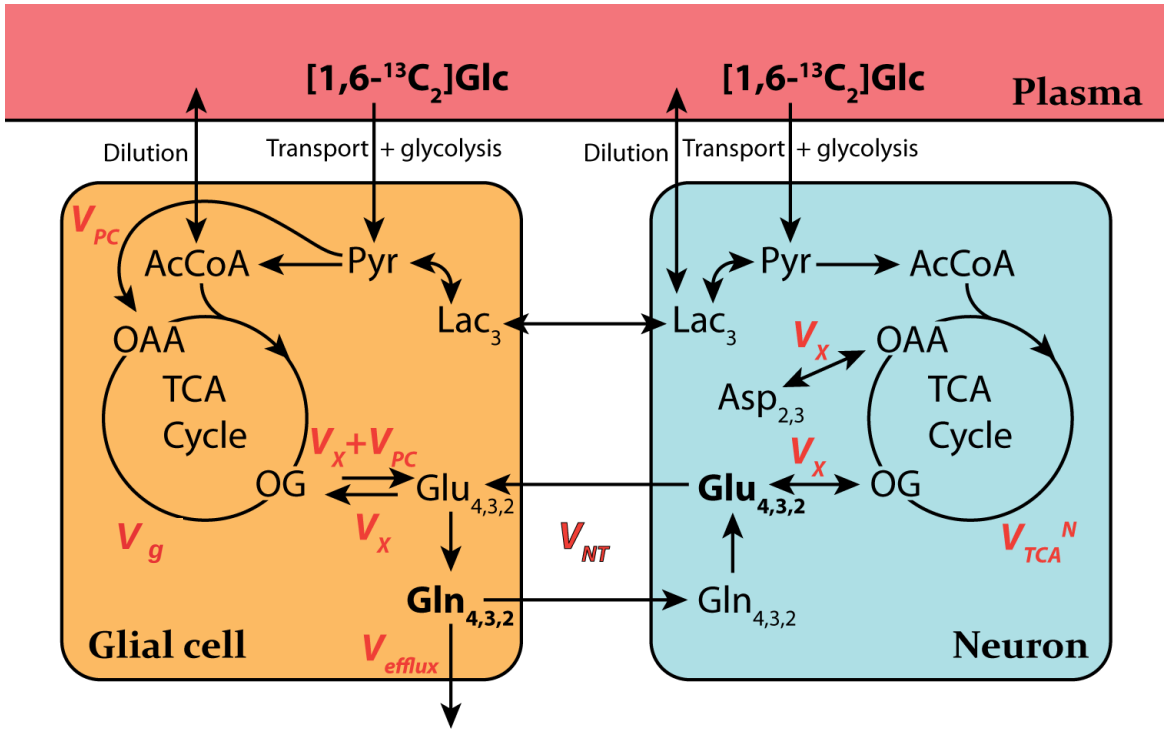

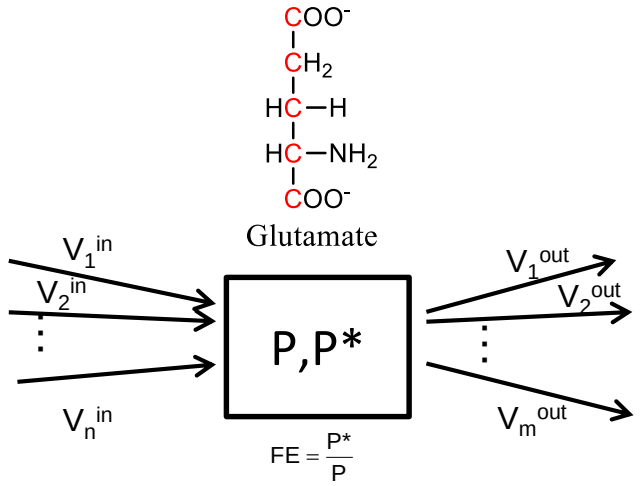

$$\frac{dP(t)}{dt} = \sum_i V_i^{in} - \sum_j V_j^{out} = 0$$

$$\frac{dP^*(t)}{dt} = \sum_i V_i^{in} \cdot \frac{S_i^*(t)}{S} - \sum_j V_j^{out} \cdot \frac{P^*(t)}{P}$$

In ^{13}C MRS, the metabolites with sufficient concentration are measured (> 1mM)

→ **Glu, Gln, Asp and Lac**

Each labelling position is described by a mass balance equation and a labelling equation

[1] Duarte et al., *Front. Neuroenerg.* , 2011

[2] Lanz et al., *J. Neurochem.* , 2013

[1,6-$^{13}C_2$] GLUCOSE DYNAMIC MRS STUDIES

METHODS

Experimental protocol:

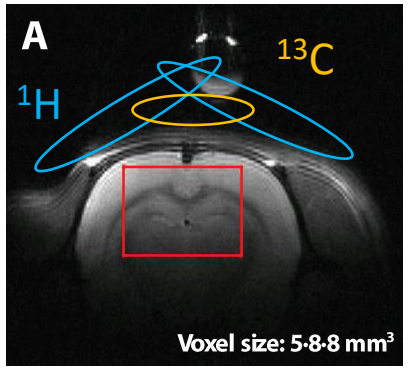

- Fasted Sprague-Dawley rats (n=6) anesthetized with alpha-chloralose infusion
- A bolus of 99% enriched [1,6-$^{13}C_2$] glucose is given over a 5 min period (based on the measured basal glycemia) and followed by constant infusion of 70% enriched [1,6-$^{13}C_2$] glucose
- Generates a « step function » shaped glucose fractional enrichment in blood (FE=70%)
- Saturate glucose transport

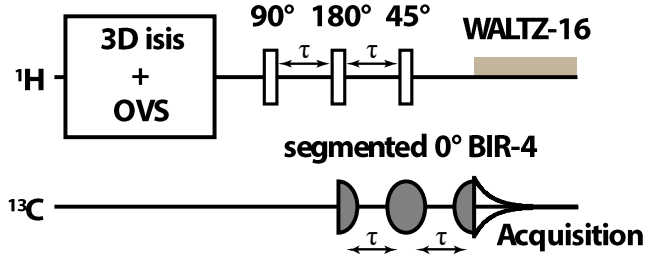

Localized DEPT

with $\tau = 1/2J_{CH}$

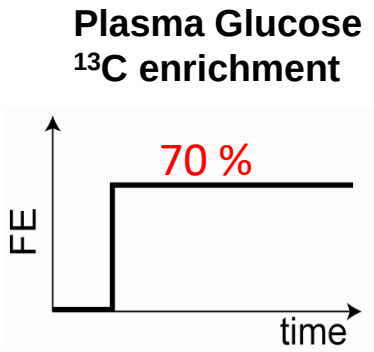

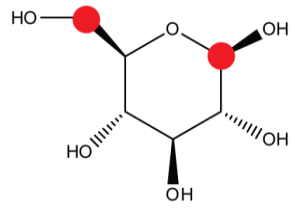

[1,6-^{13}C]Glucose

[1,6-$^{13}C_2$] GLUCOSE DYNAMIC MRS STUDIES

METHODS

Workflow:

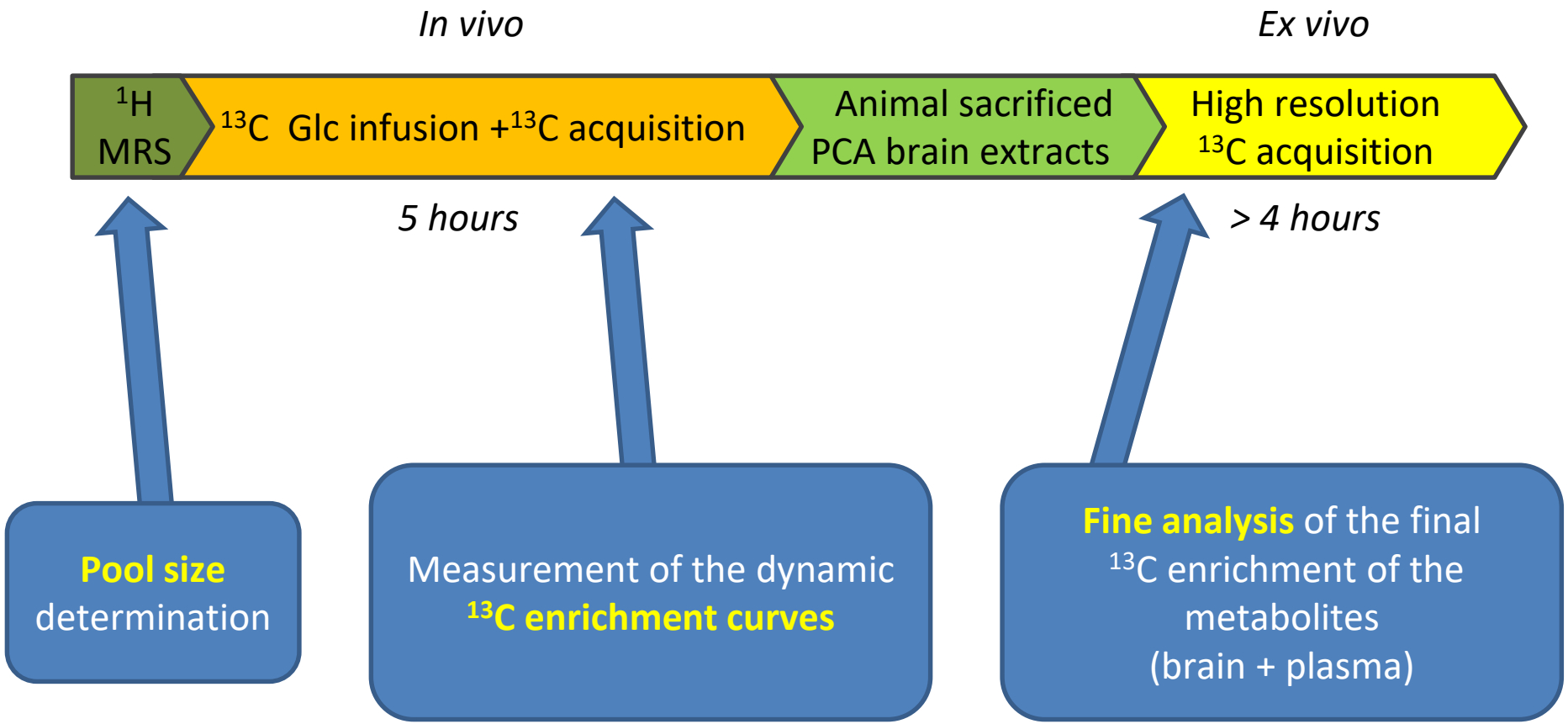

[1,6-$^{13}C_2$] GLUCOSE DYNAMIC MRS STUDIES

METHODS

→ separate measurement of the labeling turnover:

In glutamate :

GluC4
GluC3
GluC2

In glutamine :

GlnC4
GlnC3
GlnC2

In aspartate:

AspC3
AspC2

(time resol.= 5.3 min)

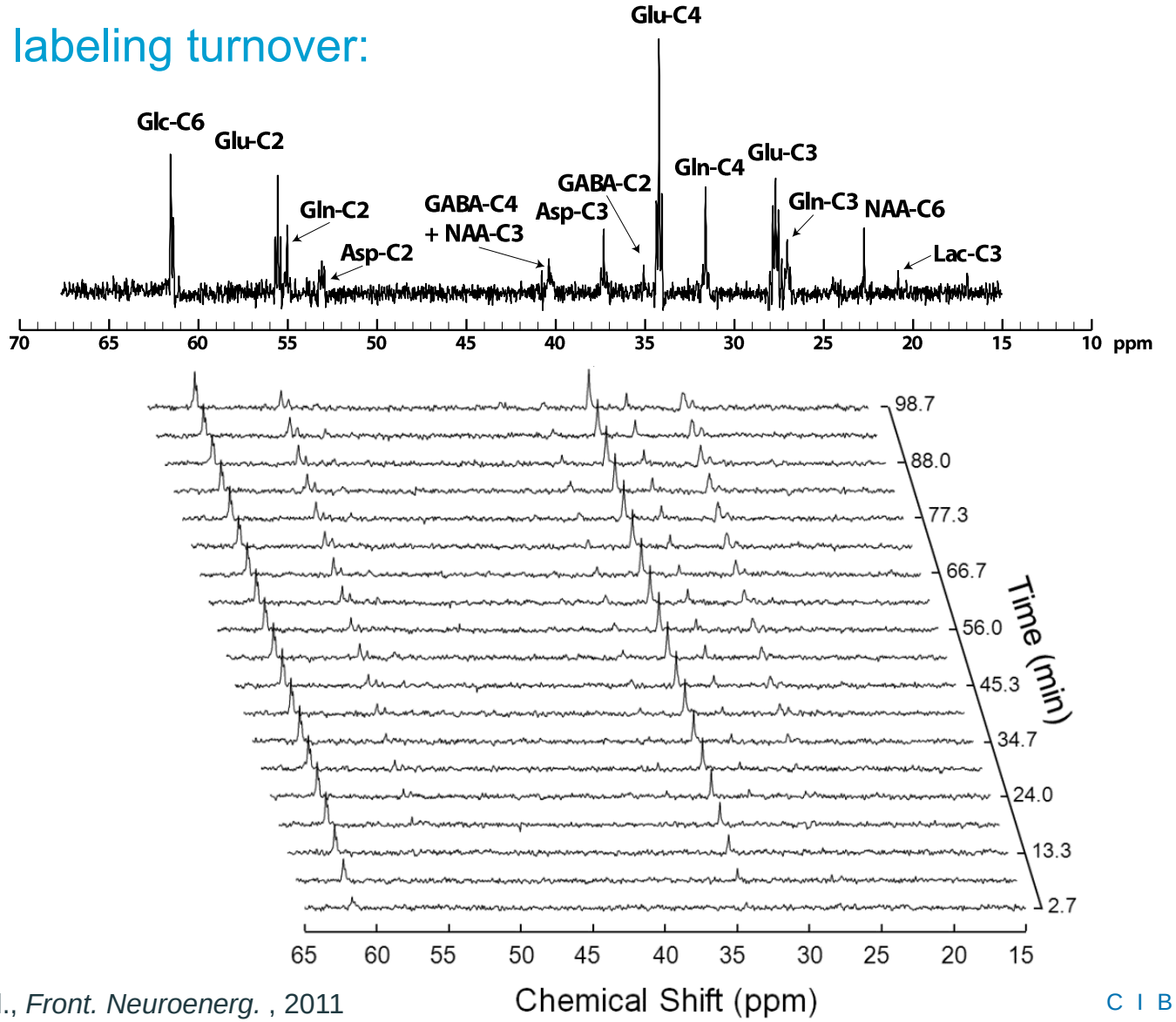

Duarte et al., *Front. Neuroenerg.* , 2011

[1,6-^{13}C] GLUCOSE DYNAMIC MRS STUDIES AT 14T

METHODS

Results :

Two-compartmental model fitted to the experimental turnover curves.

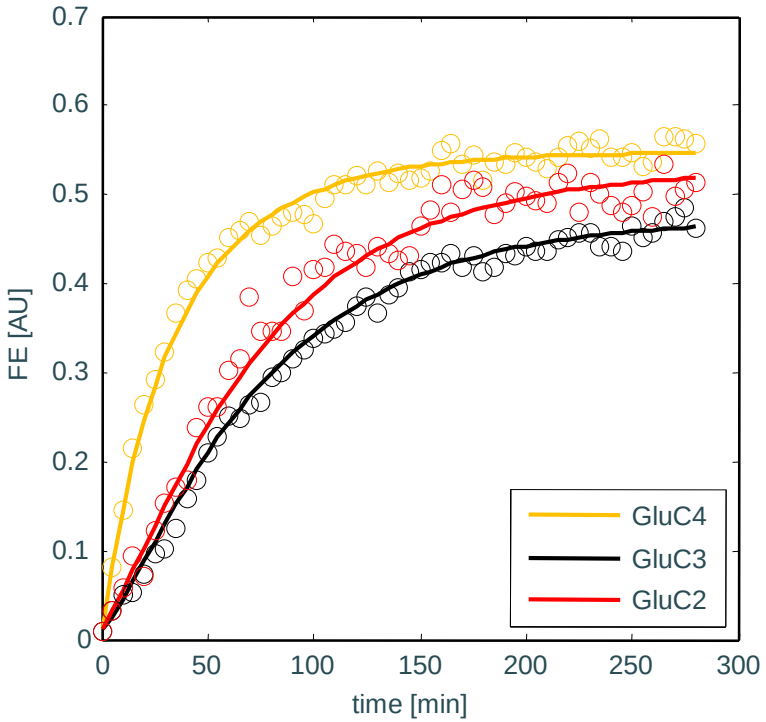

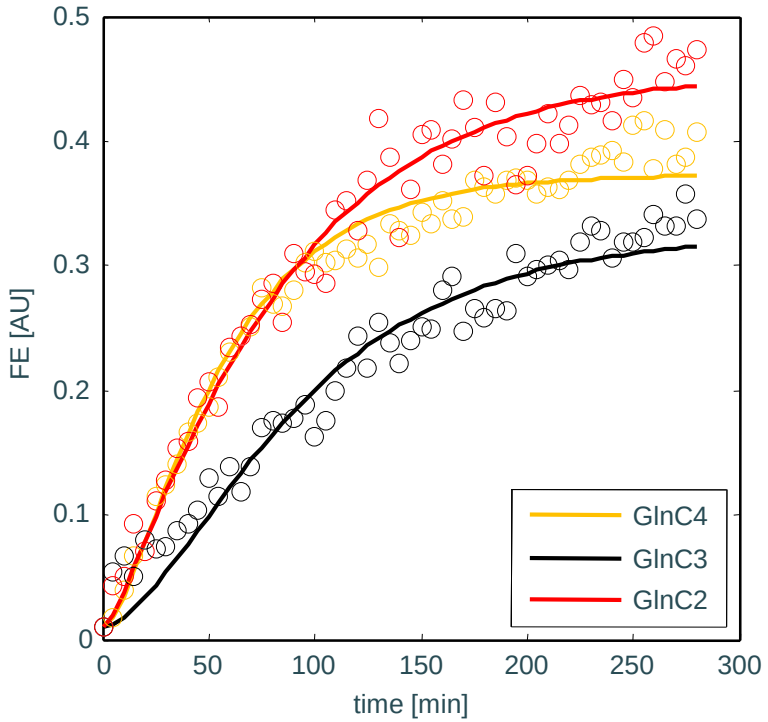

V_g	0.23	+-	0.02
V_x^g	0.17	+-	0.06
V_{nt}	0.12	+-	0.01
V_{tca}^n	0.44	+-	0.01
V_x^n	0.76	+-	0.07
V_{pc}	0.07	+-	0.01

[µmol/g/min]

Duarte et al., *Front. Neuroenerg.* , 2011

TWO-COMPARTMENT MODELLING

OF [1,6-^{13}C] GLUCOSE DYNAMIC MRS STUDIES AT 14T

Results :

Characterization of brain oxidative metabolism.

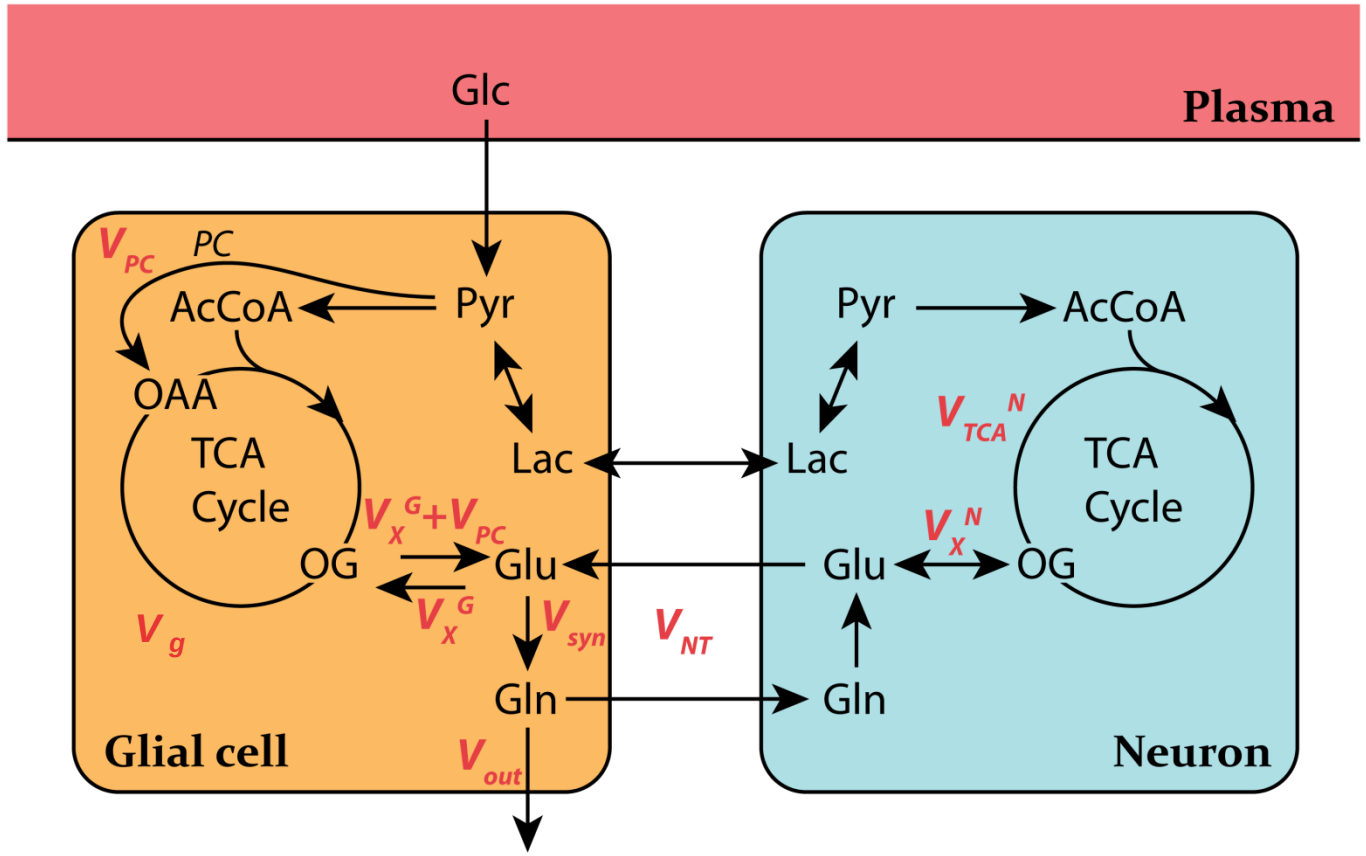

V_g	0.23	+-	0.02
V_x^g	0.17	+-	0.06
V_{nt}	0.12	+-	0.01
V_{tca}^n	0.44	+-	0.01
V_x^n	0.76	+-	0.07
V_{pc}	0.07	+-	0.01

[µmol/g/min]

EXTENSION OF IN VIVO ^{13}C STUDIES TO MICE

Rat (~270 g)
Blood volume ≈ 15 ml

Voxel 320 µL
5x8x8mm^3

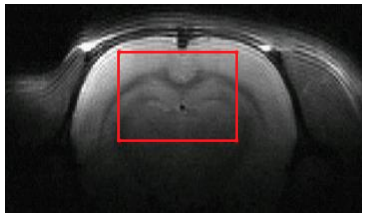

Mouse (~30 g)
Blood volume ≈ 2.5 ml

Voxel 112 µL
3.6x6.9x4.5mm^3

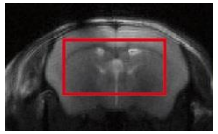

Additional difficulties in mice studies:

- smaller brain
  - smaller VOI and -> low SNR
  - Tissue inhomogeneities -> difficult B_0 shimming
- small blood volume
  - Blood sampling in the magnet almost impossible -> standardization of the input function or image-derived input function

CURRENT PROJECTS:

EXTENSION OF IN VIVO ^{13}C STUDIES TO MICE

Methods:

Animals and physiology:
- Nude male mice (8weeks old, 20-30g, n=3)
- 7 hours fasted
- Isoflurane anaesthesia (1-2%)

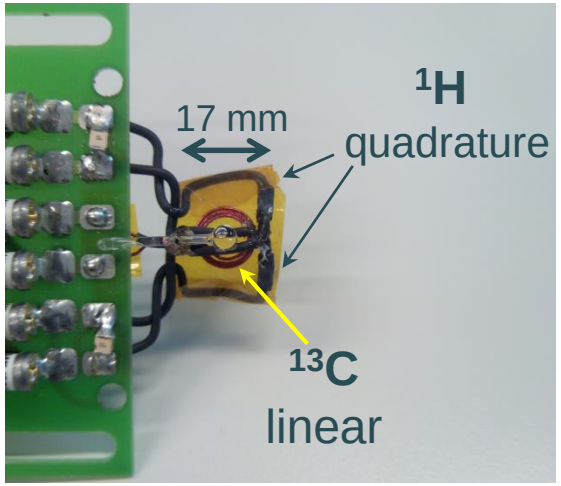

Infusion protocol (target FE = 70%, metabolic steady-state):
- Tail vein catheter
- 5 min exponential bolus of 99%-enriched [1,6-$^{13}C_2$] Glc
- 5 hours adjustable continuous infusion of 70%-enriched [1,6-$^{13}C_2$] Glc (target glycemia = 300mg/dL)

Data acquisition:
- Voxel 112µL
- 14.1 Tesla system (Varian/Magnex)
- Home-built surface coil
- Semi-adiabatic DEPT sequence

Lai et al., *JCBFM* , 2018

EXTENSION OF IN VIVO ^{13}C STUDIES TO MICE

Results:

Voxel 112µL
3.6x6.9x4.5mm^3

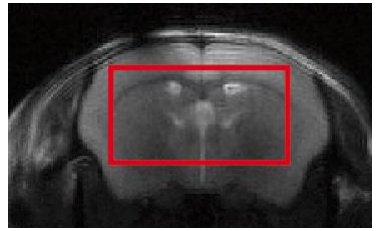

IN VIVO data
32min acq. after 4.5h infusion
SNR= 16

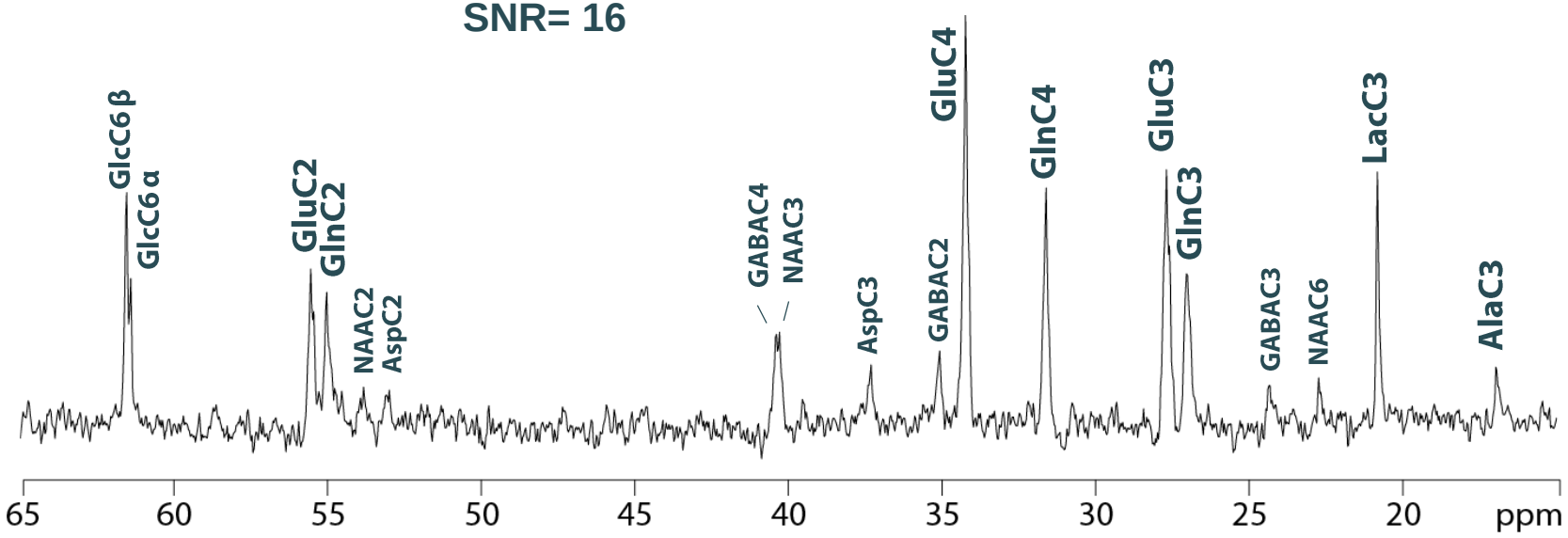

Lai et al., *JCBFM* , 2018

EXTENSION OF IN VIVO ^{13}C STUDIES TO MICE

Results:

Glutamate and **Glutamine**

(temp. resol = 10min):

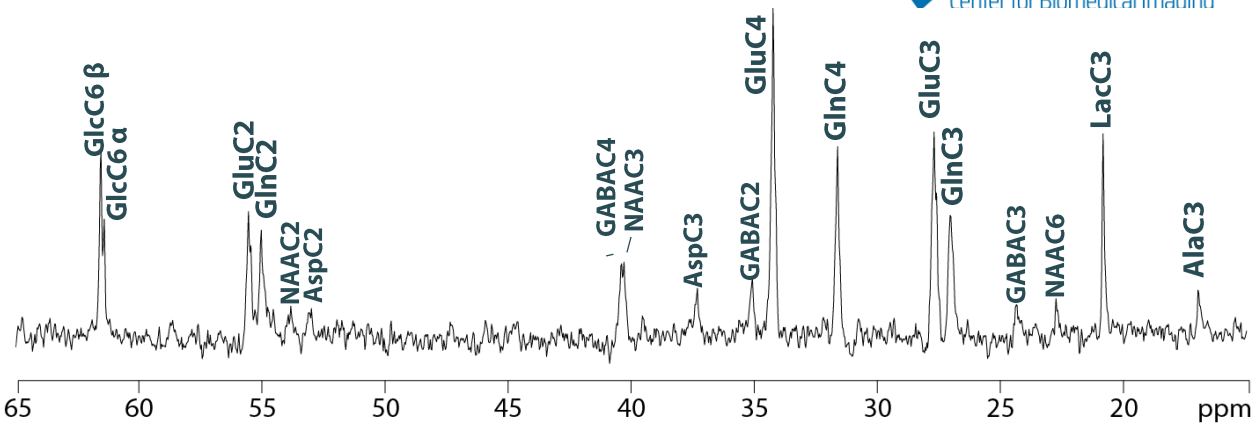

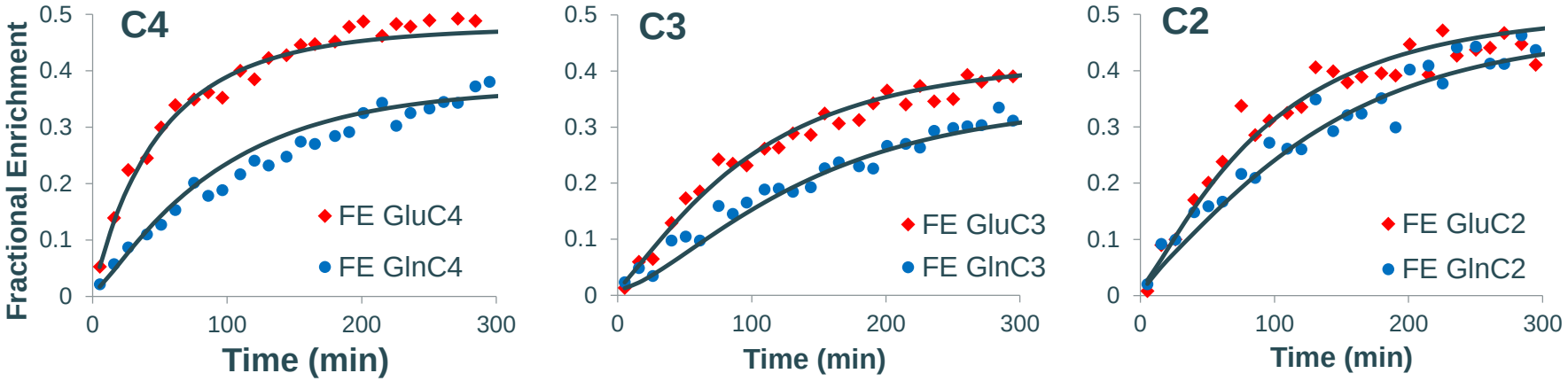

Fluxes	V_g	V_{PC}	V_{NT}	V_{tca}^n	V_x	V_{dil}^g
[µmol/g/min]	0.11	0.051	0.21	0.33	0.20	0.82
SD	0.02	0.005	0.03	0.02	0.03	0.04

Voxel 112µL

3.6x6.9x4.5mm^3

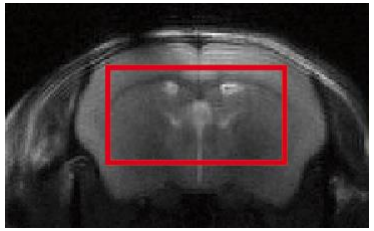

Lai et al., *JCBFM* , 2018

GLUCOSE CONSUMPTION

MEASURED WITH FDG-PET

Fluorodeoxyglucose (FDG) -> glucose metabolism

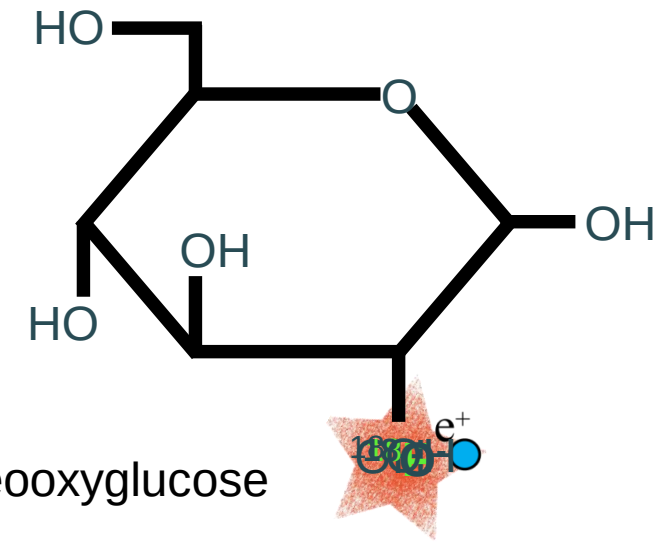

Fluorodeooxyglucose

FDG half-life : 110 min

Mean free path the emitted β^+ in water : ~ 1mm

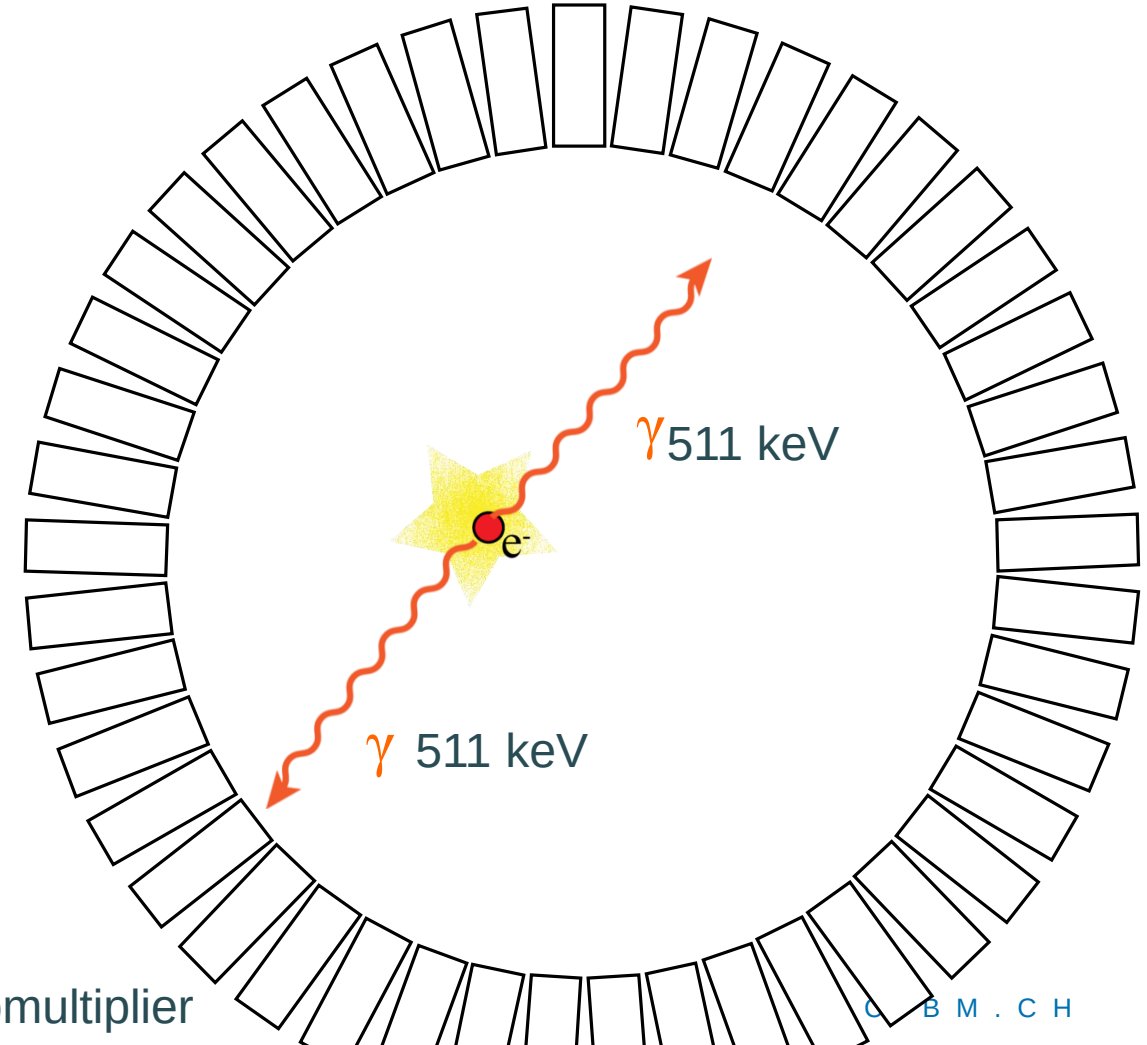

PET detectors:
Scintillator + photomultiplier

PARTICULARITY OF FDG

In the particular case of FDG, there is actually no «cold» tracer present in the system.

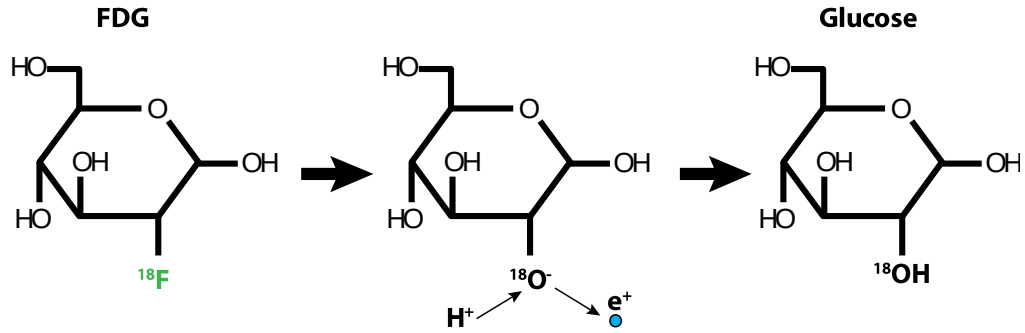

→ direct conversion of activity (in kBq/ml) to concentration is possible.

$$A(t) = A_0 \, exp\left(\frac{-\ln(2)\, t}{T_{1/2}}\right)$$

$$C(t) = \frac{100}{96.86}\int_t^\infty A(t')dt' = \frac{100}{96.86}\, A(t)\left(\frac{T_{1/2}}{\ln(2)}\right)$$

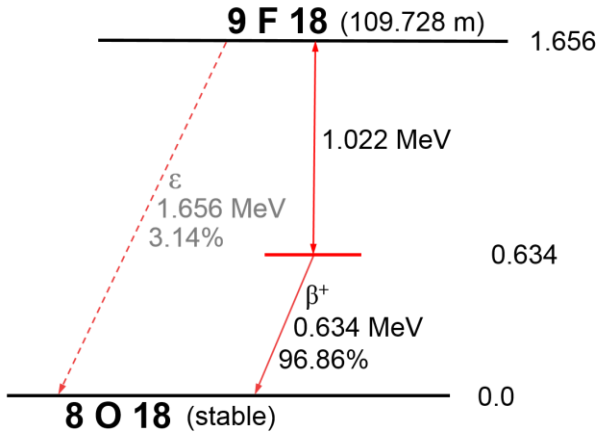

With $A \cong 500$ kBq/ml → $C \cong 5 \cdot 10^9$ molecules/ml $\cong 8$ pmol/l

METABOLISM OF FDG

BBB / Cell membrane

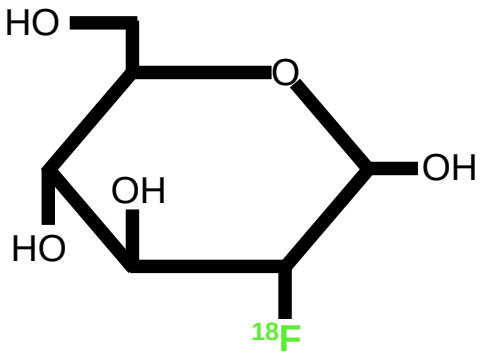

Fluorodeoxyglucose
FDG

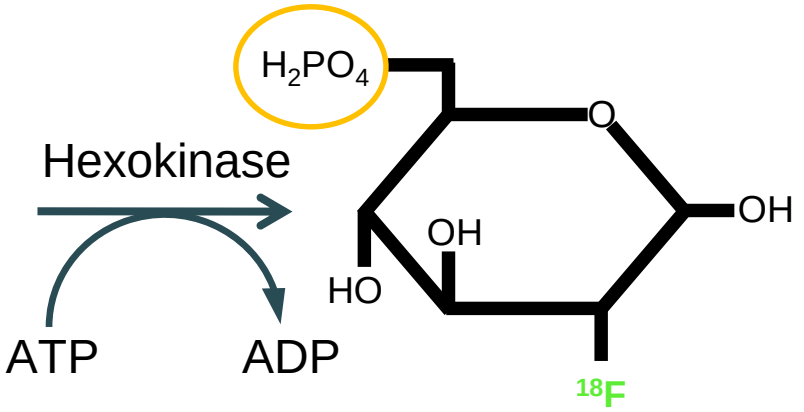

FDG-6P

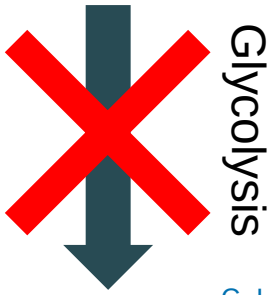

MODELLING OF GLUCOSE AND FDG METABOLISM:

AIF

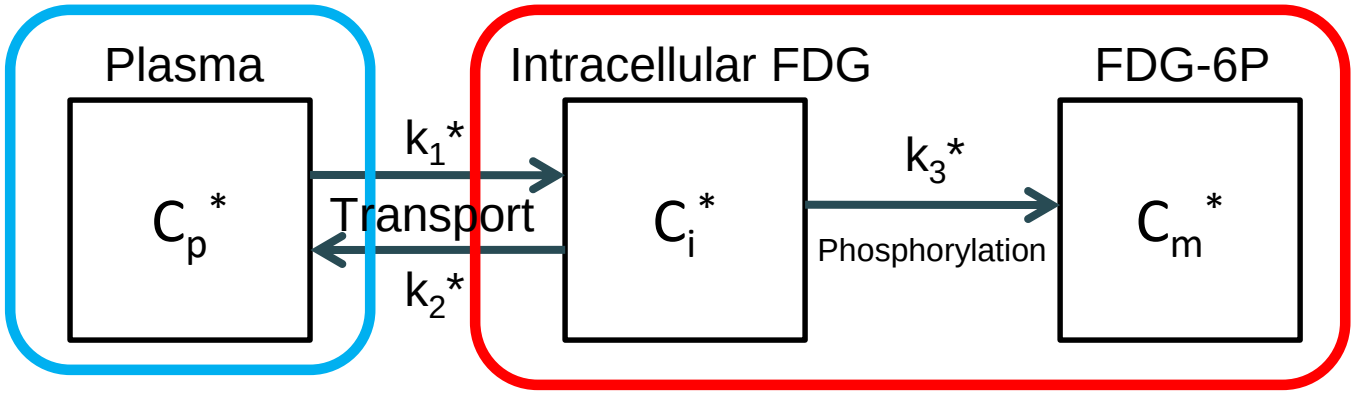

PET measured quantity

$$C_i^*(t) = \frac{k_1^*}{k_2^* + k_3^*}\left((k_2^* + k_3^*)e^{-(k_2^*+k_3^*)t}\right) \otimes C_p^*(t)$$

$$C_m^*(t) = \frac{k_1^* k_3^*}{k_2^* + k_3^*}\left(1 - e^{-(k_2^*+k_3^*)t}\right) \otimes C_p^*(t)$$

MODELLING OF GLUCOSE AND FDG METABOLISM:

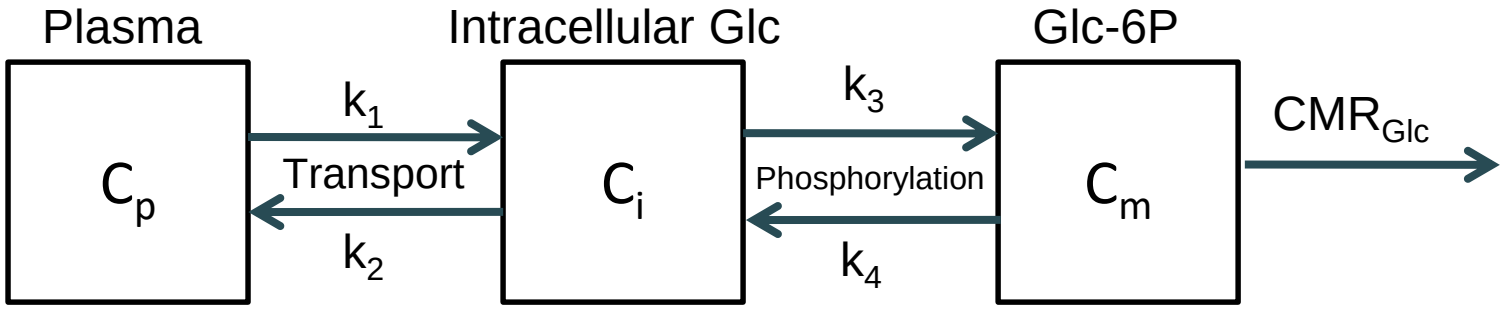

Mass balance equations at metabolic steady-state:

$$\frac{dC_i(t)}{dt} = k_1 C_p + k_4 C_m - (k_2 + k_2) C_i = 0$$

$$\frac{dC_m(t)}{dt} = k_3 C_i - (k_4 C_m + CMR_{Glc}) = 0$$

$$CMR_{Glc} = k_3 C_i - k_4 C_m = C_p \frac{k_3 k_1}{k_2 + k_3}$$

$$MR_{Glc} = \frac{C_p}{LC} \frac{k_1^* k_3^*}{k_2^* + k_3^*}$$

with

$$LC = \frac{\left[\frac{k_1^* k_3^*}{k_2^* + k_3^*}\right]}{\left[\frac{k_1 k_3}{k_2 + k_3}\right]}$$

MATHEMATICAL PRINCIPLES OF COMPARTMENTAL MODELLING

The measurement of the substrate concentration:

The arterial input function (AIF)

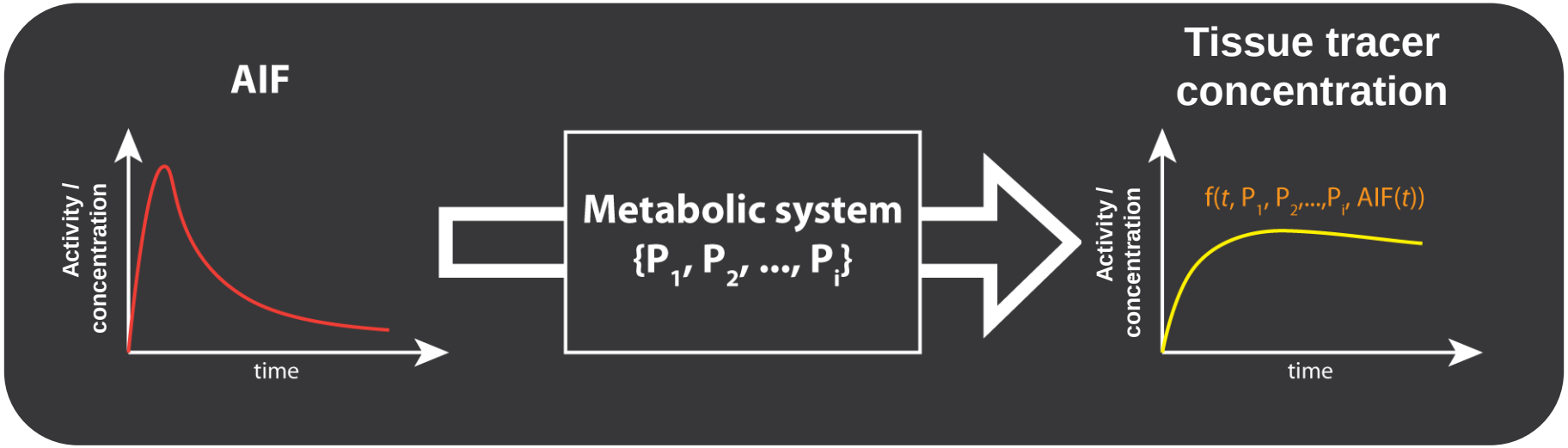

The AIF needs to be measured continuously over the entire infusion period or

The infusion protocol is designed to reach a desired input function.

QUANTITATIVE CMR_{GLC} MAPPING WITH PRECLINICAL PET

Non-invasive tracer input function measurement

JNM
The Journal of Nuclear Medicine

Research Article | Basic Science Investigations

Image-Derived Input Function from the Vena Cava for ^{18}F-FDG PET Studies in Rats and Mice

Bernard Lanz[1], Carole Poitry-Yamate[2], and Rolf Gruetter[1–4]

[1]Laboratory for Functional and Metabolic Imaging (LIFMET), Ecole Polytechnique Fédérale de Lausanne, Lausanne, Switzerland; [2]Center for Biomedical Imaging, Ecole Polytechnique Fédérale de Lausanne, Lausanne, Switzerland; [3]Department of Radiology, University of Lausanne, Lausanne, Switzerland; and [4]Department of Radiology, University of Geneva, Geneva, Switzerland

THE JOURNAL OF NUCLEAR MEDICINE • Vol. 55 • No. 8 • August 2014

QUANTITATIVE CMR_{GLC} MAPPING WITH PRECLINICAL PET

Non-invasive tracer input function measurement

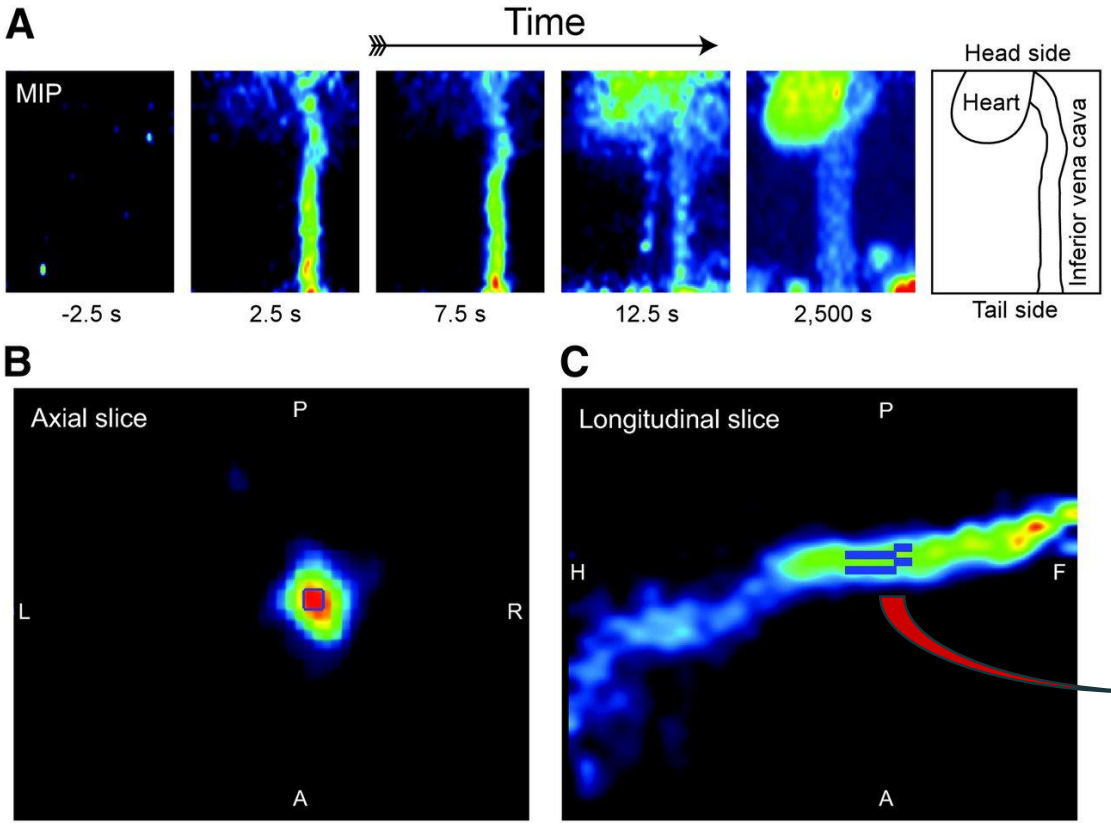

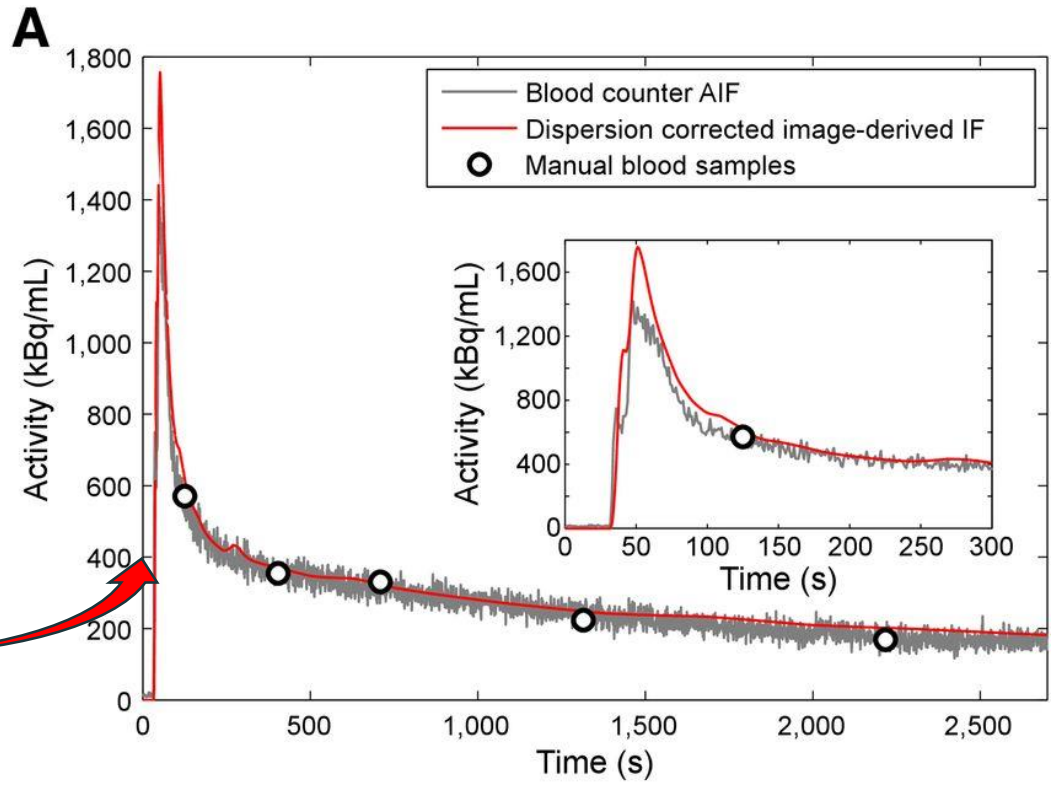

PET images of vena cava in rat during first passage of ^{18}F-FDG bolus, used to define VOI for image-derived input function

Lanz et al., J. Nucl. Med., 2014

QUANTITATIVE CMR_{GLC} MAPPING WITH PRECLINICAL PET:: APPLICATIONS [1]

3D maps in Bq/mL
0.5x0.5x1.18 mm^3
nominal resolution

Injection of ^{18}F-FDG bolus in the tail vein

dynamic acquisition on the vena cava

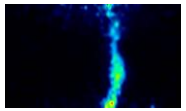

static acquisition on the brain

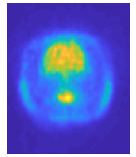

67.6 ± 11.9 MBq

Arterial input function (AIF) [2]

(Correction for blood versus plasma content)

45 min

T_f

60 min

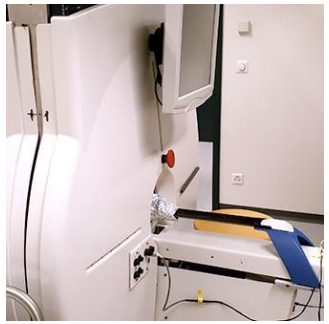

Avalanche photodiode LabPET 4 scanner
Reconstruction:

- MLEM (5 iterations on vena cava ; 15 on brain)
- Built-in quantitative calibration on FDG phantom
- Correction for inelastic scattering and radioactive decay

Sokoloff approach: [4]

Quantitative 3D CMR_{glc} maps

Glycemia

$$CMR_{glc}(T_f) = \frac{C_p}{LC} \frac{C_t^*(T_f)}{\int_0^{T_f} C_p^*(t)dt}$$

Lumped constant
0.71 [3]

Minimal invasiveness (FDG injection + one blood sample)

[1] Mosso et al., Anal. Biochem., 2022
[3Tokugawa et al., J Nucl Med., 2007
[2] Lanz et al., J. Nucl. Med., 2014
[4] Sokoloff et al., J. Neurochem., 1977

QUANTITATIVE CMR_{GLC} MAPPING WITH PRECLINICAL PET:: APPLICATIONS [1] (HEPATIC ENCEPHALOPATHY)

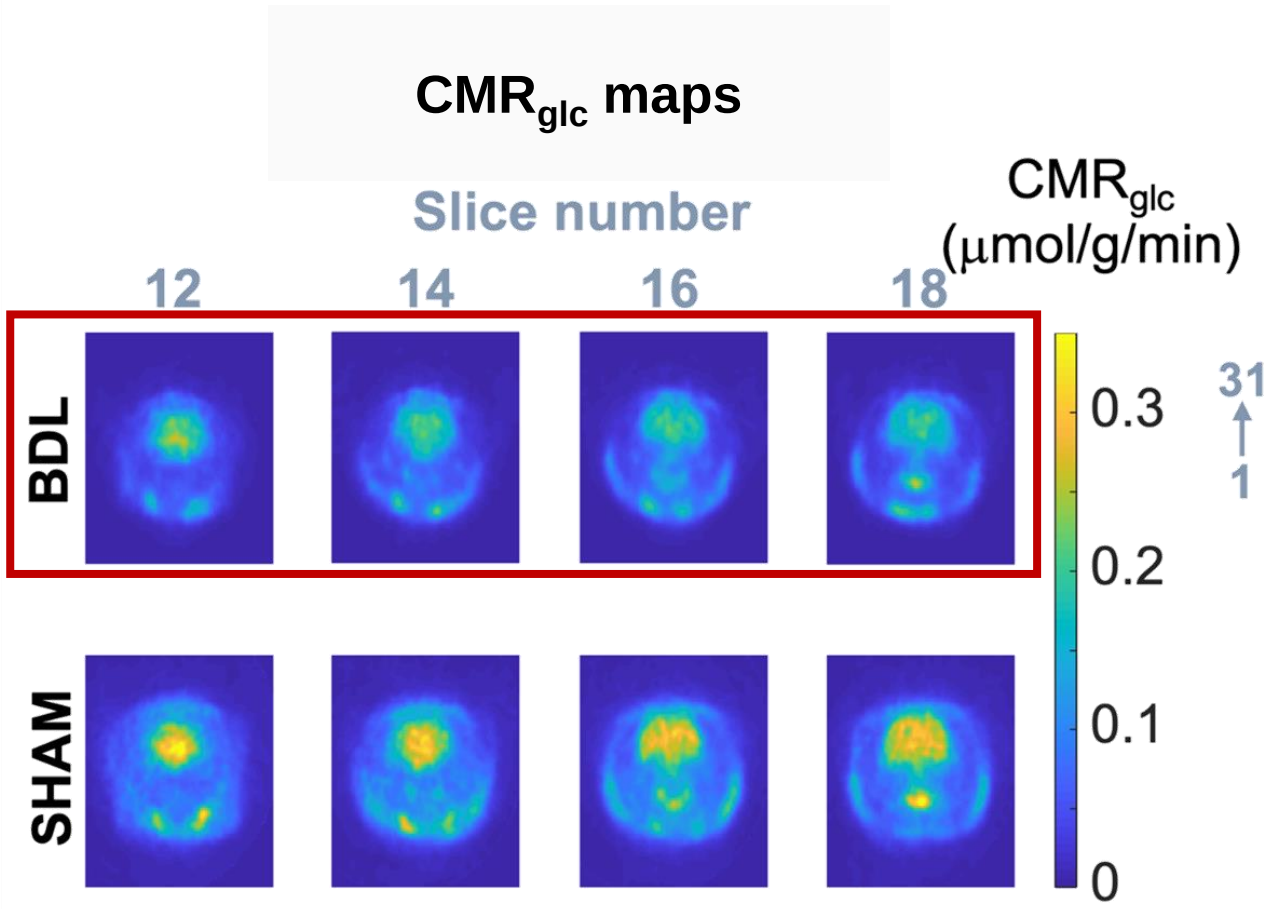

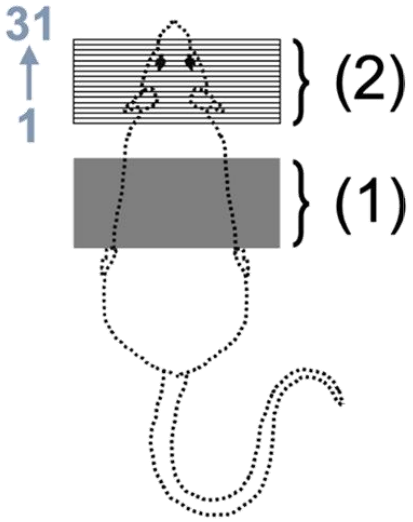

- Limitations of the SUV when systemic metabolic effects occur
- Added power of quantitative mapping of glucose uptake (CMR_{glc}) using an image-derived IF

Hippocampus

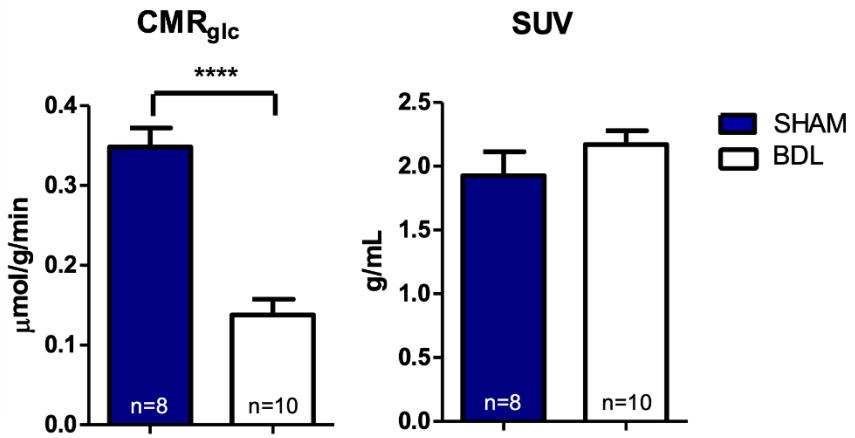

glucose cerebral metabolic rate in BDL rats over all slices

Mosso et al., Anal. Biochem., 2022

QUANTITATIVE CMR_{GLC} MAPPING WITH PRECLINICAL PET

Minimally invasive metabolic flux measurement in rats and mice

- Image-derived tracer input function
- Calibrated PET images in Bq/ml
- Adapted metabolic modelling with dynamic (mice) or steady-state (rats) FDG radioactivity density maps

→ CMR_{glc} 3D parametric maps with PET scanner nominal resolution (main limitation is the positron mean free path)

QUANTITATIVE METABOLIC MODELLING

GOAL: compare, validate and combine multimodal results

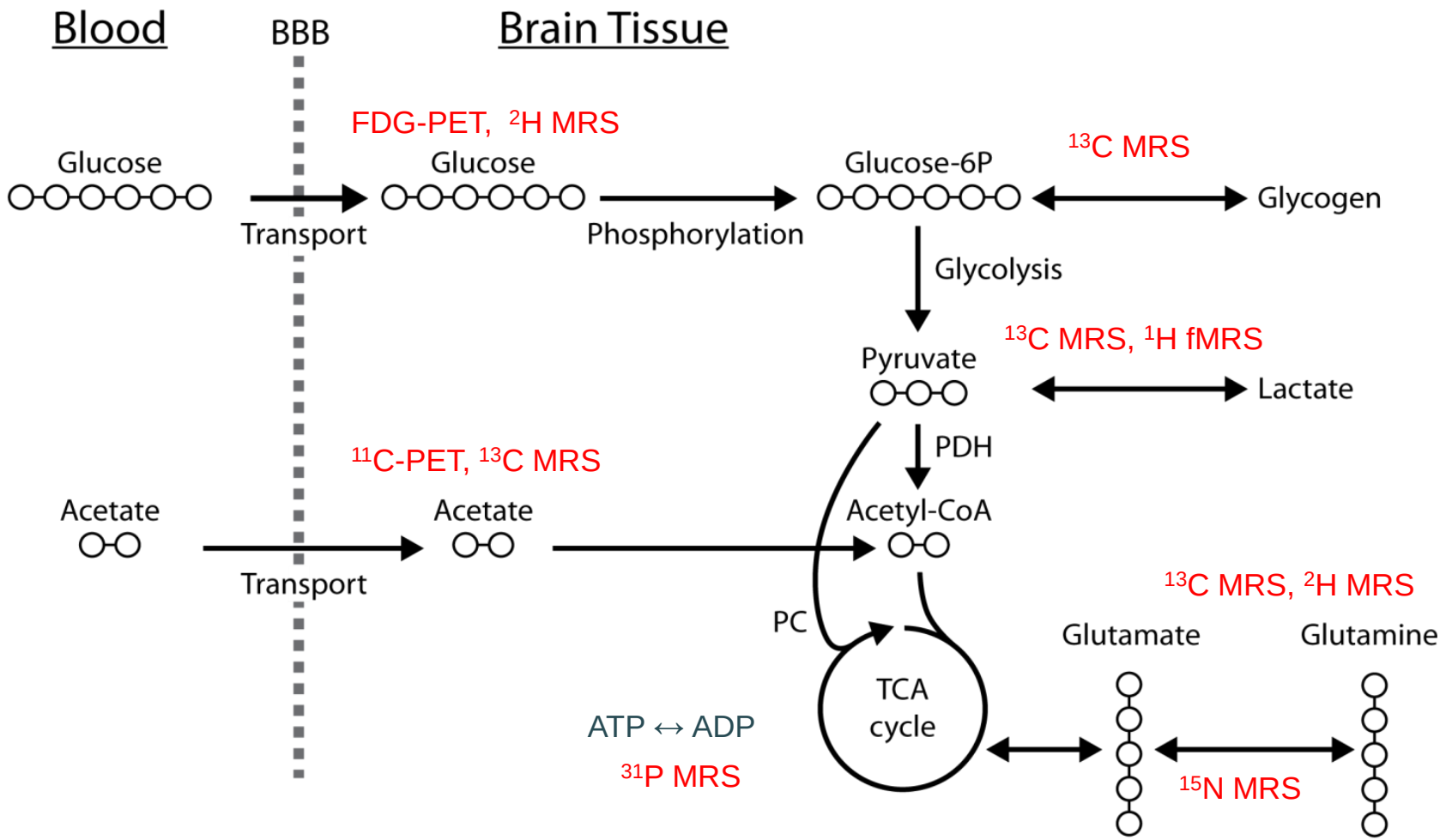

Deuterium MRSI

(also called DMI, deuterium metabolic imaging)

- Labelling experiment to study metabolic pathways (like in FDG-PET or ^{13}C MRS)
- Low background signal (water lipids)
- Short relaxation times (T1 and T2)
  -> faster temporal averages

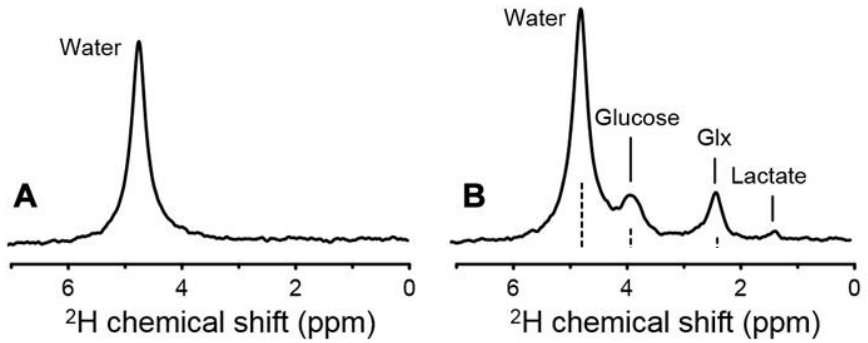

rat brain in vivo at 11.7 T before infusion of any ^{2}H-labeled substrate

rat brain after infusion of [6,6′-$^2H_2$]glucose in vivo

De Feyter *et al.*, *Sci. Adv.* 2018

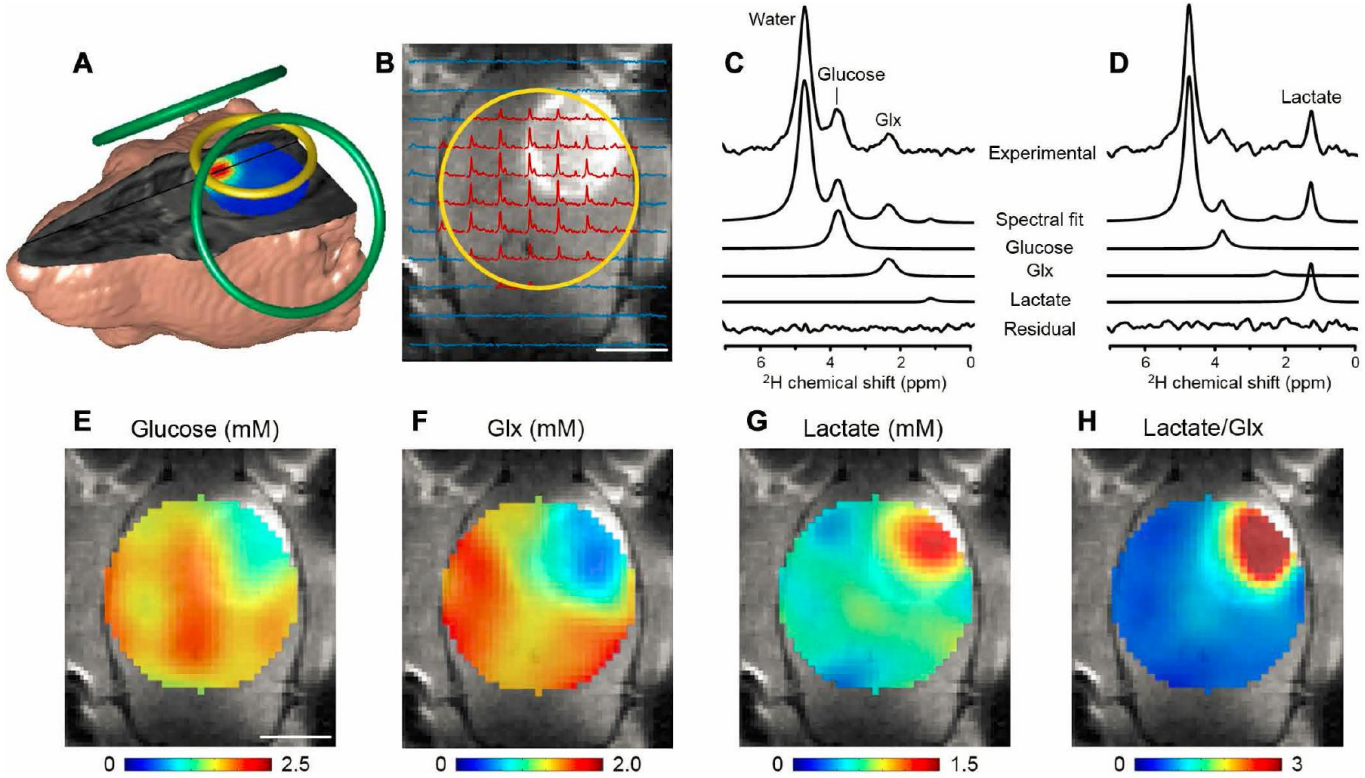

Deuterium MRSI

(also called DMI, deuterium metabolic imaging)

- Labelling experiment to study metabolic pathways (like in FDG-PET or ^{13}C MRS)
- Low background signal (water lipids)
- Short relaxation times (T1 and T2)
  -> faster temporal averages

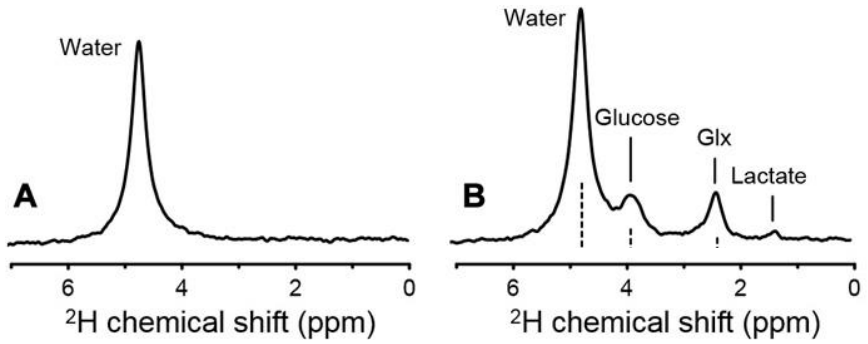

rat brain in vivo at 11.7 T before infusion of any ^{2}H-labeled substrate

rat brain after infusion of [6,6′-$^2H_2$]glucose in vivo

De Feyter *et al.*, *Sci. Adv.* 2018

Specific challenges:

- label losses
- Isotopic effects

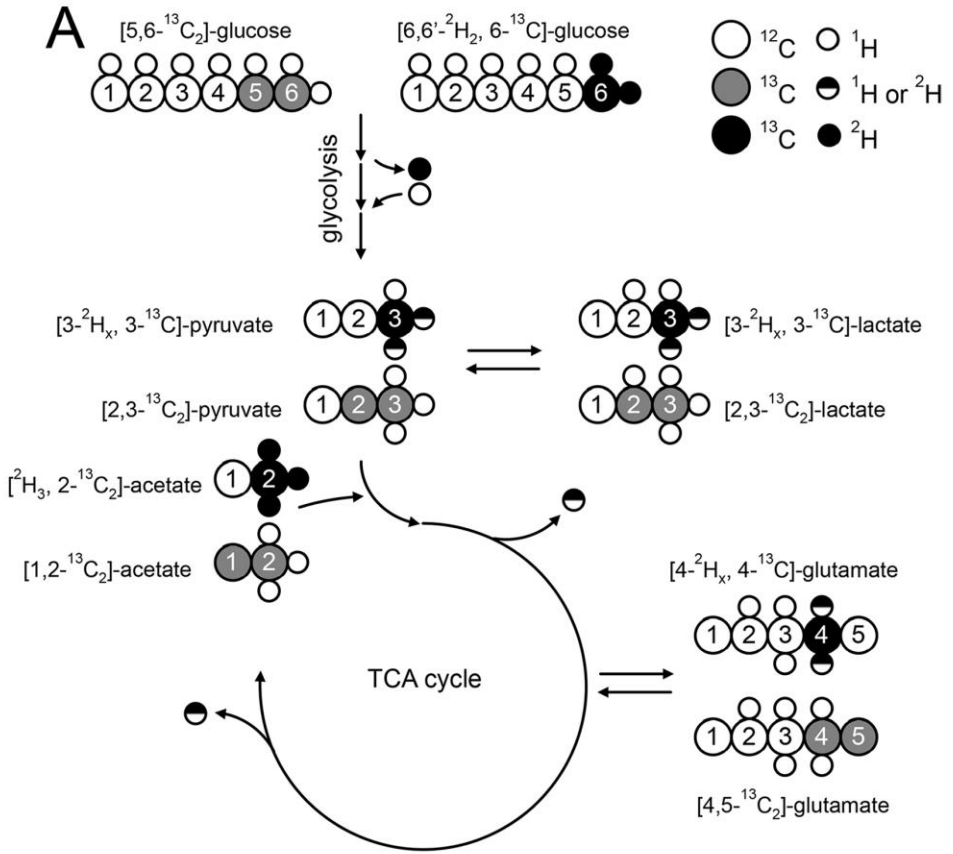

De Graaf *et al.*, *ACS Chem. Neurosci.* 2021

Towards quantitative Deuterium MRSI

- Deuterium MRSI :
  intermediary spatial resolution as compared to FDG-PET and in vivo ^{13}C MRS (one single voxel)
- It is <u>able to distinguish</u> $CMR_{Glc}(ox)$ et $CMR_{Glc}(non\text{-}ox)$
  (chemical specificity)
- It is non-radioactive and safe
  (strong clinical potential)

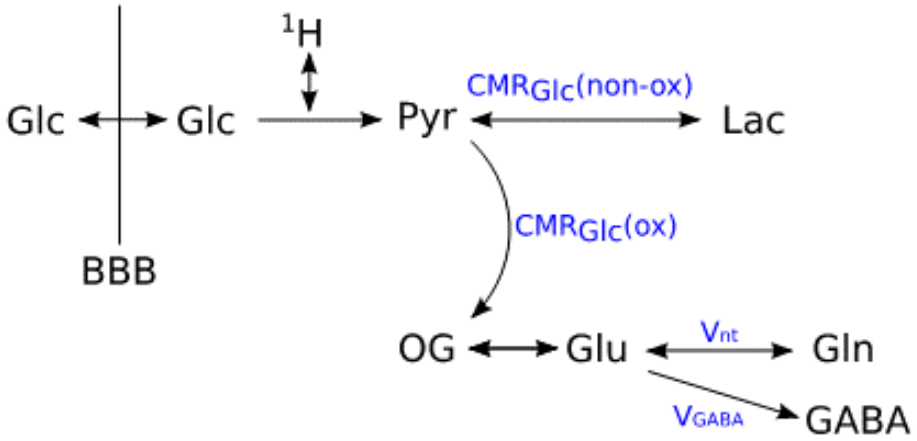

- Further developments need to be done to acquire
  <u>metabolic maps dynamically</u>
  -> new spatial encoding strategies
  -> obtain metabolic time courses for each voxel
  -> derive $CMR_{Glc}(ox)$ et $CMR_{Glc}(non\text{-}ox)$ in micromol/g/min
- Validate results in preclinical experiments with FDG-PET et ^{13}C MRS

BIBLIOGRAPHY

Contact: bernard.lanz@epfl.ch

- Cudalbu, C. & Lanz, B.
  Methods | Magnetic Resonance Spectroscopy for the Measurement of In Vivo Brain Metabolism. in *Encyclopedia of Biological Chemistry III (Third Edition)* (ed. Jez, J.) (Elsevier, 2021). doi:10.1016/B978-0-12-819460-7.00295-4.

- Lai, M., Gruetter, R. & Lanz, B.
  Progress towards in vivo brain 13C-MRS in mice: Metabolic flux analysis in small tissue volumes. *Anal Biochem* **529**, 229–244 (2017).

- Cobelli, C., Foster, D. and Toffolo, G. (2007) *Tracer kinetics in biomedical research: from data to model,*
  Kluwer Academic Publishers.

- Berliner, L. J. and Robitaille, P. M. (2002)
  In vivo carbon-13 NMR,
  Kluwer Academic Publishers.

- *http://infoscience.epfl.ch/record/182628/files/EPFL_TH5468.pdf*

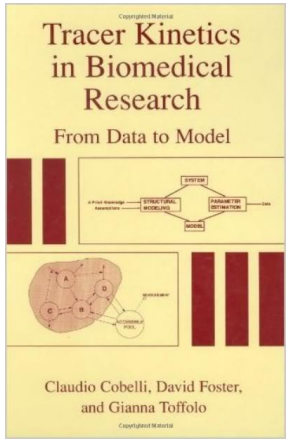

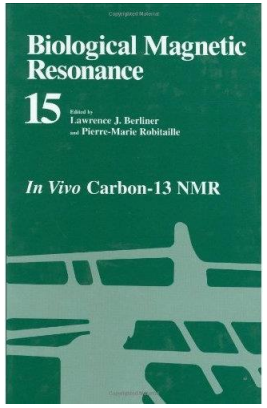

Thank you for your attention

Contact: bernard.lanz@epfl.ch

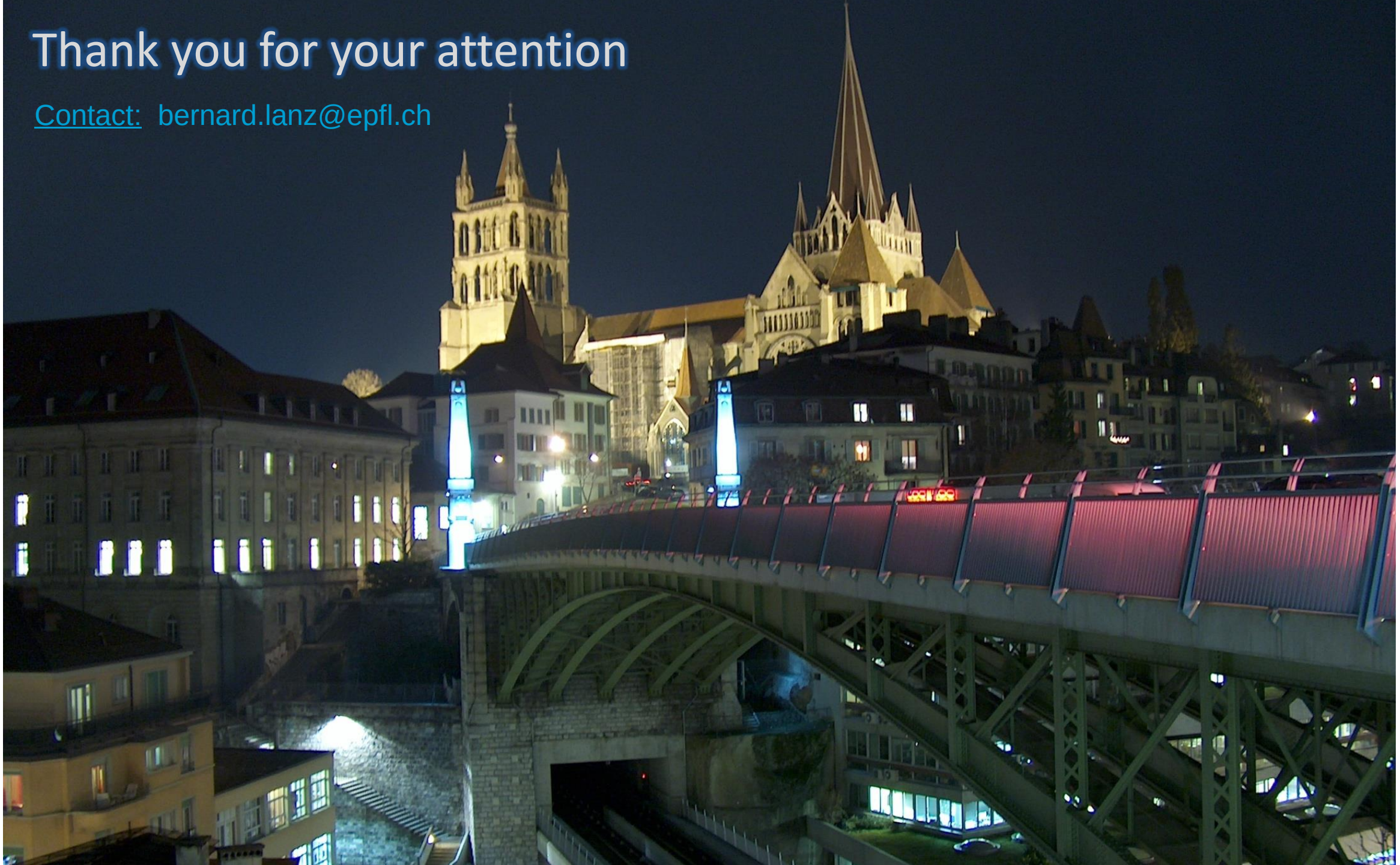

PREPROCESSING ^{13}C IN VIVO DATA – RAT BRAIN

AGILENT

- Open the fid
- Preprocessing/**Conjugate**
- Phase the signal using the zero and first order phase and afterwards use the option “Preprocessing/**Hard phase**” to save the changes. GluC4 at 34.3 ppm
  - If this option is not used the phasing is only visual
- Save the data as .mrui

^{13}C IN VIVO RAT BRAIN SIGNAL AFTER PREPROCESSING (SUM OF ONE HOUR OF SCAN)

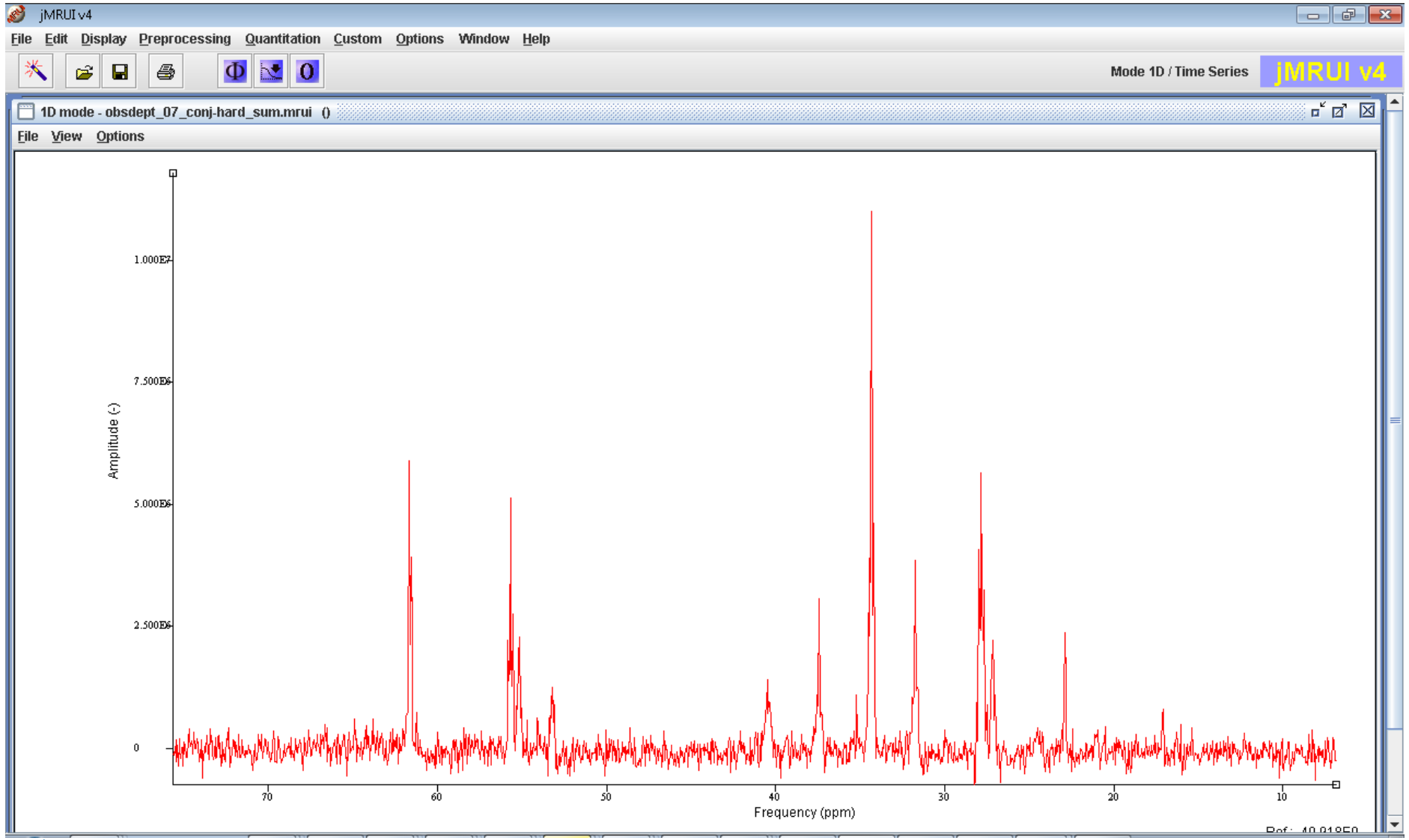

STARTING VALUES

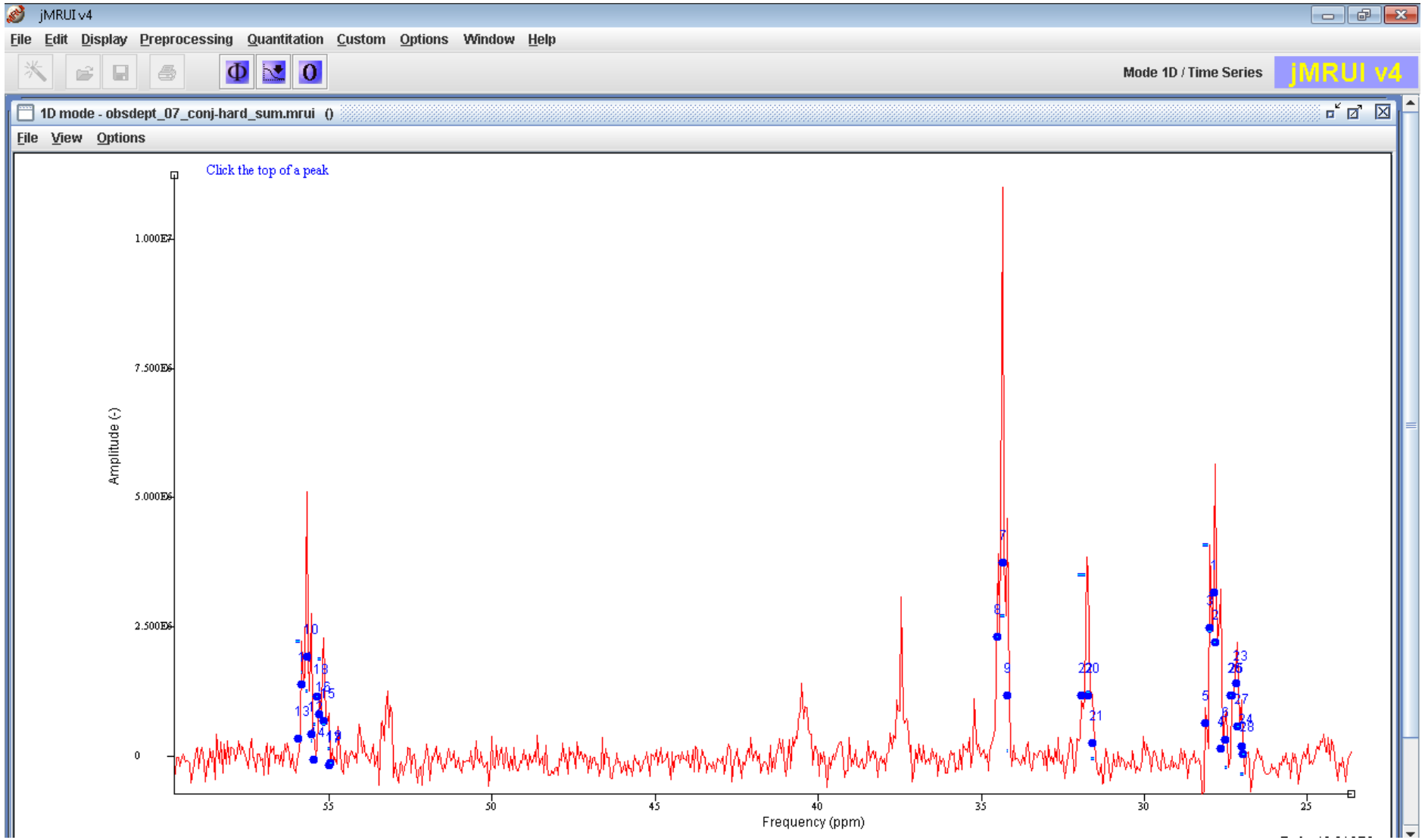

STARTING VALUES

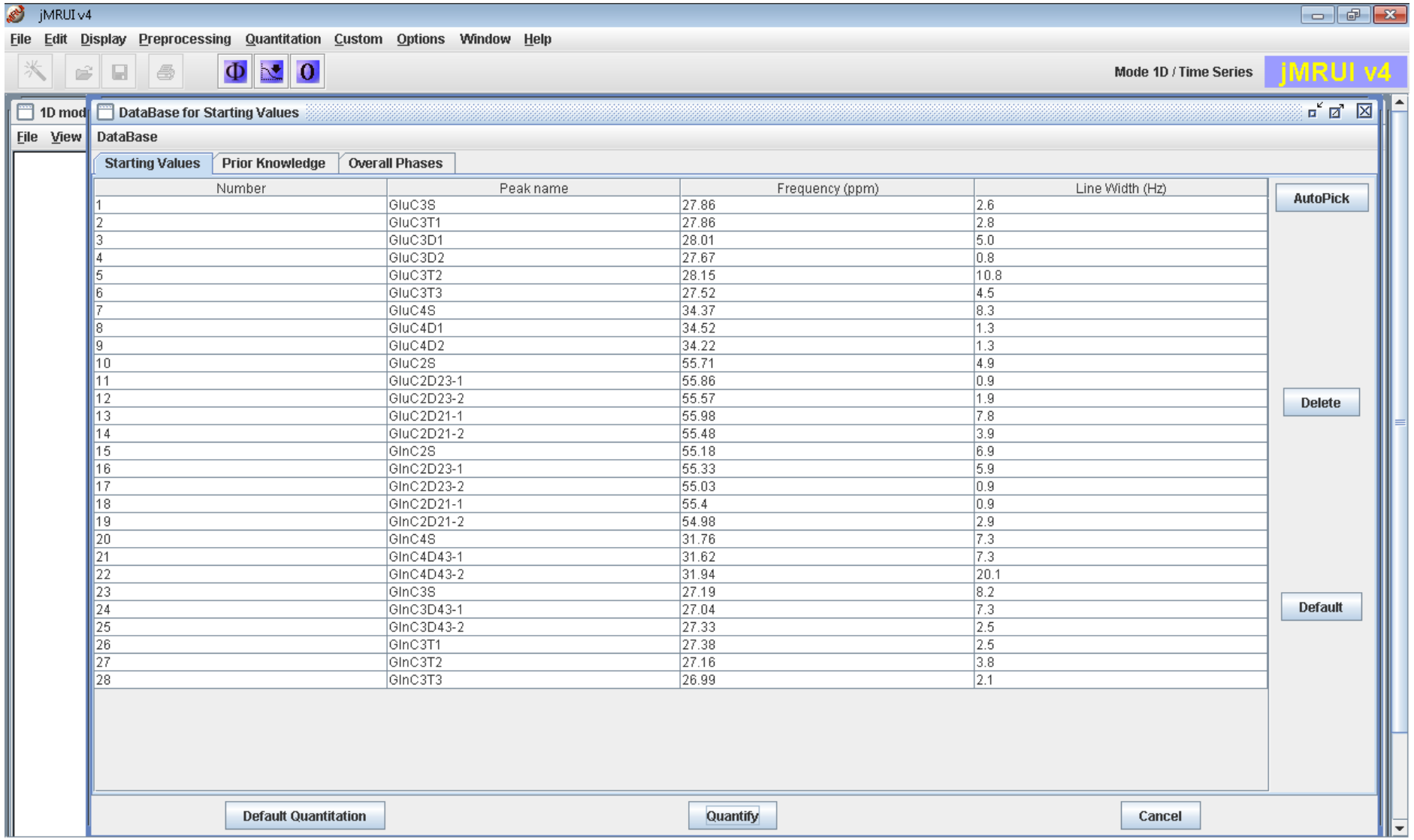

PRIOR KNOWLEDGE:

^{13}C-^{13}C J-EVOLUTION

Localized DEPT:

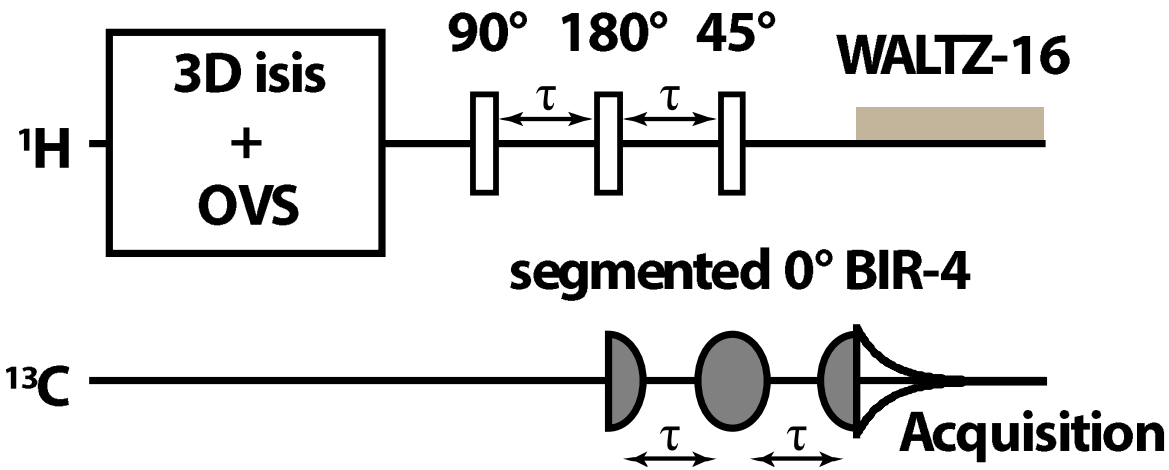

- Relative phase evolution:

with $\tau = 1/2J_{CH}$

- Triplets: $\theta_0:0:-\theta_0$
- Doublets: $\theta_0:-\theta_0$

with $\theta_0 = \pi \cdot \tau \cdot J_{cc}$
and $\tau = 2.75$ ms

Lanz B, et al. Magn Reson Med. 2013 **Henry** PG, et al NMR Biomed. 2003

PRIOR KNOWLEDGE

Table 1
Details on the High-Level Prior Knowledge Used in AMARES for the Quantifications with the 2nd and 3rd Approach

Resonance	Multiplet	Frequency	Relative phase	Amplitude
GlnC3	GlnC3S	27.15–27.25 ppm	0.0	Estimated
	GlnC3D-1	GlnC3S–18.45 Hz	34.6	Estimated
	GlnC3D-2	GlnC3S+16.45 Hz	–34.6	GlnC3D-1*1.0
	GlnC3T-1	GlnC3S+32.9 Hz	–69.1	GlnC3T-2*0.5
	GlnC3T-2	GlnC3S–2 Hz	0.0	Estimated
	GlnC3T-3	GlnC3S–36.9 Hz	69.1	GlnC3T-2*0.5
GluC3	GluC3S	27.8–27.9 ppm	0.0	Estimated
	GluC3D-1	GluC3S+16.3 Hz	–34.3	Estimated
	GluC3D-2	GluC3S–18.3 Hz	34.2	GluC3D-1*1.0
	GluC3T-1	GluC3S–2 Hz	0.0	Estimated
	GluC3T-2	GluC3S+32.6 Hz	–68.5	GluC3T-1*0.5
	GluC3T-3	GluC3S–36.6 Hz	68.5	GluC3T-1*0.5
GlnC4	GlnC4S	31.74–31.84 ppm	0.0	Estimated
	GlnC4D43-1	GlnC4S–18.45 Hz	34.6	Estimated
	GlnC4D43-2	GlnC4S+16.45 Hz	–34.6	GlnC4D43-1*1.0
GluC4	GluC4S	34.3–34.4 ppm	0.0	Estimated
	GluC4D43-1	GluC4S+16.3 Hz	–34.3	Estimated
	GluC4D43-2	GluC4S+18.3 Hz	34.3	GluC4D43-1*1.0
GlnC2	GlnC2S	55.15–55.25 ppm	0.0	Estimated
	GlnC2D23-1	GlnC2S+17.45 Hz	–34.6	Estimated
	GlnC2D23-2	GlnC2S–17.45 Hz	34.6	GlnC2D23-1*1.0
	GlnC2D21-1	GlnC2S+25.7 Hz	0.0	Estimated
	GlnC2D21-2	GlnC2S–27.7 Hz	0.0	GlnC2D21-1*1.0
GluC2	GluC2S	55.65–55.75 ppm	0.0	Estimated
	GluC2D23-1	GluC2S+16.3 Hz	–34.3	Estimated
	GluC2D23-2	GluC2S-18.3 Hz	34.3	GluC2D23-1*1.0
	GluC2D21-1	GluC2S+25.7 Hz	0.0	Estimated
	GluC2D21-2	GluC2S–27.7 Hz	0.0	GluC2D21-1*1.0

Lanz B, et al. Magn Reson Med. 2013

PRIOR KNOWLEDGE - AMPLITUDES

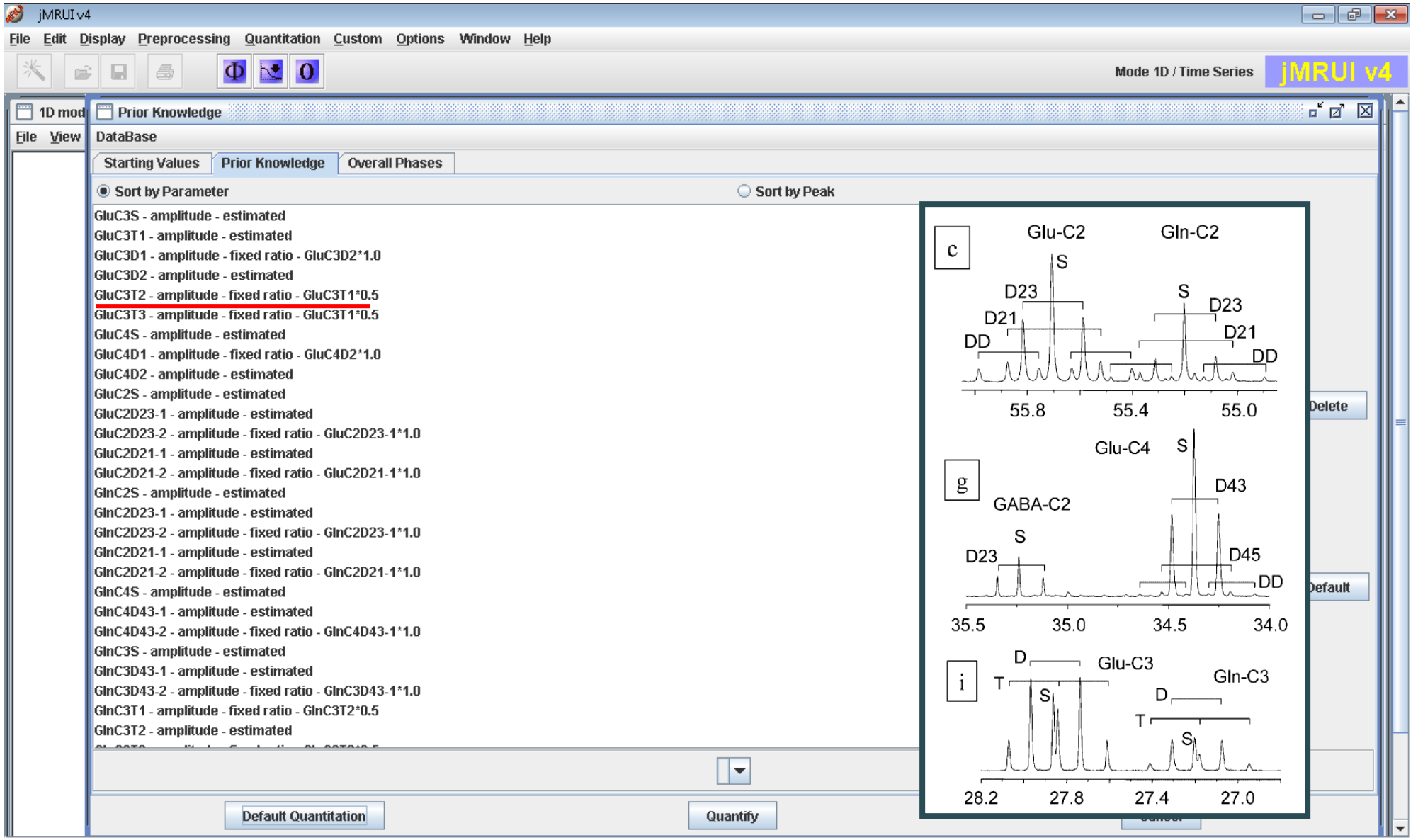

PRIOR KNOWLEDGE – RELATIVE PHASE

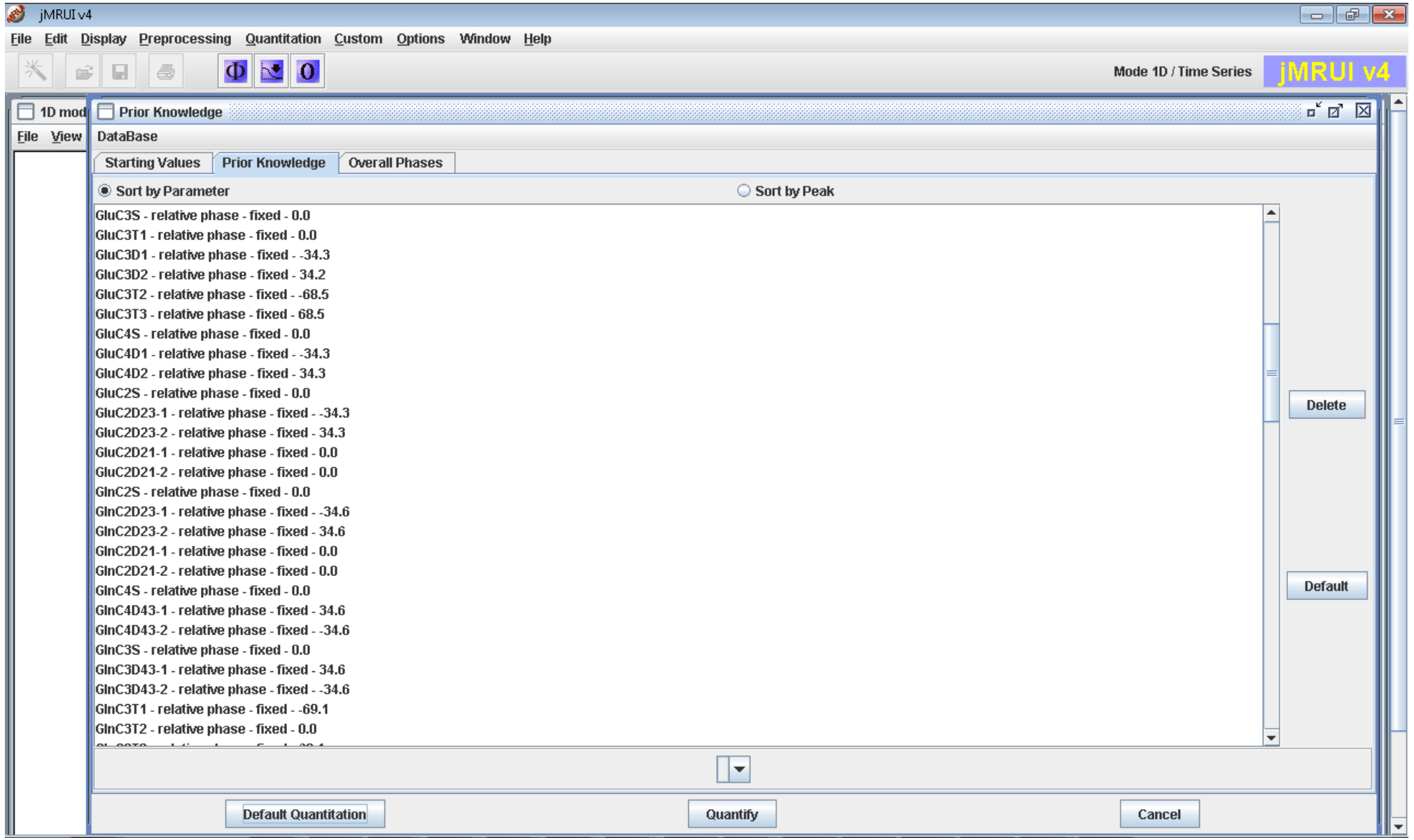

PRIOR KNOWLEDGE - LINEWIDTH

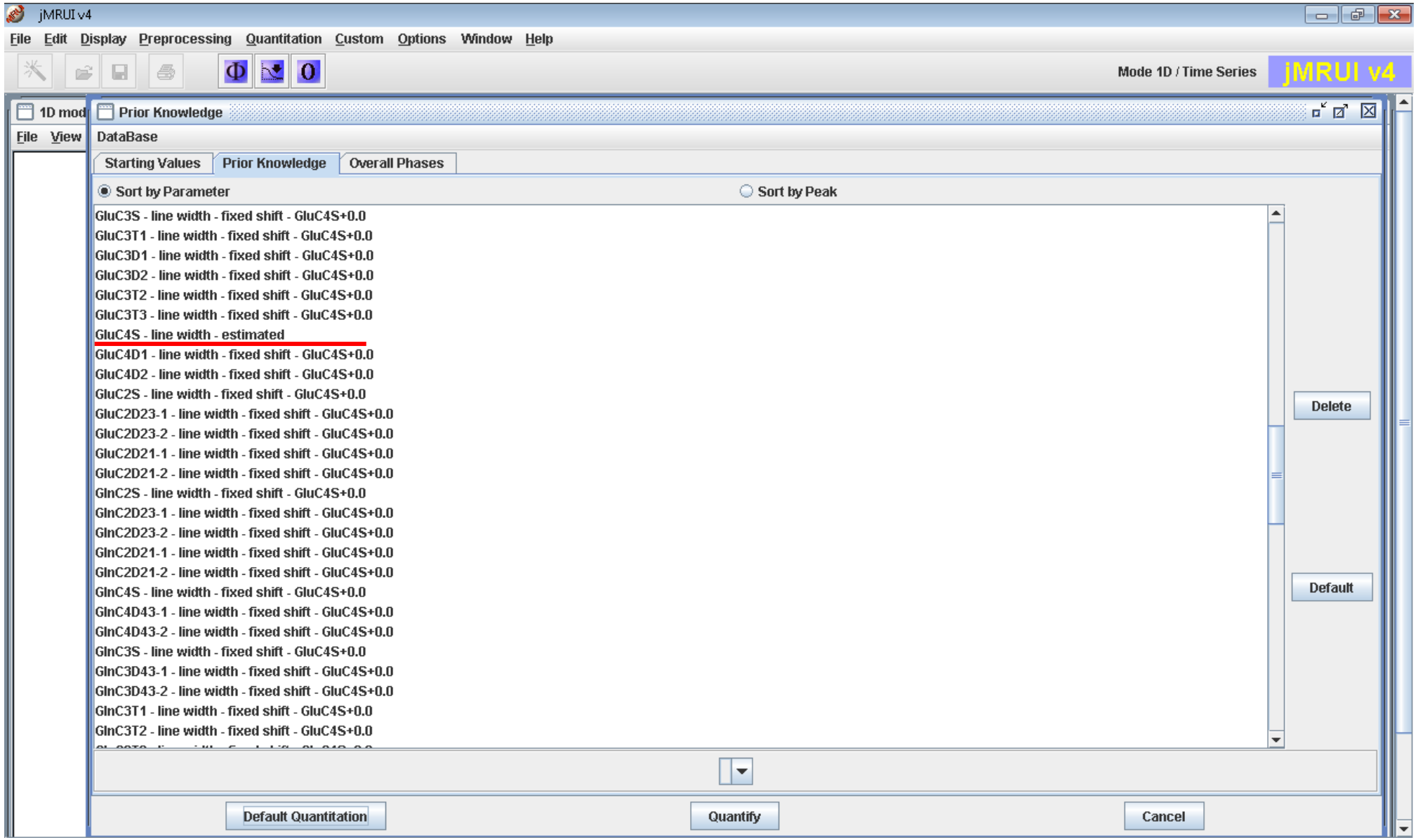

PRIOR KNOWLEDGE - FREQUENCY

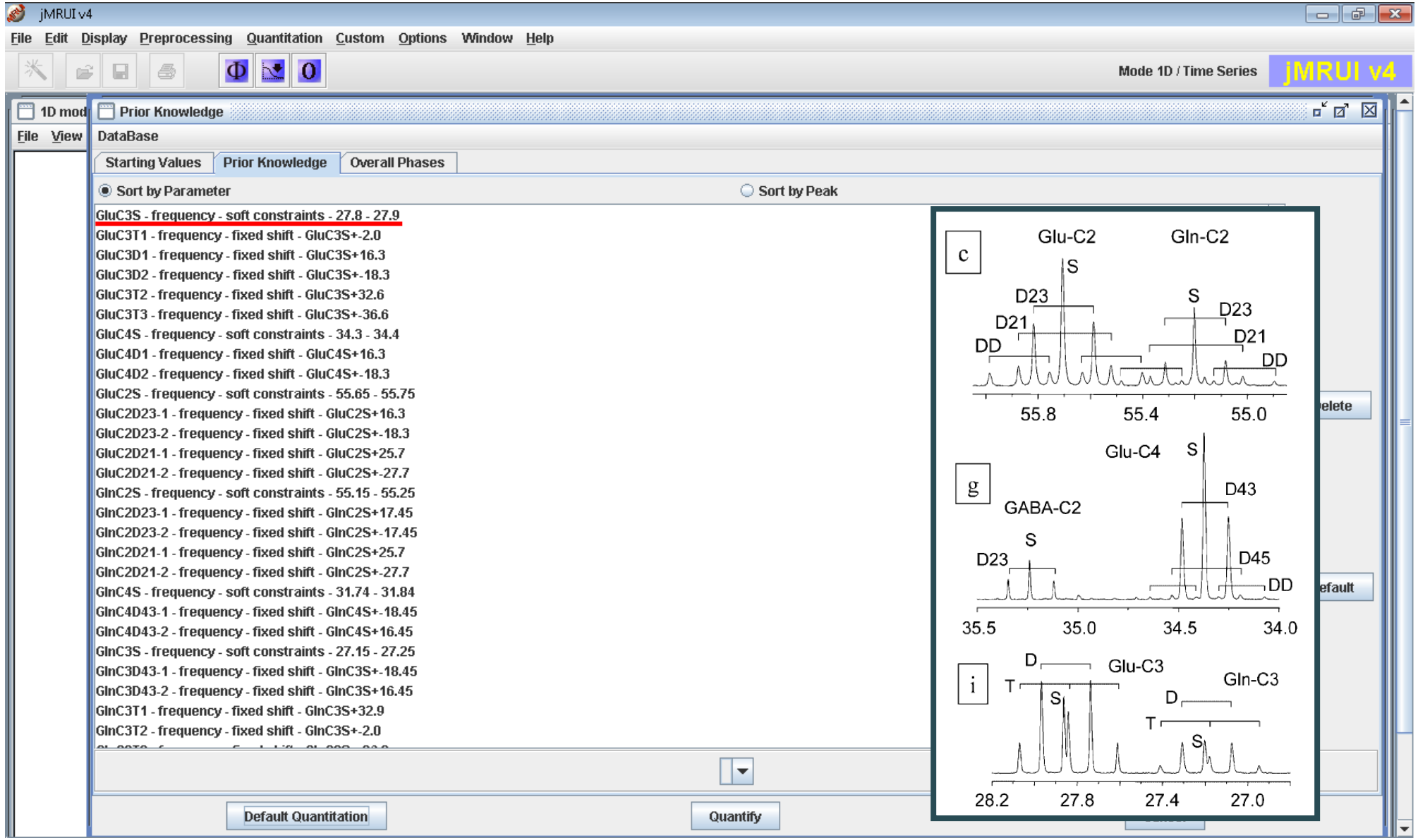

RESULTS

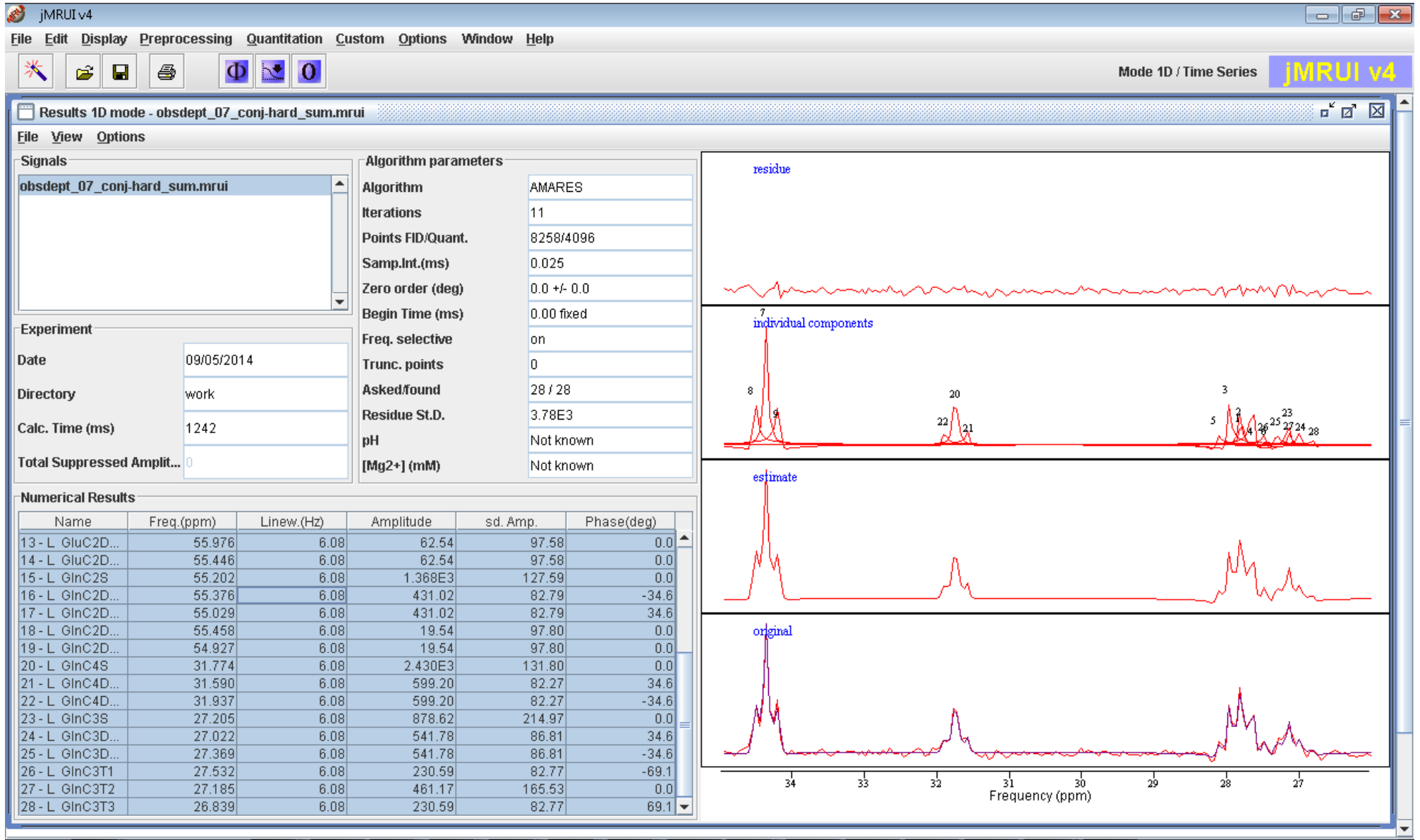

RESULTS

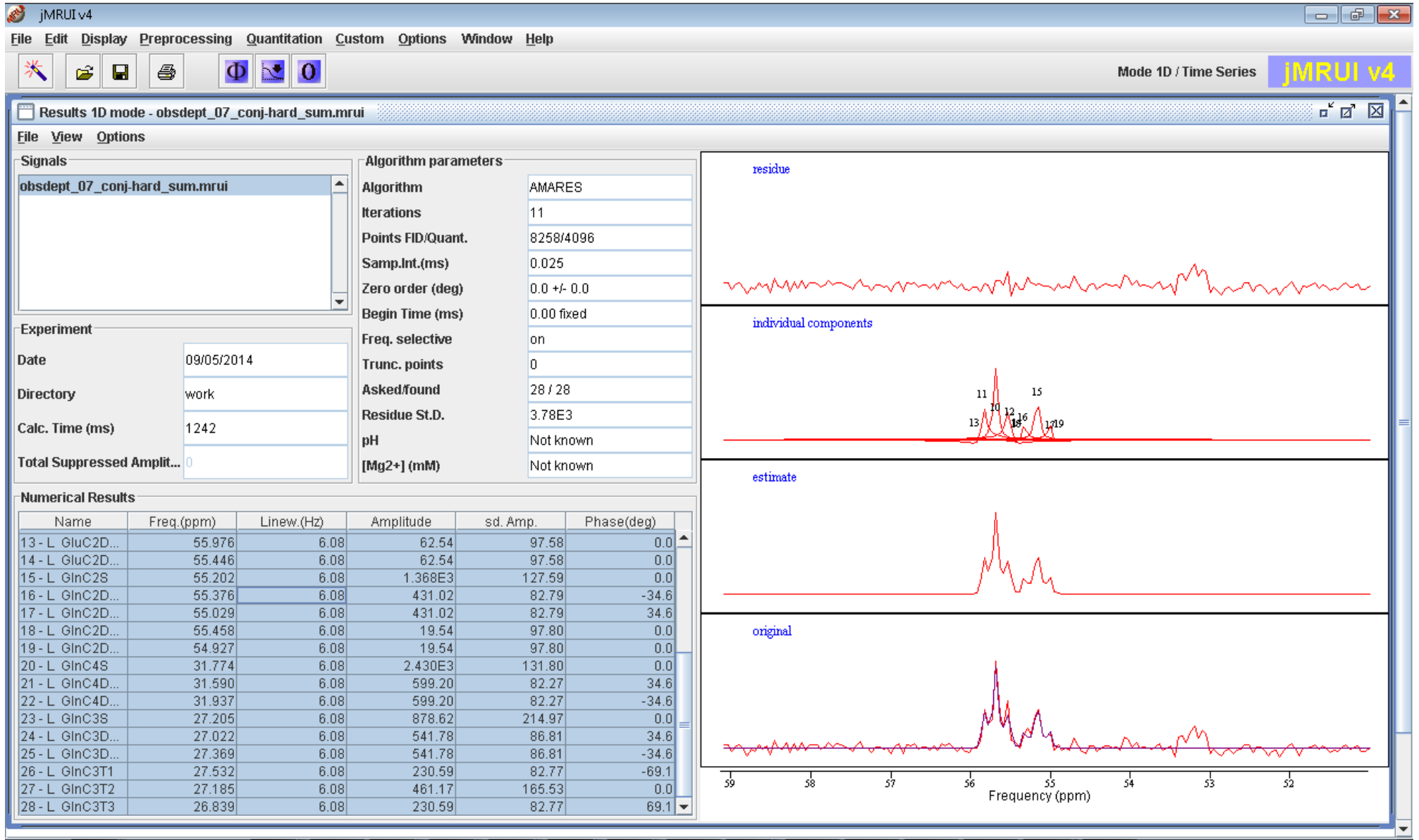

TIME CURVES

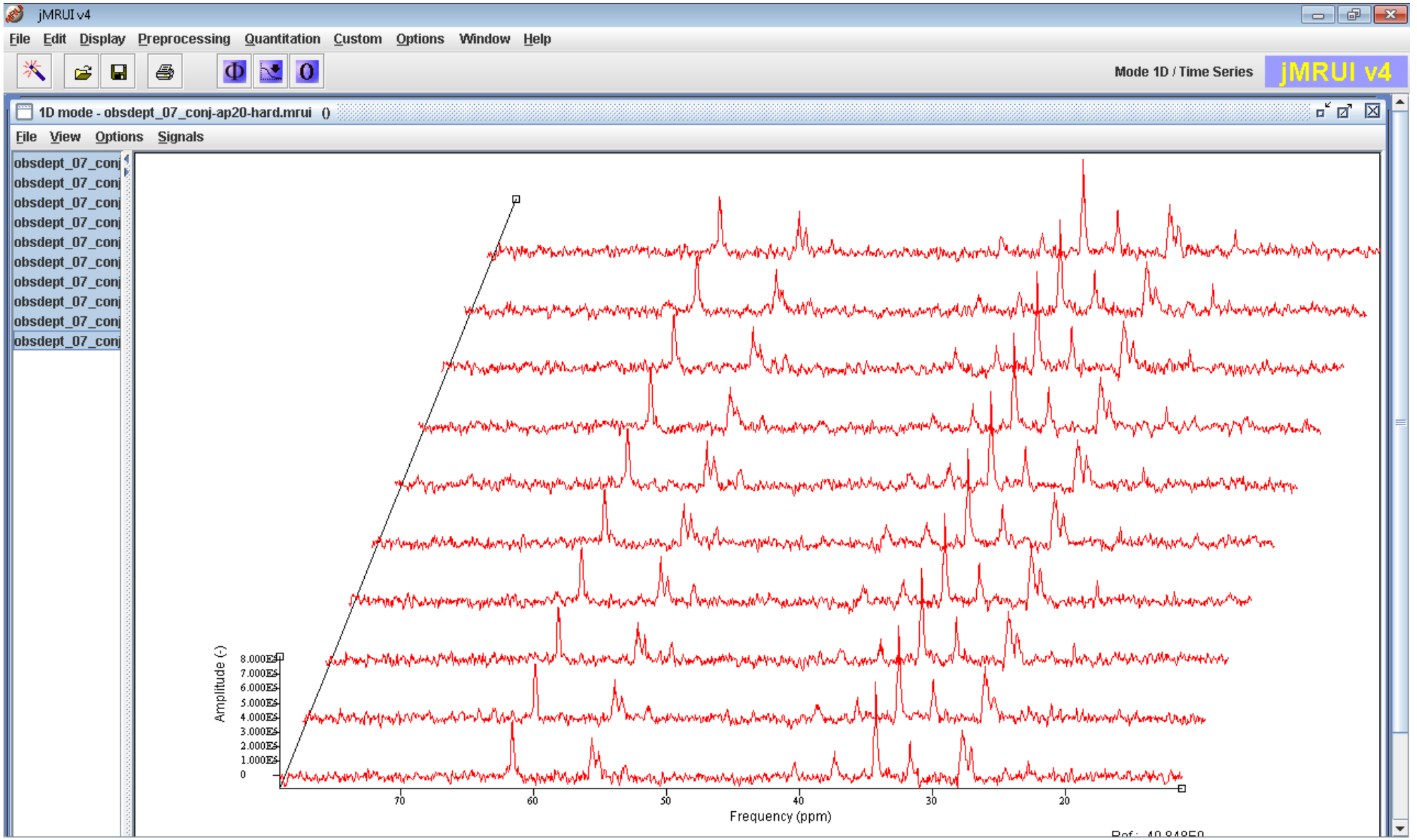

SAVE THE RESULTS AS .TXT FILE

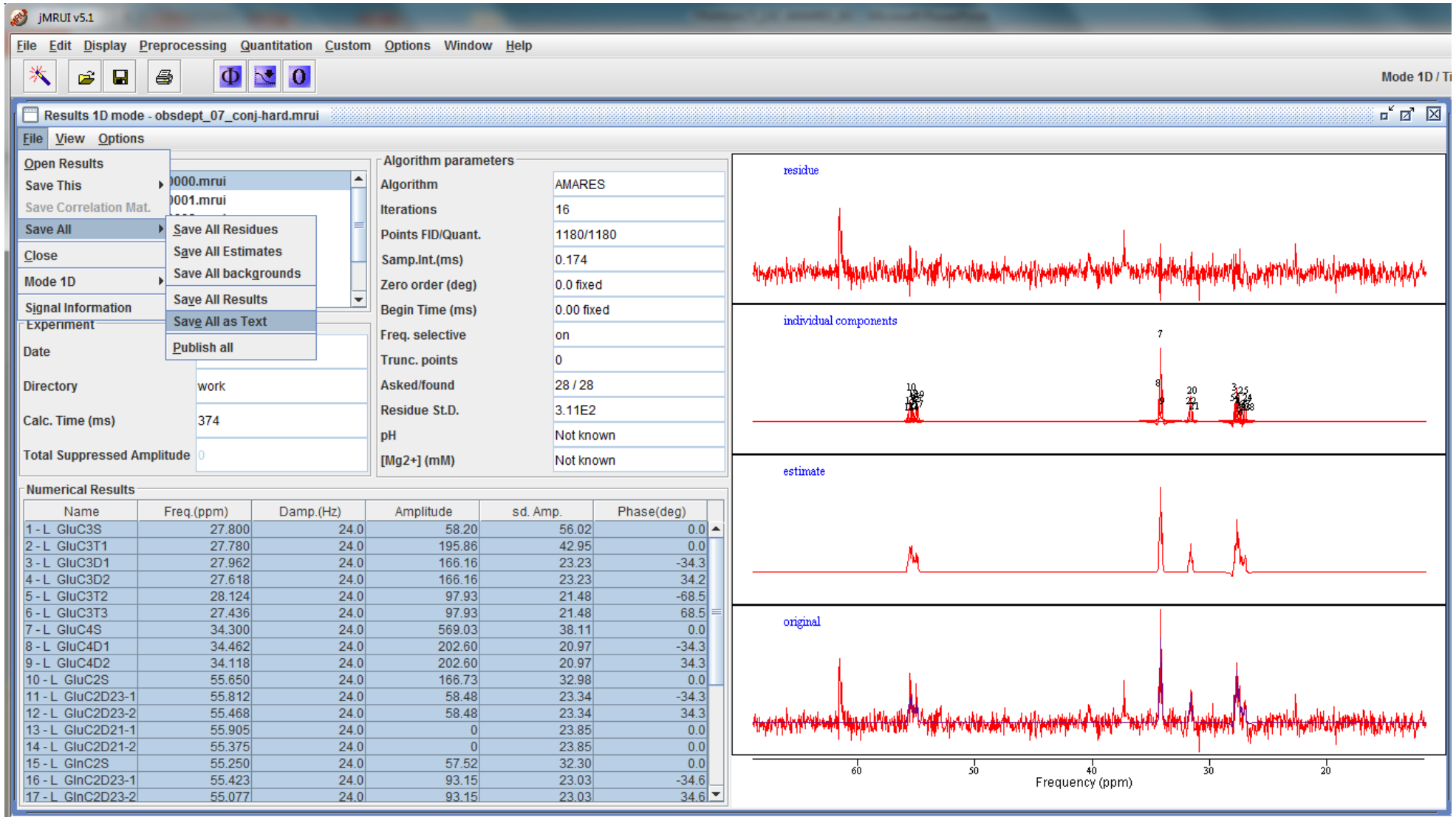

TIME CURVES

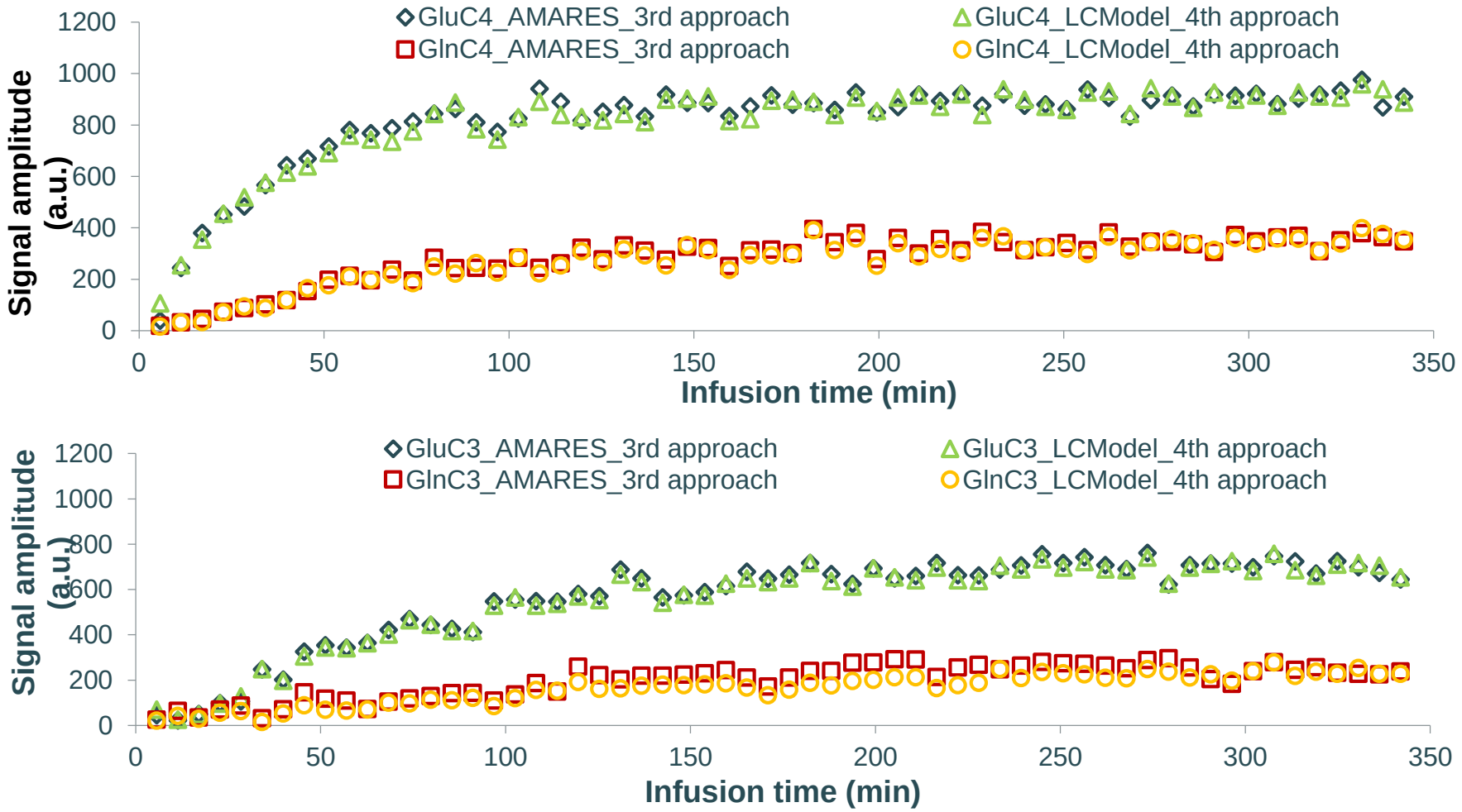

Lanz B, et al. Magn Reson Med. 2013